



**COLOR IMAGE SEGMENTATION BASED ON
REGION GROWING ALGORITHM**

By
Mohammad Ibrahim Al-Fraheed

Supervisor
Dr. Yas Al-Sultanny

**A Thesis Submitted in Partial Fulfillment of the Requirements for
the
Degree of Master of Science
In Computer Science**

**Department of Computer Science
Graduate College of Computing Studies
Amman Arab University for Graduate Studies
May, 2007**

Authorization of Dissemination

I, the undersigned " Mohammad Ibrahim Al Fraheed" authorize hereby " Amman Arab University for Graduate Studies " to provide copies of this dissertation to libraries, institutions, agencies, and any other parties upon their request.

Name: Mohammad Ibrahim Al Fraheed .

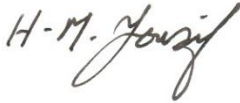



Signature:



Date: 11/9/2007

Resolution of the Examining Committee

This dissertation titled " Color Image Segmentation Based on Region Growing Algorithm" , has been defended and approved on 23/7/2007 .

<u>Examining Committee</u>	<u>Title</u>	<u>Signature</u>
Prof. Hilal Al - Bayatti	President	
Prof. Ala'a Al-hamami	Member	
Dr. Yas Al - Sultanny	Member and Supervisor	
Dr. Basel kasasbah	Member	

Dedication

To My Mother and My Father...

To My Brothers...

To My Fiancée...

Acknowledgement

I would like to thank my supervisor, Dr. Yas Al-Sultanny, for his invaluable guidance and support throughout the entire process of this thesis research work and for his important suggestions during my research.

Also I would like to thank my family, colleagues and friends for their great support.

Table of Contents

Table of Contents	vi
List of Figures	ix
List of Tables.....	xiv
List of Abbreviations.....	xv
Abstract	xvi
Arabic summary	xix
Chapter One Introduction and Literature Review	1
1.1. Introduction.....	1
1.2. Image Segmentation.....	1
1.3. Image segmentation technique.....	3
1.3.1.Thresholding techniques	3
1.3.2. Boundary Based Techniques.....	3
1.3.3. Region- based techniques.....	4
1.4. The Wavelet Transform and Segmentation.....	4
1.5.Image Segmentation Application.....	5
1.5.1.Face Recognition.....	5
1.5.2. Inspecting Machined Parts	5
1.5.3.Planning Radiation Therapy.....	6
1.5.4.Merging Medical Images	6
1.5.5.Surveying by Satellite	7
1.5.6. Number-Plate Identification.....	7
1.5.7.Aerial Navigation.....	8
1.6. Statement of the Problem.....	8
1.7. Image acquisition	9
1.8. Literature Review.....	10
1.8.1. Region Growing.....	10
1.8.2.Wavelets Transform.....	16
1.9.Outline of Thesis	21
Chapter Two Image Segmentation.....	23
2.1.Introduction.....	23
2.2. Segmentation Technique.....	23
2.3. Color Spaces (Models).....	25
2.3.1.RGB Color Model.....	25

2.3.2.The HSI Color Model.....	26
2.3.3.Converting Colors From RGB Model to HSI Model.....	27
2.4.Image Segmentation.....	27
2.4.1.Intensity Discontinuities Category.....	28
2.4.1.1.Point Detection.....	28
2.4.1.2.Line Detection.....	28
2.4.1.3.Edges Detection Using Canny Edge Detector.....	29
2.4.2.Intensity Similarity Category.....	32
2.4.2.1.Basic Formulation.....	32
2.4.2.2.Region Growing.....	32
2.5.The Proposed First Technique For Color Image Segmentation to the RGB and HSI Model Based on Region Growing Algorithm.....	33
2.6.Implementation and Results.....	39
2.6.1.RGB Image Segmentation.....	39
2.6.2.HSI Image Segmentation.....	48
2.7. Conclusions and Discussions.....	51
Chapter Three Image Segmentation by Wavelets.....	56
3.1.Introduction.....	56
3.2. Image Representation in Multi-Resolution.....	56
3.2.1. Image Pyramids.....	57
3.2.2.Haar Transform.....	57
3.3. Multiresolutions Expansion.....	59
3.3.1.Scaling function.....	59
3.3.2.Wavelet Function.....	60
3.4. Wavelet Transform in One Dimension Based on the Discrete Wavelet Transform.	62
3.5.Wavelet Transform in Two Dimensions.....	62
3.6.Two-Dimensional Wavelet Transform by Averaging and Differencing Method.....	66
3.7. The Proposed Second Technique for medical image segmentation.....	68
3.7.1. The Proposed Second Technique (Part a) for Edge Detection and Medical Image Segmentation by Using Wavelet.....	69
3.7.2.The Proposed Second technique (Part b) for Medical Eye Images Segmentation by Canny Edge Detector.....	75
3.7.3.The Proposed Second Technique (Part c) for extracting high light region using wavelet.....	80
3.8. Conclusions and Discussions.....	83
Chapter Four Segmentation Based on 2D Wavelet.....	87
4.1.Introduction.....	87

4.2.The Proposed Third Technique for Colored Image Segmentation Based on Region Growing Algorithm and 2DWT.....	87
4.2.1.The first stage to the proposed third technique for Extracting Edges of RGB images.....	87
4.2.2.The Second Stage of The Proposed Third Technique for Determining Seed Regions	95
4.2.3.The Third Stage of the Proposed Third Technique for Region Growing Algorithm	101
4.3.Implementation and Results.....	102
4.4.Conclusions and Discussions.....	109
Chapter 5 Conclusions and Future Work.....	115
5.1. Introduction.....	115
5.2. Conclusions.....	116
5.3. Suggestions for Future Work.....	118
References.....	120

List of Figures

Figure No	Description	Page No
Chapter Two		
2.1	Schematic of the RGB color cube.	24
2.2	A mask for Point detection.	26
2.3	Line detector masks.	27
2.4	steps for proposed first technique to the region growing by using seed regions	32
2.5	Splitting the three bands of the RGB image	33
2.6	The results which are produced by applying edge Canny detector on bands of images.	33
2.7	Edge detection to the three bands is different by applying Dilation	34
2.8	Seed regions of red band in figure (2.7-a), marked from R_01 to R_15 .	34
2.9	Re-arrange the images in figure (2.5).	35
2.10	Merge seed region with neighboring pixels.	36
2.11	The difference between region before and after merge process, for region R_06.	36
2.12	Segmentation to the three bands of the image	37
2.13	Segmentation to the Africa map	38
2.14	Segmentation to the photo image.	39
2.15	Brain image segmented	39
2.16	City map image.	40
2.17	Red band of the city map image and its histogram	40
2.18	Regions of segmented image for red band of city map image.	40
2.19	Green band of city map image and its histogram	41
2.20	Regions of segmented image for green band of city map image.	41
2.21	Blue band of city map image and its histogram	41

2.22	Regions of segmented image for blue band of city map image.	42
2.23	The red band regions segmentation to the city map image colored with blue color.	43
2.24	The green band regions segmentation of the city map image colored with blue color.	43
2.25	The blue band region segmentation of the city map image colored with blue color.	44
2.26	Segmentation to the HSI model.	45
2.27	Segmentation by the HSI model of the city map image.	45
2.28	Histogram of intensity band.	46
2.29	Regions segmentation to the image for intensity band of the city map image.	46
2.30	Regions segmentation to the intensity band of the map image colored with blue color.	47
2.31	The relationship between the number of dilation operation and number of color region in the three band of RGB model and HSI model	50
2.32	The relationship between the values of the expand intervals, and the number of the color region in the three bands of RGB model and HSI model.	50
Chapter Three		
3.1	Pyramidal image structure	53
3.2	The basic Haar scaling function.	55
3.3	The basic Haar wavelet function.	57
3.4	The process of transform $j+1$ scale to j approximation and detail coefficient	60
3.5	Decomposition process at two scales.	61
3.6	Diagram shows the process of reconstruct j approximation and detail coefficients to scale $j + 1$	61
3.7	Medical images that are used to extract their edges by using wavelet	64
3.8	steps for proposed second technique (part a) to the edge detection and medical image segmentation by using wavelet	65
3.9	First scale of wavelet transform of the front view of the human head	66
3.10	Edge detection and image segmentation by using wavelet to the front view of the human head	67
3.11	First scale of wavelet transform to the back view of the human head	67
3.12	Edge detection and image segmentation using wavelet to the back view of the human head	68

3.13	Edges for image that was tested using proposed algorithm.	69
3.14	steps for proposed second technique (part b) for medical eye image segmentation using canny edge detector.	70
3.15	Sketch to determine the iris dimension	71
3.16	Applying segmentation by using algorithm 1	72
3.17	Applying segmentation to another image, by using algorithm1	72
3.18	The discrete wavelet frame decomposition with low pass (L), and high pass (H) filters, the input image decomposed into four sub bands.	73
3.19	steps for second stage of the proposed second technique (part c) for extracting high light region.	74
3.20	Applying segmentation by using wavelet algorithm to determine the ill region in the iris	76
3.21	Applying segmentation by using wavelet algorithm to determine plastic lens.	77
3.22	Relationship between the scale and number of regions.	78
3.23	Image of edges at different scales.	78
3.24	Edges to the human head.	79
3.25	Edges by using different methods.	80
Chapter Four		
4.1	The basic scaling and wavelet function of symlets wavelet family.	83
4.2	steps of the first stage to the proposed third technique for extract edges of RGB image	83
4.3	Splitting the three band of the RGB image.	84
4.4	Histograms of three bands of map image in figure (4.3).	84
4.5	Image of the city map before and after enhancement.	85
4.6	Transformed red band of the image based on symlets wavelet family and its contents; approximation, horizontal, vertical and diagonal coefficients.	86
4.7	The transformed red band of the image after removing approximation coefficient from it.	87
4.8	The three coefficients of the transformed image and the result of merging.	87
4.9	Shows the image transformed after replacing each of the three coefficients with coefficient X that is produced from step 5.	88

4.10	Edge image of red band of map image and its histogram.	88
4.11	Edges of the green and blue band of the image in figure (4.3).	89
4.12	Steps to second stage of the proposed third technique for determining seed regions.	90
4.13	The binary image to the three bands of RGB image.	91
4.14	The mask that represents the operand B.	91
4.15	The binary image of the RGB image.	92
4.16	The binary image after removing isolated pixels with their isolated pixels that are removed from them.	93
4.17	Merging Image	93
4.18	Merged image after removing one-pixel gaps.	94
4.19	Flow chart to the region growing by using seed regions	94
4.20	RGB image segmentation to the city map image	95
4.21	Red band segmentation to the city map with their regions.	95
4.22	Green band segmentation to the city map with their regions.	96
4.23	Blue band segmentation to the city map image with their regions.	96
4.24	Regions segmentation to the red band of the map image colored with blue color.	98
4.25	Regions segmentation to the green band of the map image colored with blue color.	98
4.26	Regions segmentation to the blue band of map image colored with blue color.	99
4.27	The lungs image and its seed regions.	99
4.28	Region segmentation to the lungs image and its regions	100
4.29	Brain image with its seed region.	100
4.30	Image segmentation with its regions	101
4.31	Lungs image segmentation with its pixels merging.	102
4.32	Relationship between image segmentation with the enhancement and the non-enhancement	102
4.33	Relationship between the standard deviation, number of the seed regions and number of the colored regions.	104
4.34	Pixels that are merged together by Gaussian filter with the best value of the standard deviation.	104
4.35	The distributions pixels between 170 – 255 based on db2 wavelet family.	105

4.36	The distributions pixels between 170 – 255 based on haar wavelet family.	105
4.37	The distributions pixels between 170 – 255 based on sym4 wavelet family.	105
4.38	Image edge to the map image based on three types of wavelet.	106

List of Tables

Table No	Description	Page No
Chapter Two		
2.1	Intensity Ranges of Segmented Image of the City Map Image.	42
2.2	Intensity Ranges of Segmented Image to the Intensity Band of the City Map Image.	46
2.3	The relationship between the number of dilation operation, number of seed regions and the number of colored regions based on the RGB model.	48
2.4	The relationship between the values of expanded interval, the number of seed regions, the number of color regions based on the RGB model.	48
2.5	Relationship between the number of dilation operations, the number of seed regions, and the number of color regions based on HSI model.	49
Chapter Three		
3.1	Values of k, p and q	54
Chapter Four		
4.1	Intensity Ranges to the regions of city map image.	97
4.2	Intensity Ranges of the lung image.	100
4.3	Intensity Ranges of brain image segmentation.	101
4.4	The relationship between standard deviation and number of seed regions, number of colored regions and elapsed time.	103

List of Abbreviations

Abbreviation	Stands for
RGB	Red, Green and Blue Color model
HSI	Hue, Saturation and Intensity Color model
\oplus	Dilation Operation
ϕ	Scaling Function
ψ	Wavelet Function
ψ^H	Horizontal Coefficient of Wavelet Function
ψ^V	Vertical Coefficient of Wavelet Function
ψ^D	Diagonal Coefficient of Wavelet Function
DWF	Discrete Wavelet Frame
LH	Low – High sub band
LL	Low – Low sub band
HL	High - Low sub band
HH	High– High sub band
T	Threshold Value
\ominus	Erosion operation
•	Closing Operation
2DWT	Two Dimension Wavelet Transform

COLOR IMAGE SEGMENTATION BASED ON REGION GROWING

ALGORITHM

By

Mohammad Ibrahim Al-Fraheed

Supervisor

Dr. Yas Al-Sultanny

Abstract

Image segmentation is to divide the image into disjoint homogenous regions or classes, where all the pixels in the same class must have some common characteristics. The proposed first technique is proposed to segment regions in an image, which is based on determining seed regions in an image. The proposed first technique was applied on different sources of images with different complexities. The segmentation was applied on each band of the RGB images, and also tested on the HSI images, the results showed that, we can obtain good segmentation by processing only the intensity band (I) of the HSI model, which gives similar results as that obtained in RGB model. The results also showed the relationship between the number of dilation to close the regions and the number of regions that can be segmented. Good results were obtained with the number of dilation equal 2, and the results showed that the best value to expand pixel neighbor is from 1 to 4, to keep the image from degradation.

The proposed second technique (Part a) is proposed using differencing-averaging method to determine the image edges, the results showed that the first level of

transformation is enough to give good results. The edges of the image were enhanced, by using thresholding technique, followed by dilation operation to determine the closed segment regions. The segments were colored with any color to discriminate these regions from the other regions of the image.

The medical eyes images are segmented by using two proposed techniques; the proposed second technique (Part b) and the proposed second technique (Part c). The first is applied on iris image to determine edges of the iris, pupil and extract any different color regions, the technique was applied on two different sources of images and showed good results. This technique is useful when we want to detect the white water inside the eyes. The second consists of two stages, the first stage used the proposed second technique (part a) that used differencing-averaging method to determine the highlight region, and the second stage was based on drawing a circle to determine the object and it showed good results for the two different sources of medical images. The background must be selected to obtain good results, by using background of high level of darkness.

The proposed third technique is proposed to segment color regions in an image that is based on determining edges and seed regions by using two-dimension wavelet transform. By this technique, the image is enhanced by using Gaussian filter before it is transformed to first scale, and the noise that is set in the edges should be removed by using morphological algorithms. The proposed third technique was applied on different types of images, the results showed the enhancement step is necessary to reduce the number of the seed regions, number of colored regions and elapsed time. The results also showed that the best results were obtained when the value of the

standard deviation for Gaussian filter was from 1 to 3.5, after that the image was degraded. In the proposed third technique many of wavelet families were tested and the results showed that the best wavelet family was the first scale of the symlet to extract edges.

تقسيم الصور الملونة بالاعتماد على خوارزمية التدرجات اللونية

إعداد

محمد إبراهيم الفراهيد

إشراف

د. ياس السلطاني

Arabic summary

تقسيم الصور هو تجزئة الصور إلى مناطق متجانسة بحيث أن كل النقاط في المنطقة نفسها يجب أن تحمل الخصائص نفسها. خوارزمية جديدة تم اقتراحها لتقسيم الصور والتي تعتمد على تحديد مناطق البذرة في الصورة. هذه الخوارزمية طبقت على أنواع مختلفة من الصور مع اختلاف درجة تعقيدها. عملية التقسيم تم تطبيقها على كل نطاق من أنطقة الصور الملونة بالألوان الثلاثة (الأحمر، الأخضر، الأزرق)، وايضاً تم فحصها على الصور الملونة ذات الأنظمة التي تعتمد على (الشكل، الإشباع، شدة اللون) في تلوين الصور. وأظهرت النتائج بأن تقسيم نطاق شدة اللون في النوع الأخير من الصور الملونة يعطي نتائج مشابهة لتقسيم الأنظمة الملونة بالألوان الثلاثة (الأحمر، الأخضر، الأزرق)، وأظهرت النتائج بأن هنالك علاقة ما بين عمليات التخمين لإغلاق المناطق وعدد المناطق المقسمة حيث نحصل على نتائج جيدة عندما يكون عدد عمليات التخمين يساوي 2 وتم الحصول على هذه النتيجة بالتجربة. أظهرت أيضاً النتائج بأن أفضل قيمة لتوسعة المناطق ودمج النطاق المجاور تتراوح ما بين 1 الى 4 لكل مدى، للحفاظ على الصورة من التشويه.

خوارزمية جديدة أيضاً اقترحت باستخدام طريقة الفرق - المعدل لتحديد الحواف في الصورة، حيث أظهرت النتائج أن المستوى الأول من عملية التحويل كافٍ للحصول على نتائج جيدة، والحواف في الصورة تم تحسينها بعد ذلك باستخدام تقنية العتبة، متبوعة بعمليات التثخين لتحديد المناطق المغلقة، ثم تلوين الأجزاء بعد ذلك بألوان مختلفة لفصلها عن بعض.

صور العين الطبية تم تقسيمها باستخدام خوارزمتين مقترحتين؛ الأولى طبقت على صورة القزحية لتحديد حواف القزحية و البؤبؤ واستخراج أي اختلاف لوني فيها. هذه الخوارزمية طبقت على مصدرين مختلفين من الصور وأظهرت نتائج جيدة. وأن هذه الخوارزمية مفيدة عندما نريد أن نحدد منطقة الماء الأبيض في القزحية من صورة العين. الخوارزمية الثانية تتكون من مرحلتين؛ المرحلة الأولى استخدمت الخوارزمية المقترحة لتحديد الحواف والتي تعتمد على طريقة الفرق - المعدل والمرحلة الثانية تعتمد على رسم الدائرة لتحديد الجزء المطلوب و أظهرت هذه الخوارزمية نتائج جيدة لنوعين مختلفين من الصور، ولكن خلفية الصور يجب ان تحدد للحصول على نتائج جيدة باستخدام لون الخلفية الغامق.

خوارزمية جديدة اقترحت لتقسيم المناطق الملونة في الصور والتي تعتمد على تحديد الحواف ومناطق البذرة باستخدام طريقة تحويل الأمواج ذات البعدين. وفي هذه الخوارزمية الصور تم تحسينها باستخدام طريقة غاوسين قبل أن يتم تحويلها إلى المستوى الأول. والتشويه في الحواف يجب أن يزال باستخدام خوارزميات مورفولوجي كال. الخوارزمية المقترحة تم تطبيقها على أنواع مختلفة من الصور، وأظهرت النتائج أن خطوة تحسين الصور ضرورية لتقليل عدد مناطق البذرة وعدد المناطق الملونة والوقت المستهلك لتنفيذ الخوارزمية. وأظهرت النتائج بأن طريقة غاوسين من الممكن أن تعطي أفضل النتائج عندما تتراوح قيم الانحراف المعياري ما بين 1 و 3.5 غير ذلك سيتم تشويه الصورة. في هذه الخوارزمية العديد من عائلات الأمواج تم فحصها وأظهرت النتائج بان أفضل العائلات هي عائلة سمليت عند المستوى الأول لاستخراج الحدود.

Chapter One

Introduction and Literature Review

1.1. Introduction

Image processing consists of three main steps; the first is image acquisition from the world by using devices that capture it and convert it to binary data. The second step is manipulation, by using the specific algorithms in order to enhance it, segment the characters from it or compressing it ...etc, and the third step is display image after manipulation.

The first and the third step are performed by classical methods but the second step is performed by large number of algorithms and every day researchers are changing them or adding new algorithms.

1.2. Image Segmentation

Segmentation is a process in which an image is divided into different regions in order to isolate the areas of interest. Segmentation leads us, from unprocessed images, to obtain very high level of knowledge (Fondón et al.,2004).

Image segmentation is to divide the image into disjoint homogenous regions or classes, where all the pixels in the same class must have some common characteristics. We do this by translating the image into the feature space and try to find the boundaries between the different features. After that, we assign a color or label to each region or set of pixels that all have the same features. According to the nature of the image, the approach of segmentation may be either region-based approach, such as methods that find the boundary pixels of region of common features, or pixel-

based approaches, where the segmentation is done according to the pixels features such as pixel intensity (Jiasheng et al.,2006).

Segmentation is useful for image analysis -for which it is considered as an initial step, image indexing - using a signature, image compression - since homogeneous regions can be encoded more compactly. Regions of interest depend on the application of scene analysis, segmentation should delimit objects, or of document analysis, segmentation consists of separating text (words and characters), graphics and images, or of image indexing, segmentation should extract uniform (colored or textured) areas. Image segmentation is considered as a very difficult task, the main reasons for these difficulties are: there is no universal definition of objects or regions, real images suffer from several weaknesses (such as irregular illumination, shadows and reflections, objects with textured surfaces, noisy and blurred images, partially occluded objects) and Segmentation results are very sensitive to parameter choices. In most cases, segmentation should provide a set of regions having the following properties: connectivity and compactness, regularity of boundaries, homogeneity in terms of color or texture and differentiation from neighbor regions¹.

Edge detection is by far the most common approach for detecting meaningful discontinuities in intensity values, such discontinuities are detected by using first- and second-order derivatives. Edge detection plays important role in image segmentation. In many cases, boundary delineation is the ultimate goal for the image segmentation and a good edge detector can then fulfill the requirement of segmentation. On the other

¹ Rolf Ingold,2005, available: http://diuf.unifr.ch/courses/05-06/improc/slides/projections/09_Segmentation.pdf

hand, many segmentation techniques require an estimation of object edges for their initialization. So the final result of the segmentation method depends heavily on the accuracy and completeness of the initial edge map (Rajpoot and Rajpoot, 2003).

1.3. Image segmentation technique

Basically, the technique for image segmentation may be divided into four categories; (Gonzalez et al, 2002)

1.3.1.Thresholding techniques

Pixels are classified by comparing their values (intensity or other function) with one or several thresholds. Thresholds are determined by histograms and can be fixed globally, locally, dynamically. The choice of good thresholds is mandatory and it is determined perfectly if the histogram peaks are separated by deep valleys. We can use thresholding techniques when the regions are homogeneous or the objects and background have a strong contrast. But the thresholding is inappropriate when regions have an important gradient and regions are strongly textured.

1.3.2. Boundary Based Techniques.

These techniques use the assumption that pixel values change rapidly at the boundary between two regions. Edge detectors used in these techniques can be simple ones such as the Sobel or Roberts operators, or more complex ones such as the Canny operator. The output of most existing edge detectors can only provide candidates for the region boundaries, because these obtained color edges are normally discontinuous or over-detected. However, the actual region boundaries should be closed curves. Therefore, some post-procedures, such as edge tracking

, gap filling, smoothing, and thinning, should be performed to obtain the closed region boundaries. All of these post-procedures are very time-consuming; converting the edge candidates to the region boundaries is thus not an easy task. The time-consuming post-procedures can be avoided by integrating the results of the boundary-based approach and those of the region-based approach (Jiasheng et al.,2006).

1.3.3. Region- based techniques.

Region growing requires a seed to begin. A new segment is grown from the seed by assimilating as many neighboring pixels as possible that meet the homogeneity criterion. The resultant segment is then removed from the process. A new seed will be chosen from the remaining pixels. This continues until all pixels have been allocated to a segment. As pixels are aggregated, the parameters for each segment have to be updated. Thus the resulting segmentation could depend heavily on the initial seed chosen and the order in which neighboring pixels are examined. Ideally the seed would be a region, but it could be a single pixel.

1.4. The Wavelet Transform and Segmentation

Wavelets were first introduced to medical imaging research in 1991 in a journal paper describing the application of wavelet transforms for noise reduction in MRI images. Wavelet transforms have been successfully applied to many topics including tomographic reconstruction, image compression, noised reduction, image enhancement, texture analysis/segmentation and multi-scale registration. One important feature of wavelet transform is its ability to provide a representation of the

image data in a multi-resolution fashion (Din Yuen Chan et al, 2005).

Wavelets were developed independently in the fields of mathematics, quantum physics, electrical engineering, and seismic geology. Interchanges between these fields have led to many new wavelet applications such as image compression, turbulence, human vision, radar, and earthquake prediction (Gunawan, 2001). In 1987, wavelets were first shown to be the foundation of a powerful new approach to signal processing and analysis called Multiresolution. Multiresolution theory is concerned with the representation and analysis of signals or images at more than one resolution because the features that might go undetected at one resolution may be easy to spot at another (Tuduki, 2000).

1.5. Image Segmentation Application

Segmentation is one of the important fields in image analysis, and there are many applications which are based on segmentation of an object in an image such as:

1.5.1. Face Recognition

Face recognition has many potential uses, such as characterizing and retrieving mug-shots for police purposes, and in security systems. One approach to recognition is to create a statistical model of the human face, by analyzing the shapes, position and relationship between features for a large number of faces¹.

1.5.2. Inspecting Machined Parts

Inspection of machined parts often requires 3D information. One way to achieve this is to use laser striping. When a laser stripe is projected on to an object, it is

¹ Adrian F. Clark, 2005, available: <http://www.bmva.ac.uk/apps/inspection.html>

distorted by the object's shape and features. 3D information can be obtained by viewing the distortion through a pair of cameras. Combining the information from a series of stripes produces a 3D model. Segmentation techniques can be used to group together areas which distort the laser stripe in the same way. This allows the individual planes and features of the part to be identified¹.

1.5.3.Planning Radiation Therapy

When planning radiation therapy of brain tumours from MR scans of the head, it is necessary to apply the most effective dose of radiation to the tumour, yet cause least damage to the surrounding tissue. This is a complex task demanding 3D visualization. An interactive system is being developed to produce 3D representations of the head, by combining the information from a series of cross-sectional images. Segmentation techniques are used to semi-automatically identify the tumour and other anatomical structures. One approach is for the clinician to select a point within an area of interest, such as the tumour. The system then locates the surrounding points which possess similar characteristics, within a given range of variability².

1.5.4.Merging Medical Images

Different types of medical image yield different information. For example, MR scans provide soft tissue information, yet nothing regarding bones. The converse is true of computed tomography (CT) scans. When planning surgery, information from both CT and MR scans may be needed. Machine vision techniques can be used to collate information from the different scans, thus producing a single 3D image showing

¹ Adrian F. Clark, 2005, available: <http://www.bmva.ac.uk/apps/inspection.html>

² Adrian F. Clark, 2005, available: <http://www.bmva.ac.uk/apps/medical.html>.

the relationship between important features. This has been achieved, for example, by interactively labeling 12-16 matching features in the original images. Identifying tissue structures in the MR scan requires more sophisticated segmentation techniques¹.

1.5.5. Surveying by Satellite

Satellite images are a valuable source of information. Machine vision techniques can be used to produce 3D models of the earth's surface, yielding data useful for geological, geographical and environmental applications. 3D models can be produced from pairs of images taken from different angles. As the images are acquired by the SPOT satellite at different times, the quality of the two images may vary. For example, features such as clouds and jet contrails may appear on one image and not on the other. When producing a digital elevation model (DEM), these atmospheric features are excluded by using segmentation technique. Data from subsequent images can be used to fill these removed areas. By merging data in this way, greater accuracy can be achieved².

1.5.6. Number-Plate Identification

Machine vision techniques have made it possible to read the registration number of a vehicle from a video image. This technology can be used in many applications including stolen vehicle recovery and journey time analysis. This information can be used locally, or sent via communication channels to a database or control computer. Four stages of processing are involved. Firstly, the number-plate is

¹ Adrian F. Clark, 2005, available: <http://www.bmva.ac.uk/apps/medical.html>.

² Adrian F. Clark, 2005, available: <http://www.bmva.ac.uk/apps/rs.html>.

detected and located in the image by using edge detection technique. Next, the plate area is analyzed in detail, and regions that could be characters are extracted by using segmentation technique. The extracted characters are each then matched against a set of templates. The statistical results from this process are used in the final stage, where registration number formats and syntax rules are used to derive the output result¹.

1.5.7. Aerial Navigation

At present, the navigation of airborne vehicles relies on the use of active remote sensing equipment. These techniques are very expensive and an automated system to interpret aerial images, using passive image sensing, combined with machine vision techniques, is being developed. The system operates by identifying road networks and matching them with stored maps of the roads. The roads are identified by processing the image with computational filters that pick out road-like features. Further processing modifies the roads into a series of straight line segments. The characteristics and relationships between these segments can be compared with the stored map which has been similarly processed².

1.6. Statement of the Problem

In image processing, extracting features (edges, regions) from colored images is an important issue in many fields such as medical field, where many algorithms have been developed to extract such features.

¹Adrian F. Clark, 2005, available: <http://www.bmva.ac.uk/apps/surveillance.html>.

²Adrian F. Clark, 2005, available: <http://www.bmva.ac.uk/apps/transport.html>.

The segmentation is an important step in image analysis and there are many applications concerned with segmentation of object in an image, so if any error occurs during this step, the whole process will fail irremediably.

Automatic image segmentation is one of the fundamental problems of early computer vision. It is often the first and most vital step in an image analysis task. If any error occurs during this step, the whole process will fail irremediably, that is, effective segmentation can usually dictate the eventual success of the analysis. This is the reason why segmentation is a matter that has been studied by many researchers all over the world (Fondón et al.,2004).

The main objectives of this study are:

1. Develop a new technique for segmenting colored images based on regions growing algorithm and determine its seed regions automatically using canny edge detector.
2. Develop a new technique for extract edges from colored images based on different-averaging method and use it to segment medical images for human eyes.
3. Develop a new technique for segmenting colored images based on two-dimension wavelet transform and region growing algorithm.

1.7. Image acquisition

In this thesis the proposed segmentation techniques based on region growing algorithm are introduced, which were tested by using two kinds of images; the first is

the gray images and the second is the color image in order to verify the performance of the segmentation technique.

Different image types and content have been used; actually, by each developed technique, different set of images has been tested and used. However, the main types of images that have been used are: Medical images; especially for the human eyes and MRI for brain, geographical images for maps and morphological shapes.

All images in the thesis have been collected and acquired from different sources; Internet web sites and scanning images from books and magazines.

1.8. Literature Review

The historical review section consists of two sub sections that are: region growing and wavelets, which review the previous work in the field of image segmentation.

1.8.1. Region Growing

Theo Pavlidis and Yuh-Tay Liow, (1990): They suggested a method that combines region growing and edge detection for image segmentation. That started with a split-and-merge algorithm where the parameters have been set up so that an over - segmented image results. Then region boundaries are eliminated or modified on the basis of criteria that integrate contrast with boundary smoothness, variation of the image gradient along the boundary, and a criterion that penalizes for the presence of artifacts reflecting the data structure used during segmentation.

Pauwels et al, (1996): They proposed a new method to group edge-segments automatically (extracted from an image) into a fully connected line-drawing that based

on a region-growing algorithm which uses stochastically obtained geometric information to halt the region expansion.

Ikonomatakis et al, (1997): They suggested a seeded region growing and merging algorithm that was created to segment grey scale and color images. The approach starts with a set of seed pixels and from these grows regions by appending to each seed pixel those neighboring pixels that satisfy a certain predicate. Small regions of far away values were merged to neighboring regions while regions of similar values were also merged. Homogeneity functions are introduced for both grey scale and color images.

Wei and Cumming, (1999): they suggested a new region-growing algorithm for interferometer synthetic aperture radar (SAR) phases unwrapping.

Tuduki et al, (2000): They developed an automated seeded region growing algorithm for extraction of blood vessels from MRA data. That generated a binary images by thresholding the original MRA data to roughly obtain the images of blood vessels and then skeletons were generated from these images using the thinning algorithm based on the Euclidean distance transformation. Finally these skeletons were used as the seeds for region growing.

Cufi et al (2000): they suggested a proposal for the image segmentation problem, which has been based on the integration of edge and region information. That began by detecting the main contours of the scene, which are later used to guide a concurrent set of growing processes. And they suggested a new homogeneity criterion based on

clustering analysis and convex hull construction.

Potocnik and Zazula, (2000): They suggested an algorithm for ovarian follicle detection in ultrasound images. This fully automated recognition algorithm has been presented in this study. Initial homogeneous regions are determined. then, these initial regions are grown. Growing is controlled by average grey-level and by a newly introduced weighted gradient of the image.

Xiaohui et al,(2000): They suggested a region growing method for ultrasound image segmentation, that is performed in a multi-feature vector space. It developed three criteria for region growing control. First, instead of using the local information as do the conventional region growing methods, this method uses global information. Second, to overcome the effects of speckle noise and attenuation artifacts, a “geographic similarity” is used. Third, an equal opportunity competence criterion is employed to make results independent of processing order.

Jianping et al, (2001): they proposed an automatic image segmentation method. First, they have determined the color edges in an image by combining an improved isotropic edge detector and a fast entropic thresholding technique because it provides a major geometric structure in an image. After that the centroids between these adjacent edge regions are taken as the initial seeds for seeded region growing (SRG). These seeds are then replaced by the centroids of the generated homogeneous image regions by incorporating the required additional pixels step by step.

Rao and Gillies, (2001) : They suggested a technique that identifies first vortex centers in the velocity field, and then grows regions about these points using a criterion based

on the Jacobians evaluated at the candidate points, and the size and shape of the region already determined. A convexity constraint is also employed to enforce coherency in the resulting regions.

Shu-Yen and Nung, (2001): They suggested symmetric region-growing (SymRG) approach that is suitable for processing medical CT images. They reviewed the concept and definitions of SymRG and described its seed-invariant property and computational separability. These significant factors govern the region growing behavior (unidirectional region growing and inter-slice merging) and computational and memory-usage efficiency.

Wesolkowski and Fieguth,(2003): they suggested that each region is characterized using two parameters: within region color contrast and between region color contrast. The first parameter is the distance between the two most distant pixels in terms of color. The second parameter is the distance between the candidate pixel and its nearest neighbor in the region.

Cheng, (2003): Suggested a segmentation algorithm for color images based on a series of region growing and merging processes. This algorithm starts with the region growing process, which groups pixels into homogeneous regions by combining the 3-D clustering and relaxation labeling techniques. Each resulting small region is then merged to the region which was the nearest to it in terms of color similarity and spatial proximity.

Wan and Higgins, (2003): They defined a set of theoretical criteria for a subclass of region-growing algorithms that were insensitive to the selection of the initial growing

points. This class of algorithms, referred to as Symmetric Region Growing, leads to a single-pass region growing algorithm applicable to any dimensionality of images.

Xu and Shi, (2003): They proposed a new method for natural color image segmentation using integrated features. Edges were first detected in terms of the high phase congruency in the gray-level image. K-means cluster is used to label long edge lines based on the global color information to roughly estimate the distribution of objects in the image, while short ones were merged based on their position and local color differences to eliminate the negative affection caused by texture or other trivial features in image. This method unified edges, both the whole and local color distribution, as well as the spatial information to solve the natural image segmentation problem.

Hu et al, (2003): They suggested the adaptive region-growing algorithm to estimate the location of face region. So, they present a visual recognition system for interactively controlling a mobile robot. It first did, the robot identified the operator by human facial recognition, and then determined the actions analyzing the human hand gestures.

Fondón, (2004): They proposed a new method to segment colour images. It is based on a novel region growing technique whose tolerance step is automatically adapted to make the method useful and totally valid for all kinds of images.

Han et al, (2004) : They suggested a method to the segmentation of breast masses in digitized mammograms and it operated on the whole mammograms instead of manually selected regions. Pixels with local maximum gray levels were flagged as

seeds, from which many candidate objects were grown using modified region-growing technique. Then False Positive (FP) reduction using decision tree was applied to discard the normal tissue regions.

Camapum et al, (2004): They suggested a new system for automatic segmentation of images of clinical structures. That was based on multi-region growing followed by watershed transform. The main contributions were the method of seed pixels selection and predicate of the multi-region growing algorithm and the segmentation results achieved.

Wenlong et al, (2004): They suggested an automatic method to segment the Sylvain fissure (SF) from T1-weighted Magnetic Resonance (MR) images. That consisted of four steps. The First, morphological methods are applied to remove non-brain tissues. The second stage was 2D region growing used to segment the cerebral spinal fluid (CSF) and gray matter (GM) in the SF, in which spatial relationships are used to control the region growing. The third step is, to get 3D volume of the SF through segmenting CSF and GM slice by slice. The forth step, CSF in the SF is extracted incorporating the anatomical information on a constant cortex thickness.

Yu-Bu et al, (2005): They presented a region growing algorithm based on gradient magnitude for tumor segmentation from small animal PET images. And they proposed a region growing algorithm to extract tumor from adjacent regions with similar intensity values using gradient magnitude difference.

Din and et al, (2005): They proposed a fast wavelet-based color segmentation

(FWCS) technique and a modified directional region-growing (DRG) technique for semantic image segmentation.

Daw-Tung et al, (2006) : They suggested an effective model-based approach for computer-aided kidney segmentation of abdominal (CT) images with anatomic structure consideration. This automatic segmentation system expected to assist physicians in both clinical diagnosis and educational training.

Jiasheng et al,(2006) : They suggested a level set framework combined with region-growing algorithm for the segmentation of complicated structures from volumetric medical images. That reduced the computational complexity while the accuracy remains. This framework should also be suitable for other 3-D image segmentation that the region of interest to be segmented has a relatively large size in width, height or both.

Mendonca and Campilho, (2006): They suggested an automated method for the segmentation of the vascular network in retinal images. That starts with the extraction of vessel centerlines, which is used as guidelines for the subsequent vessel filling phase.

1.8.2.Wavelets Transform

Graps, (1995): explained the wavelets equations and viewed a historical perspective for wavelets and how they were performed at every interval, and he mentioned some of the applications of wavelets and how research can do wavelets in these applications.

Strickland and Hee, (1996): They developed a two-stage method based on wavelet

transforms for detecting and segmenting calcifications. The first stage based on an undecimated wavelet transform, which is simply the conventional filter bank implementation without down sampling, so that the low-low (LL), low-high (LH), high-low (HL), and high-high (HH) sub-bands remain at full size. Detection takes place in HH and the combination LH and HL.

Yanjiang and Baozong, (2000): They presented a method for the detection and localization of human eyes in a color image. The face-like regions located using an evolutionary color clustering algorithm. Then, wavelet decomposition was applied to each region to detect the possible facial features. If the features are distributed like a predefined human face model, the eyes can be located; otherwise, a three-layer BP neural network is used to check if there is an eye in the region.

Liming and Lenders, (2001): They presented an approach to detect human head boundary in plain background image using 2D Morlet continuous wavelet transform. And they utilized the rich edge information provided by continuous wavelet in various directions to detect the head boundary, and then fused this information to get the final result.

Gunawan, (2001): suggested a method for detecting micro calcification using wavelet transform based on statistical methods. Digitized mammograms were decomposed by using the wavelet transform without down sampling the process at several levels in the transform space. They applied the multiscale adaptive to improve the contrast enhancement of images, then skewness, kurtosis and box plot outlier were applied as

detection method of the previous modification image with a specific size of region of interest (ROI).

Leandro et al, (2001): They developed an approach based on the continuous wavelet transform using the Morlet wavelet to segment the blood vessels in retinal angiographic images. And they used shape analysis techniques for the detection and quantitative characterization of the vascular branching pattern in the retina, the wavelets would also be important with respect to performing fractal and multifractal image analysis.

Neyhart et al, (2001): They presented an image segmentation technique for identifying tissue and non-tissue regions of a digital x-ray images. The approach involves the generation of a segmentation mask developed by using discrete wavelet transform technique.

Mostafa et al, (2001): They developed Multiresolution algorithm that extends the well-known expectation maximization (EM). The proposed algorithm was based on generating scaled version of the original image using wavelet analysis. And they introduced an algorithm for image segmentation based on EM algorithm and it was based on a Multiresolution analysis of the image.

Mei, (2002): They developed an analytic model for segmentation of tumors which used Multiresolution analysis in concert with a Bayesian classifier to identify the possible tumors. The method choosed thresholds to segment tumors from background, by using multiscale analysis of the image probability function. A performance analysis based on a Gaussian distribution model was used to show the proposed adaptive threshold.

Jong et al, (2002): They suggested a method to detect a human skin region from a given head and shoulder image. That consisted of two stage: region segmentation and facial region detection. In the first stage the input image was segmented into an appropriate set of arbitrary regions using the wavelet – based watershed algorithm. In the second stage the facial regions were identified from the segmented results using a skin-color model.

Kurnaz et al, (2003): They suggested a feature extraction method for the segmentation of ultrasound images. They used Wavelet transform for determination of the textures in the ultrasound images. Elements of the feature vectors were formed by the wavelet coefficients at several decomposition levels. Incremental self-organized neural network (INeN) was proposed as the classifier.

Rajpoot and Rajpoot, (2003): They suggested an algorithm for unsupervised segmentation of hyperspectral human colon tissue cell images into its constituent parts by exploiting the spatial relationship between these constituent parts. That employed a modification of the conventional wavelet based texture analysis, on the projection of hyperspectral image data in the first principal component direction.

Jung, (2003): suggested a multiscale segmentation technique based on wavelet decompositions and watersheds. The wavelet transform was applied to the image, producing detail and approximation coefficients. The watershed is applied to the approximation image at a certain resolution 2^j , and projected up to higher resolutions using the inverse wavelet transform.

Leandro et al, (2003): They described a framework for automatic analysis of optic fundus non-Mydriatic images, focusing on the segmentation of the blood vessels by

using pixel classification based on pattern recognition techniques. They represented each pixel by a feature vector composed of color information and measurements at different scales taken from the continuous wavelet transform as well as from mean and order filtering applied to the green channel.

Zhu et al, (2004): They presented an efficient method for automatic segmentation of blood vessels in retinal images. A set of directional basis filters based on dyadic wavelet transform is designed to enhance blood vessels. That attempts to utilize the linear combination of the wavelet transforms to fix on the blood vessels directional information in retinal images. The directional maps are processed by thresholding scheme in order to segment blood vessels from the background. 2-D entropies are evaluated by the proposed thresholding approach based on the gray level-gradient co-occurrence matrix. The 2-D thresholding vector maximizes the edge class entropies selected. The thresholding method utilizes the gray level and gradient information in the enhanced image.

Amira and Farrell, (2005): They presented an automatic system based on wavelet transforms for face recognition. A range of wavelet decompositions together with different threshold types and segmentation algorithms had been implemented in order to investigate the best performances.

Chen and Liu, (2005): They first transformed the original image into a morphological gradient image by using morphology methods and treating it with an opening-closing filter bank to get a reference image with less noise interference; then they segmented the reference image by using the watershed algorithm. After that they merged the

segment field according to the test criterion with respect to the gray mean of the region boundary and the region area.

Haihua et al, (2005): They suggested an efficient segmentation method for medical image analysis which combines pyramidal image segmentation with hierarchical watershed segmentation algorithm. The segmentation procedure consists of pyramid representation, image segmentation, region merging and region projection. Each layer of pyramid was split into a number of regions by a root labeling technique, and the regions were projected onto next higher-resolution layer by reverse wavelet transform. The projection gradually was achieved onto full resolution layer so that segmentation was ended.

1.9.Outline of Thesis

The thesis is divided into the following five chapters:

- Chapter-1 a general description of the image segmentation and wavelets. Some of segmentation application was described. A literature review in region growing algorithm and segmentation using wavelet transform was introduced.
- Chapter-2 presents concepts of segmentation technique and the basic region growing algorithm. It also presents a new algorithm to segment regions in an image, which is based on determining seed regions in an image. This chapter shows also the results of applying algorithm on different sources of images complexity.
- Chapter 3 presents the concept of wavelet transform and two-dimension wavelet transform. It also presents a new algorithm using wavelet applied to determine the image edges by using wavelet. It also presents two algorithms of segmentation, the

first algorithm is applied on iris image to determine edge of iris, pupil and extract any different color region on it. The second algorithm consists of two stages, the first stage uses the wavelet to determine the highlight region, and the second stage based on drawing a circle to determine object.

- Chapter 4 presents a new approach to segment color regions in an image that is based on determining edges and seed regions by using two-dimension wavelet transform. After that, applying region growing algorithm to extract regions and color it with specific color.

- Chapter 5 presents conclusions and future work.

Chapter Two Image Segmentation

2.1.Introduction

Segmentation is a process in which an image is divided into different regions in order to isolate the areas of interest on it . Segmentation leads us, from unprocessed images, to obtain a very high level of knowledge (Bogdan et al, 1997).

Color image segmentation is a process of extracting from the image domain one or more connected regions satisfying uniformity (homogeneity) criterion which is based on features derived from spectral components. These components are defined in a chosen space colour space model. The segmentation process could be augmented by some additional knowledge about object in the scene such as geometric and optical properties (Gonzalez et al, 2002).

Segmentation is one of the important fields in image analysis. There are many applications based on object extraction from an image such as face recognition which is concerned with human face by analyzing human face shapes, position and relationship between features for a large number of faces. And also, there are many applications, such as inspecting machined parts, planning radiation therapy, merging medical images, surveying by satellite, number-plate identification and aerial navigation.

2.2. Segmentation Technique

In image segmentation the problem of developing automatic segmentation procedures has always been and still is of great interest. The existing automatic

segmentation methods are generally associated with some particular applications where 'a priori' information about the result of the segmentation is known (Zheng et al, 2001).

Region-based segmentation algorithms postulate that neighboring pixels within the same region have similar intensity values, of which the split-and-merge technique is probably the most well known. The general procedure is to compare a pixel with its immediate surrounding neighbors. If a criterion of homogeneity is satisfied, the pixel can be classified into the same class as one or more of its neighbors. The choice of homogeneity criterion is therefore critical to the success of the segmentation (Sophie et al, 2004).

Some region growing methods use edge as a growth-stopping condition, and the growing seeds are selected manually. The growth occurs in the homogenous intensity regions and stops at the edges. If there are broken edges then the segmentation is incorrect (Slobodan and Branislav, 2000).

Seeded region growing algorithm (SRG) is a new approach which is based on conventional postulate of region growing algorithms where the criteria of similarity of pixels is applied, but the mechanism of growing regions is closer to the watershed algorithm. Instead of controlling region growing by tuning homogeneity parameters, SRG is controlled by choosing a usually small number of pixels, known as seeds. These seed pixels are chosen by user according to his / her own opinion of what regions to extract on the image (Yinpeng et al, 2000).

2.3. Color Spaces (Models)

Every image is represented by color models, which is a specification of a coordinate system and subspace within that system, where each color is represented by a single point. There are common color models used today, which are : RGB (red, green, blue) , CMY (cyan, magenta, yellow), CMYK (cyan, magenta, yellow, black) and HSI (hue, saturation, intensity) (Gonzalez et al, 2002).

2.3.1.RGB Color Model

In RGB Model, each color appears in its primary spectral components of red, green and blue. This model is based on a Cartesian coordinate system. The color space of interest is the cube shown in figure (2.1), in which RGB values are at three corners; red, green and blue. Black is at the origin and white is at the corner farthest from the origin. The gray scale extends from black to white along the line joining black corner and white corner.

Some of the advantages of RGB color model are that it is suited for hardware implementation and it matches nicely with the fact that the human eye is strongly perceptive to red, green, blue primaries (Gonzalez et al, 2002).

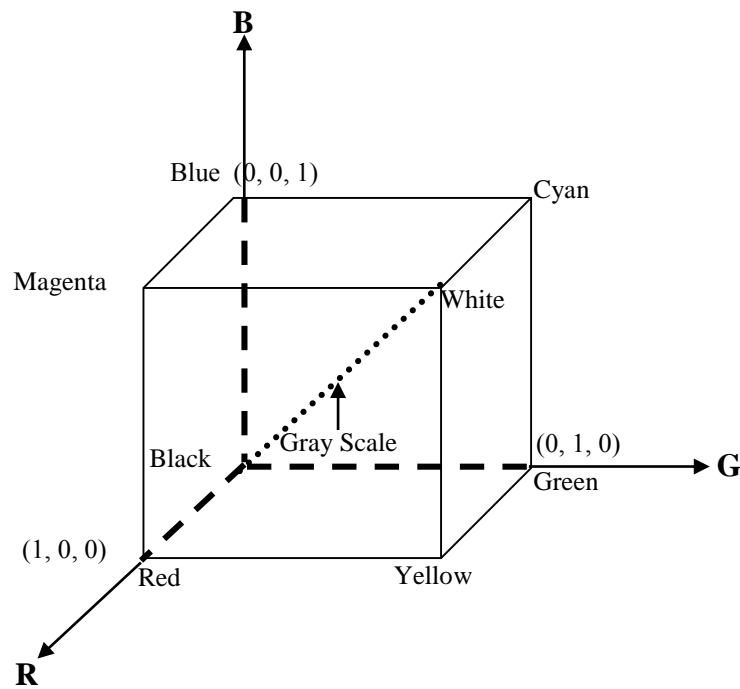


Figure (2.1) : Schematic of the RGB color cube.

2.3.2. The HSI Color Model

The characteristics generally used to distinguish one color from another are brightness, hue and saturation. Brightness embodies the achromatic notion of intensity. Hue is an attribute associated with the dominant wavelength in a mixture of light waves. Saturation refers to the relative purity or the amount of white light mixed with a hue (Gonzalez et al, 2002).

The HSI (hue, saturation, intensity) color space, decouples the intensity components from color-carrying information (hue, saturation) in a color image. It is an ideal tool for developing image-processing algorithms based on color descriptions that are natural and intuitive to humans, who are the developers and users of these algorithms (Gonzalez et al, 2002).

2.3.3. Converting Colors From RGB Model to HSI Model

To convert image from HSI model to RGB model, the image (Gonzalez et al, 2002) should be normalized to the range [0 , 1]. And then, apply the following equations:

$$H = \begin{cases} \theta & \text{if } B \leq G \\ 360 - \theta & \text{if } B > G \end{cases} \quad \dots(2.1)$$

With

$$\theta = \cos^{-1} \left\{ \frac{\frac{1}{2}[(R-G) + (R-B)]}{[(R-G)^2 + (R-B)(G-B)]^{1/2}} \right\} \quad \dots(2.2)$$

$$S = 1 - \frac{3}{(R+G+B)} [\min(R, G, B)] \quad \dots(2.3)$$

$$I = \frac{1}{3}(R+G+B) \quad \dots(2.4)$$

Where :

R : Red band in RGB model.

G: Green band in RGB model.

B: Blue band in RGB model.

H: Hue band in HSI model.

S: Saturation band in HSI model.

I: Intensity Band in HSI model.

2.4. Image Segmentation

Image segmentation is subdividing an image into its constituent parts, regions or object. So to perform this objective we should deal with image based on two gray

value properties: discontinuities and similarity. In the first category, the approach is to partition an image based on abrupt changes in intensity, such as edges in an image. The principal approaches in the second category are based on partitioning an image into regions that are similar according to a set of predefined criteria (Gonzalez et al, 2002).

2.4.1.Intensity Discontinuities Category

There are three basic types of intensity discontinuities in digital image: points, lines and edges. The most common way to look for discontinuities is to run a mask through the image so that, the center of mask move from point to point in an image.

2.4.1.1.Point Detection

The detection of isolated points embedded in areas of constant or nearly constant intensity in an image is performed by using the mask as shown in figure (2.2).

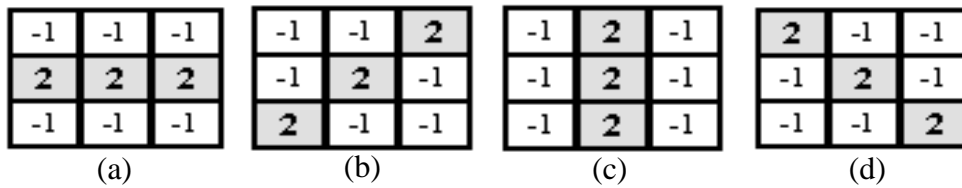
-1	-1	-1
-1	8	-1
-1	-1	-1

Figure (2.2): A mask for Point detection.

The isolated point has been detected at the location on which the mask is centered if $|R| \geq T$. Where T is a nonnegative threshold.

2.4.1.2.Line Detection

The masks in figure (2.3) are used to detect lines in an image. So that, if the center point in the image, $|R_i| > |R_j|$, for all $j \neq i$, that point is said to be more likely associated with a line in the direction of mask i.



(a) : the horizontal line mask.
 (b) : the line mask that is oriented by +45 degree.
 (c) : the vertical line mask.
 (d) : the line mask that is oriented by -45 degree.

Figure (2.3) Line detector masks.

2.4.1.3.Edges Detection Using Canny Edge Detector

Edges characterize boundaries and are therefore a problem of fundamental importance in image processing. Edges in images are areas with strong intensity contrasts. The Canny edge detection algorithm is known to many as the optimal edge detector. The algorithm steps are as follows (Gonzalez et al, 2002):

1. The image is smoothed using a Gaussian filter with a specified standard deviation, σ , to reduce noise. By applying the following :
 - a. Create array of one-dimension whose length equals N (represents the possible width of Gaussian filter) and fill it with value from 1 to N.

$$A = \begin{array}{c} \text{index} \quad 1 \quad 2 \quad \dots \quad N \\ \begin{array}{|c|c|c|c|} \hline 1 & 2 & \dots & N \\ \hline \end{array} \end{array}$$

- b. Produce the array R, which has the results of the following equation, after applying it on each cell of A.

$$R_i = e^{-(A_i)^2 / 2\sigma^2} \quad \dots(2.5)$$

Where:

i : index of array R (1 to N).

A: array produced in step (a).

σ : Standard deviation of the pixels intensity values.

e: exponential value.

- c. Find *width* which is the maximum index of array R whose value is greater than *GaussianDieOff*, Otherwise the *width* will be equal 1 because the entered standard deviation is very small.
- d. Design the Gaussian one-dimension filter, by applying the following equation:

$$gau = \frac{e^{-t^2 / 2\sigma^2}}{2\pi(\sigma)^2} \quad \dots(2.6)$$

Where:

t : One dimension of array, whose values are from – *width* to +*width* (width which is produced in step c).

σ : Standard deviation of the pixels intensity values.

e: exponential value.

- e. Find the directional derivative of 2D Gaussian (along X-axis). By applying the following equation:

$$D_{gau2d} = -x \frac{e^{-(x^2+y^2)/(2\sigma^2)}}{\pi\sigma^2} \quad \dots (2.7)$$

Where:

x: two-dimension array. Number of columns and rows equal

$width - (-width) + 1$ and the first column has value $-width$, the second column has value $-width + 1$ and third has value $-width+2$ until the last column equal the value $width$.

y: two-dimension array. Number of columns and rows equal

$width - (-width) + 1$ and the each column has value from $-width$ to $width$.

- f. Smooth the image by running the *gau* across rows and then across columns

2. Compute the local gradient, whose equation is

$$g(x, y) = [G_x^2 + G_y^2]^{1/2} \quad \dots (2.8)$$

G_x is computed by running the *Dgau2d* through image which is produced in (step 1.f).

G_y is computed by running the *Dgau2d* through image which is produced in (step 1.f), after replacing column by the corresponding row.

3. The edge points determined in step 2 give rise to ridges in the gradient magnitude image. The algorithm then tracks along the top of these ridges and sets to zero all pixels that are not actually on the ridge top so as to give a thin line in the output, a process known as *non-maximal suppression*. The ridge pixels are then thresholded using two thresholds T1 and T2, with $T1 < T2$. Ridge

pixels with values greater than T2 are said to be "strong" edge pixels. Ridge pixels with values between T1 and T2 are said to be "weak" edge pixels (Gonzalez et al, 2002).

4. Finally, the algorithm performs edge linking by incorporating the weak pixels that are 8-connected to the strong pixels.

2.4.2.Intensity Similarity Category

The main idea here is to classify a particular image into a number of regions. Thus for each pixel in the image we need to somehow decide or estimate which regions it belongs to.

2.4.2.1.Basic Formulation

Let R represent the entire image region, then segmentation is viewed as a process that partitions R into n sub regions R_1, R_2, \dots, R_n . (Gonzalez et al, 2002), such that:

$$(a) \bigcup_{i=1}^n R_i = R.$$

(b) R_i is a connected region, $i = 1, 2, \dots, n$.

(c) $R_i \cap R_j = \phi$ for all i and j, $i \neq j$.

(d) $P(R_i) = \text{TRUE}$ for $i = 1, 2, \dots, n$.

(e) $P(R_i \cup R_j) = \text{FALSE}$ for any adjacent regions R_i and R_j .

2.4.2.2.Region Growing

Region growing is a procedure that groups pixels or sub-regions into larger regions based on predefined criteria for growth. The basic approach is to start with a set of

"seed" points and from these grow regions by appending to each seed those neighboring pixels that have predefined properties similar to the seed (Gonzalez et al, 2002). So the basic region growing may be performed by the following:

1. Determine seed point value in an image, If the number of seed point value equals 1, then you would find any pixel in an image equal to this seed point value; mark it as seed point also. Otherwise the seed point value may be an array, so you should shrink it until the closed area becomes a point and un-closed area becomes rings, after that, mark this point as seed point.
2. Create a black image the size of the original image.
3. Subtract each seed point value from all pixels of original image (take absolute of result) and then if the result is less than or equals T (Threshold value) then mark the same pixel in black image as white pixel.
4. Repeat step 3 for all seed point values and each time concat a black image with previous black image.

2.5.The Proposed First Technique For Color Image Segmentation to the RGB and HSI Model Based on Region Growing Algorithm

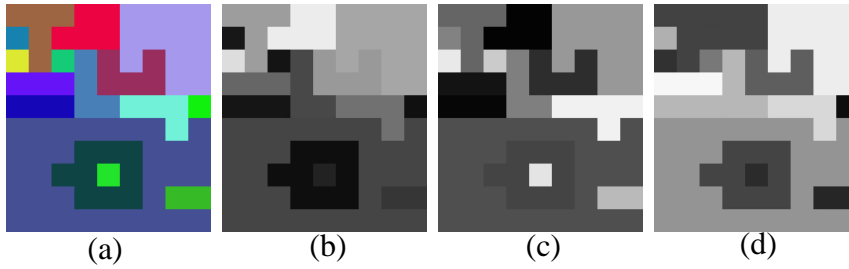
The region growing algorithm usually uses seed point to grow the regions. The seed point is determined either manually (by user) or automatically. Figure (2.4) shows the basic steps of the proposed first technique to determine the seed region.

- Step 1 Split the three bands of the (RGB) image
- Step 2 Canny mask applied on the selected band to
 obtain edges
- Step 3 Closing area by dilation
- Step 4 Determine the closed areas in the image (seed
 regions).
- Step 5 Determine the maximum and the minimum
 intensity values for every seed regio
- Step 6 Re-arrange seed regions from the largest to the
 smallest seed regions
- Step 7 Merge seed region with the neighbor pixels
 region.
- Step 8 Delete pixels which are found in more than one
 region from the smallest regions.
- Step 9 Color the regions
- Step 10 Repeat the previous steps to the other bands

Figure (2.4): steps for proposed first technique to the region growing by using seed regions

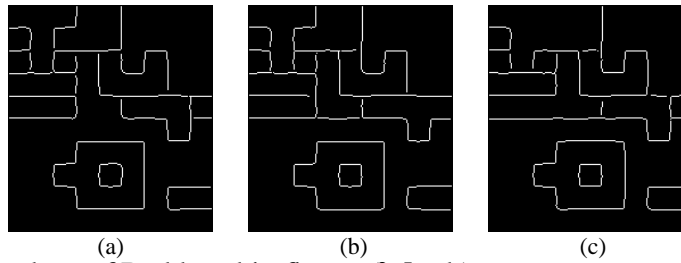
The detailed steps for the proposed first technique are:

Step1: Split the RGB bands of the image as shown in figure (2.5), each band has different appearance from the other bands.



(a) original image. (b) Red band. (c) Green Band. (d) Blue band.
 Figure (2.5): Splitting the three bands of the RGB image

Step 2: Apply canny mask to each band to determine regions edge, as shown in figure (2.6). Experimentally the canny mask gave us the best results of edge detection compared with the other methods of edge detection.



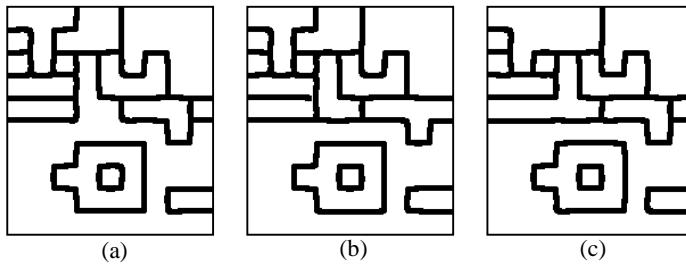
(a) edges of Red band in figure (2.5 - b).
 (b) edges of Green band in figure (2.5 - c).
 (c) edges of Blue band in figure (2.5 - d).

Figure (2.6). The results which are produced by applying edge Canny detector on bands of images.

Step3: Apply dilation operation to the connect areas. The canny mask is not always joining edges with others, so the dilatation operation joins edge of the areas and delete any disconnect pixels on the edges (Gonzalez et al, 2002).

$$A \oplus B = \{z | (\hat{B})_z \cap A \neq \phi \} \quad \dots(2.9)$$

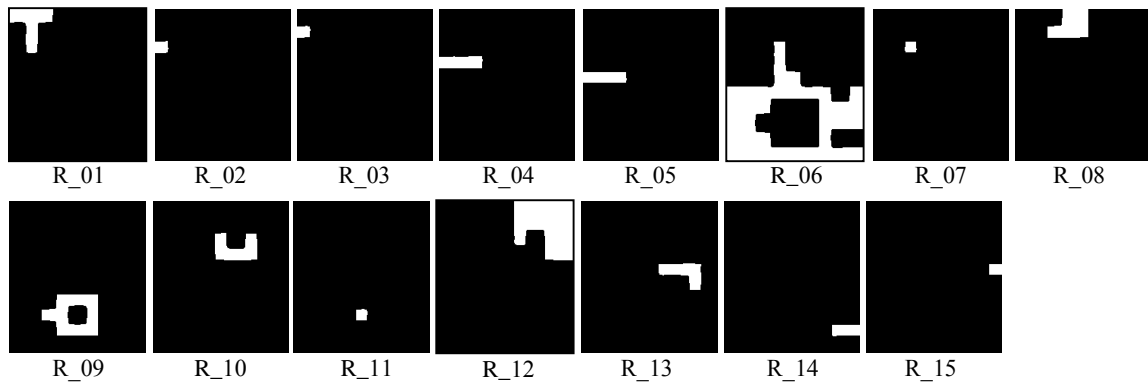
and the following figure (2.7) shows the result of dilation operation for image in figure (2.6).



- a- applying dilation to the image in figure (2.6 -a).
- b- applying dilation to the image in figure (2.6 -b).
- c- applying dilation to the image in figure (2.6-c).

Figure (2.7): Edge detection to the three bands is different by applying Dilation

Step 4: Split each closed area in a separate image, as shown in figure (2.8), these regions are called seed regions, the number of seed regions are (15), which produced (15) seed region images, to the red band image in figure (2.7-a).



Figure(2.8): Seed regions of red band in figure (2.7-a), marked from R_01 to R_15.

Every region in figure (2.8) represents a closed area in figure (2.7 – a) so they are separated to be a seed region.

Step 5: Find the maximum intensity value and the minimum intensity value for every seed region of the image in figure (2.5).

Step 6: Re-arrange seed regions from the largest area seed region to the smallest area seed region. This step is important for region growing processing, because there are pixels that may be set in two or more regions by re-arranging regions, the algorithm set them in the largest region always.

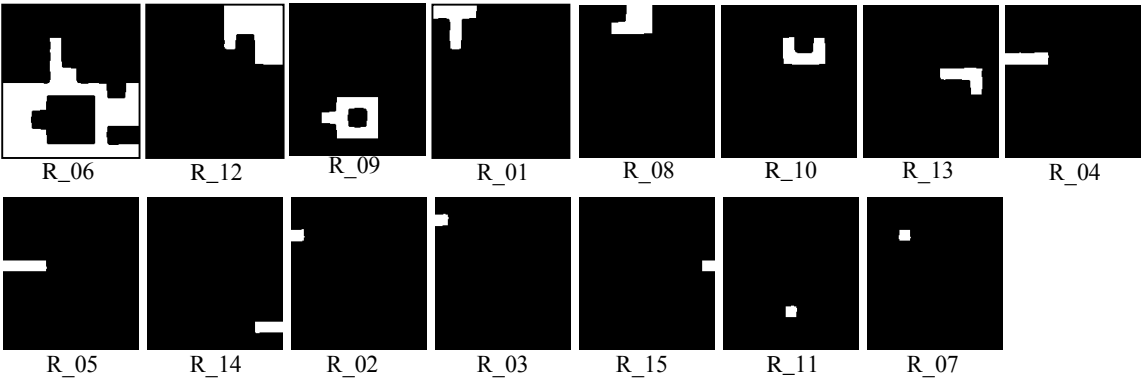
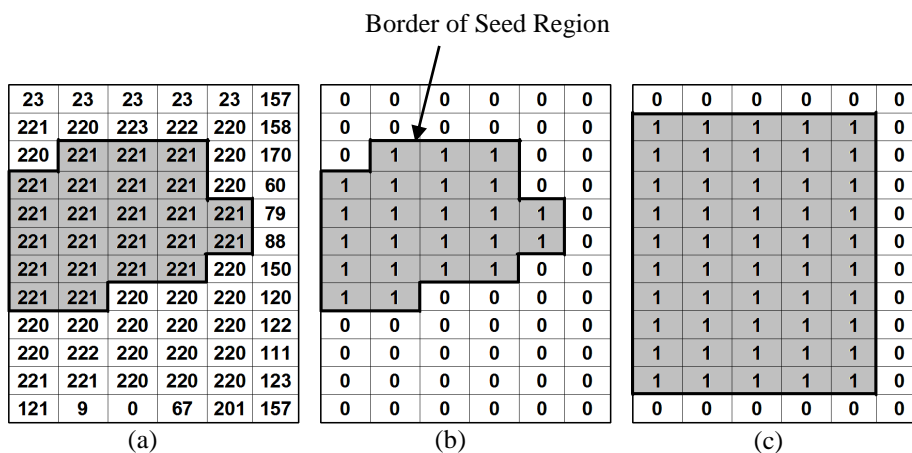


Figure (2.9): Re-arrange the images in figure (5).

Step 7: Merge seed region with every neighbor pixels whose intensity is between the (maximum intensity value + value of expand interval) and (minimum intensity value - value of expand interval). The value of expand interval is a constant value that is added to right bound of interval, which represents the maximum intensity value of seed region, and subtracted from left bound of interval, which represents the minimum intensity value of the seed region.

Figure (2.10-a) represents an array of intensity values which has a seed region marked by black border line and this array represents a band of image. So the merge seed region processes are done as follows:

- Mark each pixel by 1 if it sets at seed regions otherwise mark pixel by 0, as shown in figure (2.10 - b).
- Check the (8) pixels neighbors, which are marked by 0, if the corresponding intensity value is less than or equal to the seed region, and greater than or equal to the (minimum intensity value - value of expand interval) of seed region then merge this pixel and mark it by 1 otherwise mark it by 0.
- Repeat step b until there is no pixel marked by 1. The value of the seed region is 221, the algorithm merges pixels 221 ± 2 as shown in figure (2.10-c).



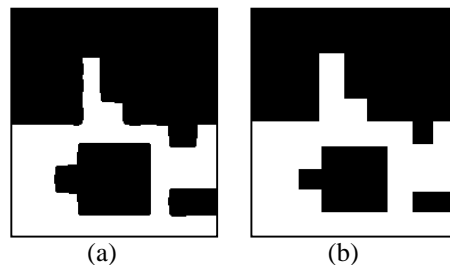
a- Initial seed region with true values of the pixels.

b- Initial seed region.

c- The result of merging seed region after iteration.

Figure (2.10): Merge seed region with neighboring pixels.

Figure (2.11), showing the result of merging process for region R_06.



a- before merge

b- after merge

Figure(2.11): The difference between region before and after merge process, for region R_06.

Step 8: Delete every pixel which sets in more than one region from all regions except the largest one. Because when the algorithm merges, seed regions and pixels may set pixel in more than one region.

Step 9: color each of region with blue color and at the same time color other regions with black color, repeat this step until all regions are colored with blue color.

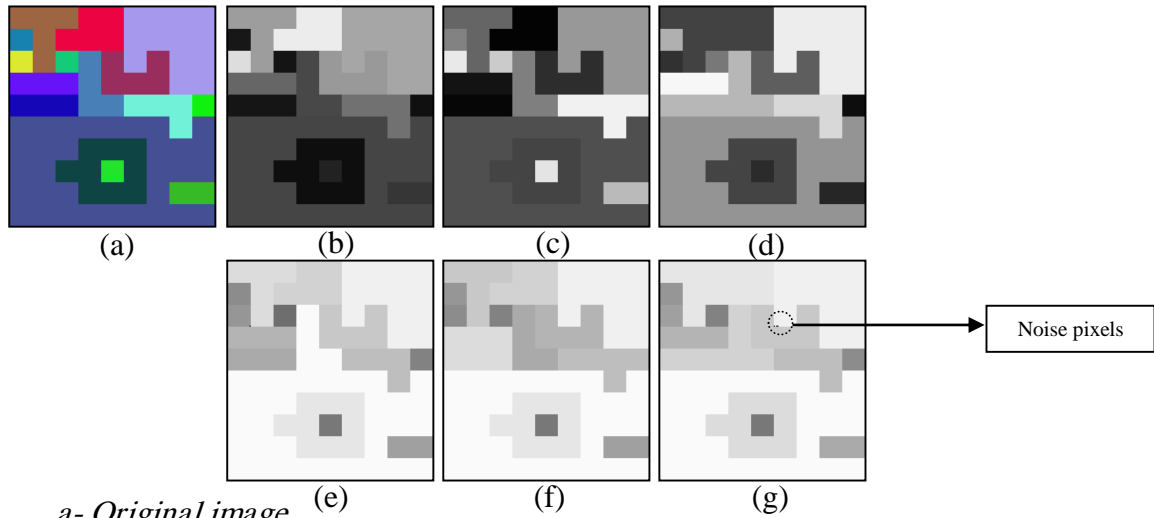
Step 10: Repeat steps from 1 to 9 on the bands of the colored image.

2.6.Implementation and Results

The first proposed technique applied to the two different images coordinated the RGB and HSI images.

2.6.1.RGB Image Segmentation

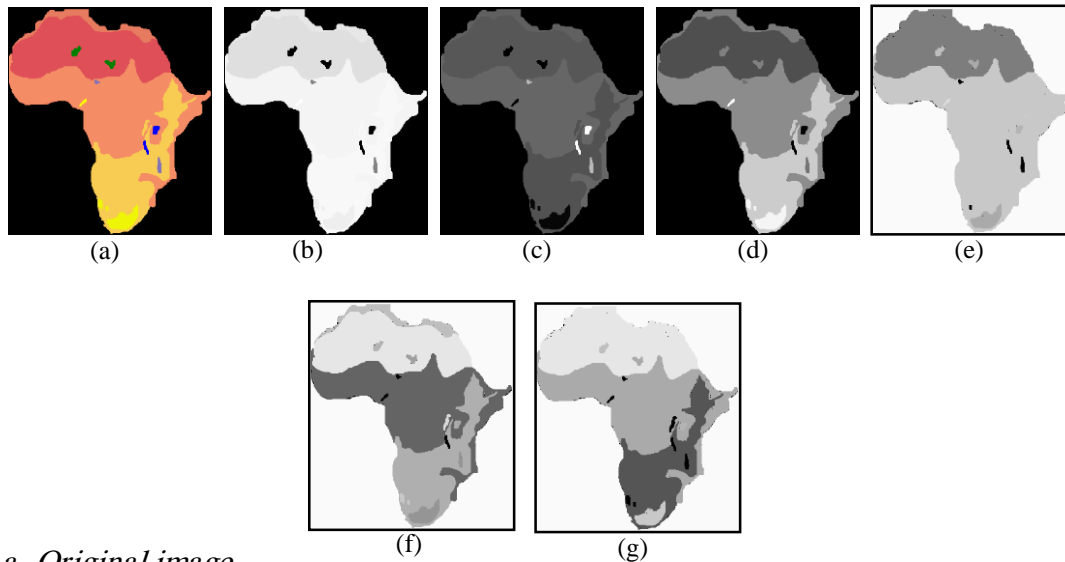
The first proposed technique was applied to the single band enhanced images (enhancement used as a preprocessing before segmentation), the algorithm gave a perfect result and it could find the noisy pixels which are colored by the black color, as shown in the Figure (2.12).



- a- Original image*
- b- Red band*
- c- Green band*
- d- Blue band*
- e- Segmentation to the Red band image*
- f- Segmentation to the Green band image*
- g- Segmentation to the Blue band image*

Figure (2.12): Segmentation to the three bands of the image

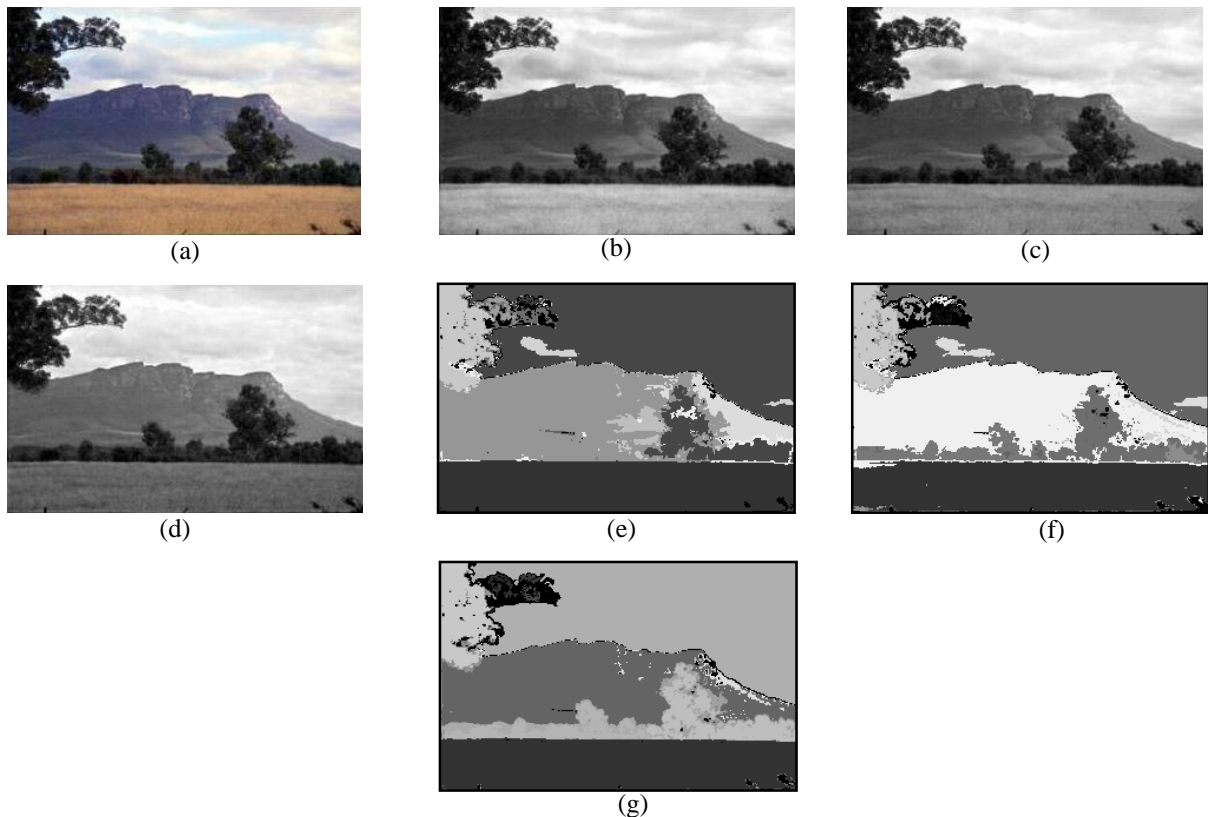
Figure (2.13) shows another application of the technique to the map of Africa, which shows a good result. There are small regions colored with black color, because these regions are very small, and the dilation process can not be applied, because they are originally closed region area, and we can not determine a border to these regions, because as we mentioned they are very small regions.



- a- Original image.*
- b- Red band image.*
- c- Green band image.*
- d- Blue band image.*
- e- Segmentation to the Red band image.*
- f- Segmentation to the Green band image.*
- g- Segmentation to the Blue band image.*

Figure (2.13): Segmentation to the Africa map

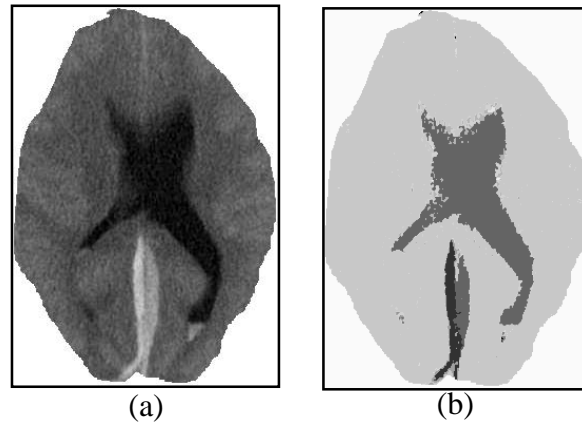
In the photo image, there are a lot of areas with different colors; the algorithm was tested using the image shown in figure (2.14), the algorithm shows that it also gives good result to complex images.



a- original image. b- Red band image. c- Green band image. d- Blue band image. e- Segmentation to the Red band image. f- Segmentation to the Green band image. g- Segmentation to the Blue band image.

Figure (2.14): Segmentation to the photo image.

The medical images also tested by the proposed first technique. Figure (2.15) shows the brain image before and after segmenting by the technique. In most medical images the three bands of RGB model in image are similar, so we show only one band of the brain image, figure (2.15-b) shows the image after segmentation to the red band.



(a) Original image.
 (b) Segmentation to the red band of the image.

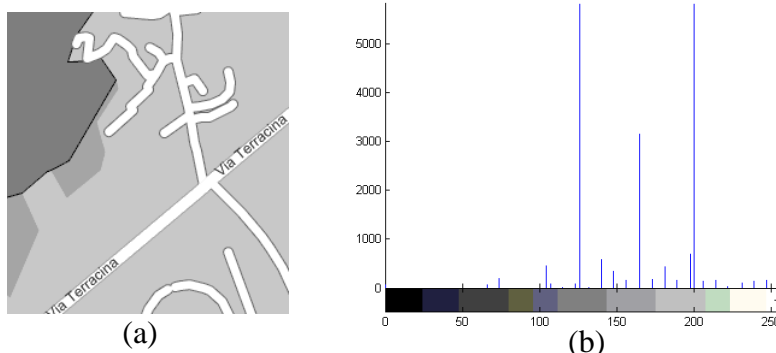
Figure (2.15): Brain image segmented

The first proposed technique also was tested using the map image in figure (2.16) the algorithm shows that it also gives good result to these images.



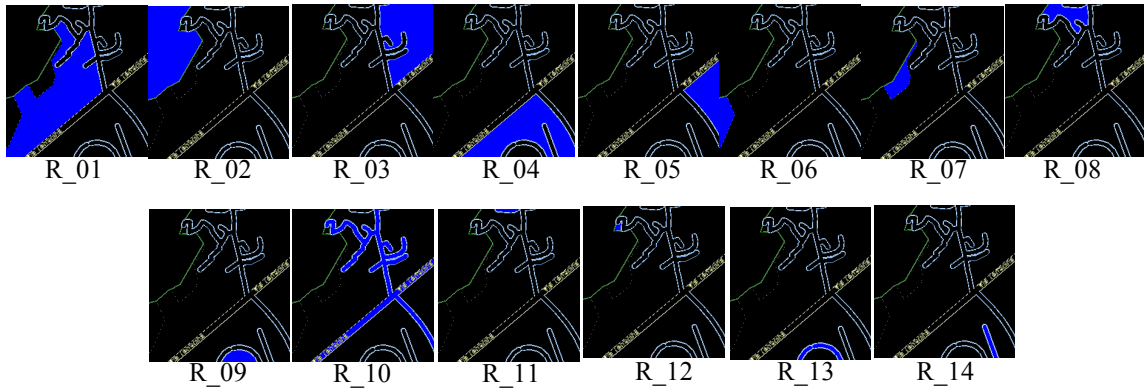
Figure (2.16): City map image.

Figure (2.17) shows the red band of the city map image and its histogram.



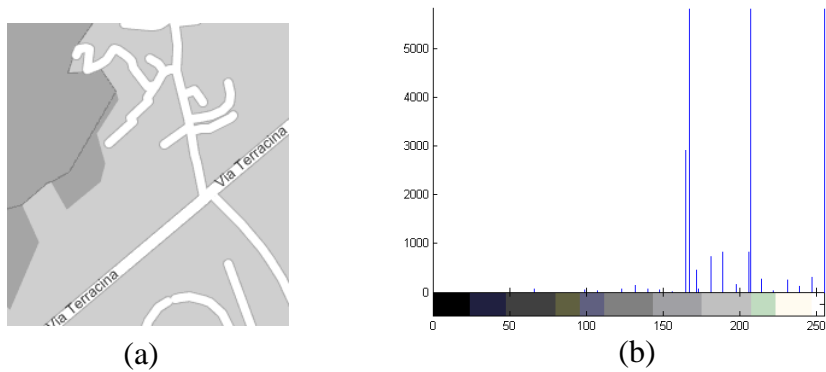
(a) Red band of the city map image. (b) Histogram of red band.
 Figure (2.17): Red band of the city map image and its histogram

Figure (2.18) shows the regions of red band of city map image after segmentation.



*R_01 to R_14: regions of segmented image of red band of city map image.
Figure (2.18): Regions of segmented image for red band of city map image.*

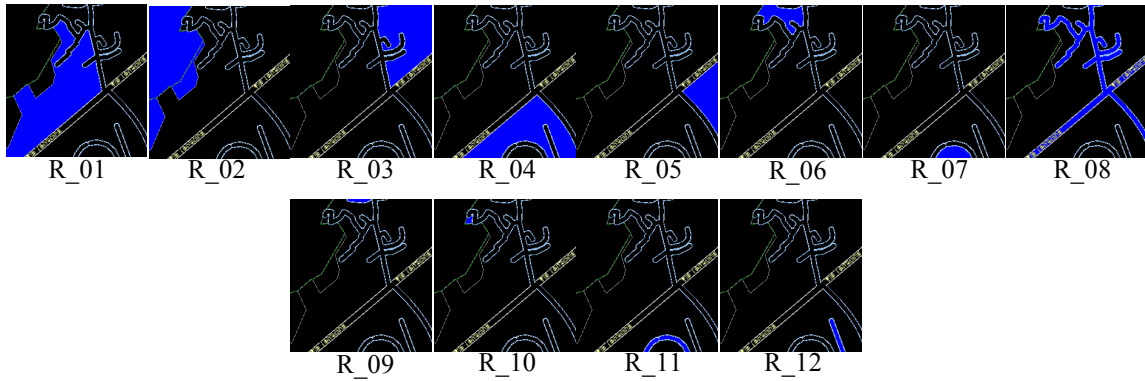
Figure (2.19) shows the green band of city map image and its histogram.



*(a) Green band of city map image. (b) Histogram of green band.
Figure (2.19): Green band of city map image and its histogram*

Figure (2.20) shows the regions of green band of city map image after segmentation.

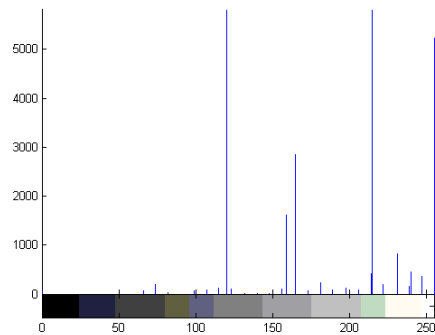
Figure (2.21) shows the blue band of city map image and its histogram.



*R_01 to R_12: regions of segmented image of green band of city map image.
Figure (2.20): Regions of / map image.*



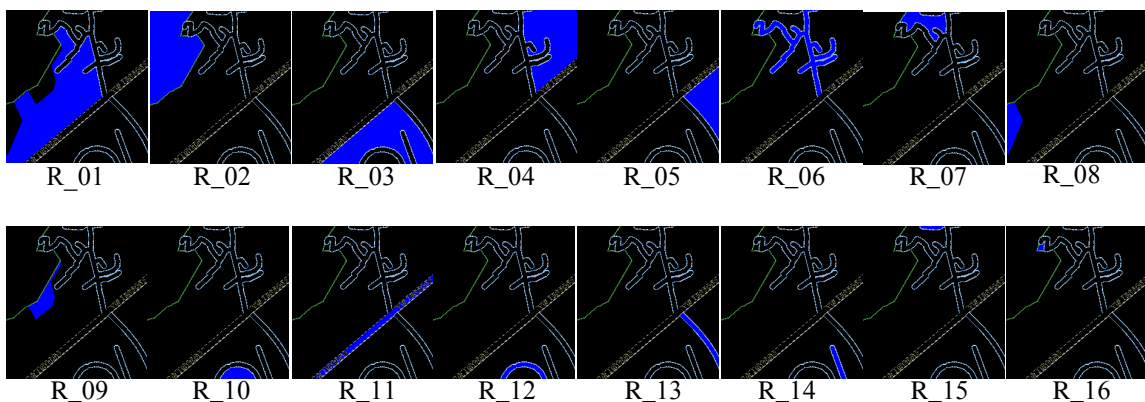
(a)



(b)

*(a) Blue band of city map image. (b) Histogram of Blue band.
Figure (2.21): Blue band of city map image and its histogram*

Figure (2.22) shows the regions of blue band of city map image after segmentation.



*R_01 to R_16: regions of segmented image of blue band of city map image.
Figure (2.22): Regions of segmented image for blue band of city map image.*

Table 2.1 shows the intensity range of each segmented region to the three bands.

Table 2.1: Intensity Ranges of Segmented Image of the City Map Image.

Region No	Range of segmented red band		Range of segmented green band		Range of segmented blue band	
	From	To	From	To	From	To
R_01	198	202	205	209	213	217
R_02	124	128	165	169	118	122
R_03	179	202	205	209	213	217
R_04	196	202	205	209	213	217
R_05	196	202	205	209	213	217
R_06	163	167	205	209	253	255
R_07	163	167	205	209	213	217
R_08	198	202	245	255	163	167
R_09	198	202	253	255	163	167
R_10	245	255	205	209	213	217
R_11	253	255	253	255	157	161
R_12	198	255	253	255	253	255
R_13	253	255	-	-	253	255
R_14	253	255	-	-	253	255
R_15	-	-	-	-	253	255
R_16	-	-	-	-	213	217

The proposed first technique supposes that:

Intensity range of region A is $[L_A \text{ to } R_A]$.

Intensity range of region B is $[L_B \text{ to } R_B]$.

Where:

L_A : is left side of intensity range of region A.

R_A : is right side of intensity range of region A.

L_B : is left side of intensity range of region B.

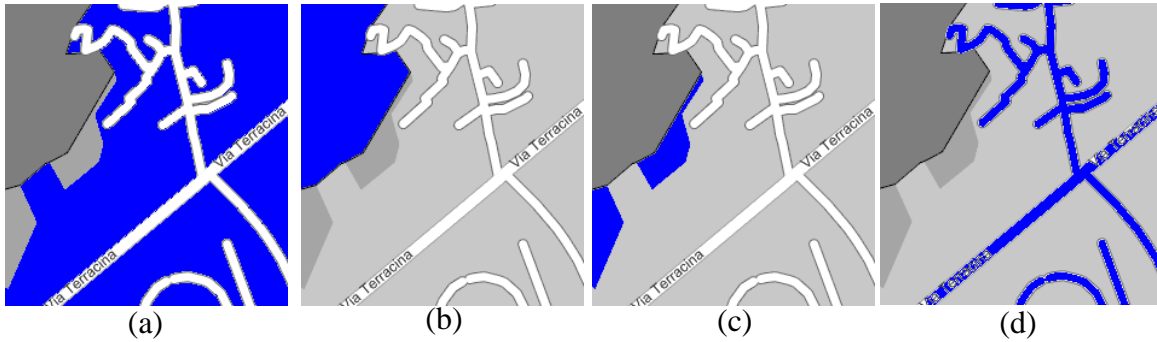
R_B : is right side of intensity range of region B.

Then

Region A is similar to region B if

$$L_A = L_B \quad \text{Or} \quad R_A = R_B$$

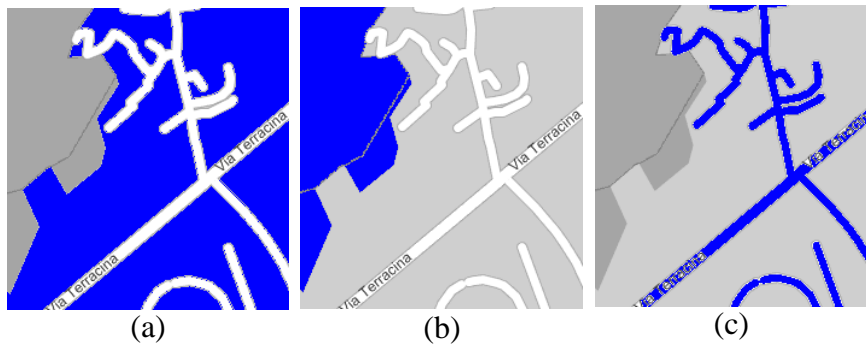
Figure (2.23) shows the similar regions in the red band of the city map image grouped together and, it is colored with blue color.



- (a): Regions whose right side of intensity range is 202 or left side is 198.
 (b): Region whose its intensity range is 124 to 128.
 (c): Regions whose left side of intensity range is 163.
 (d): Region whose right side of intensity range is 255.

Figure (2.23): The red band regions segmentation to the city map image colored with

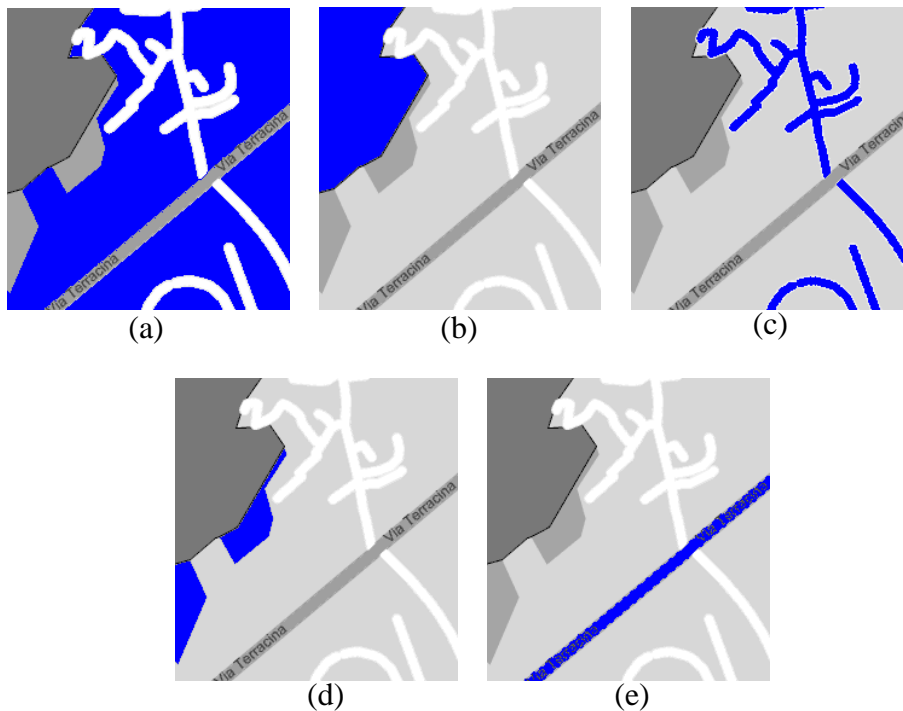
Figure (2.24) shows the similar region in the green band of map image grouped together, and are colored with blue color.



- (a): Regions whose intensity range is 205 to 209.
 (b): Region whose intensity range is 165 to 169.
 (c): Region whose right side of intensity range is 255.

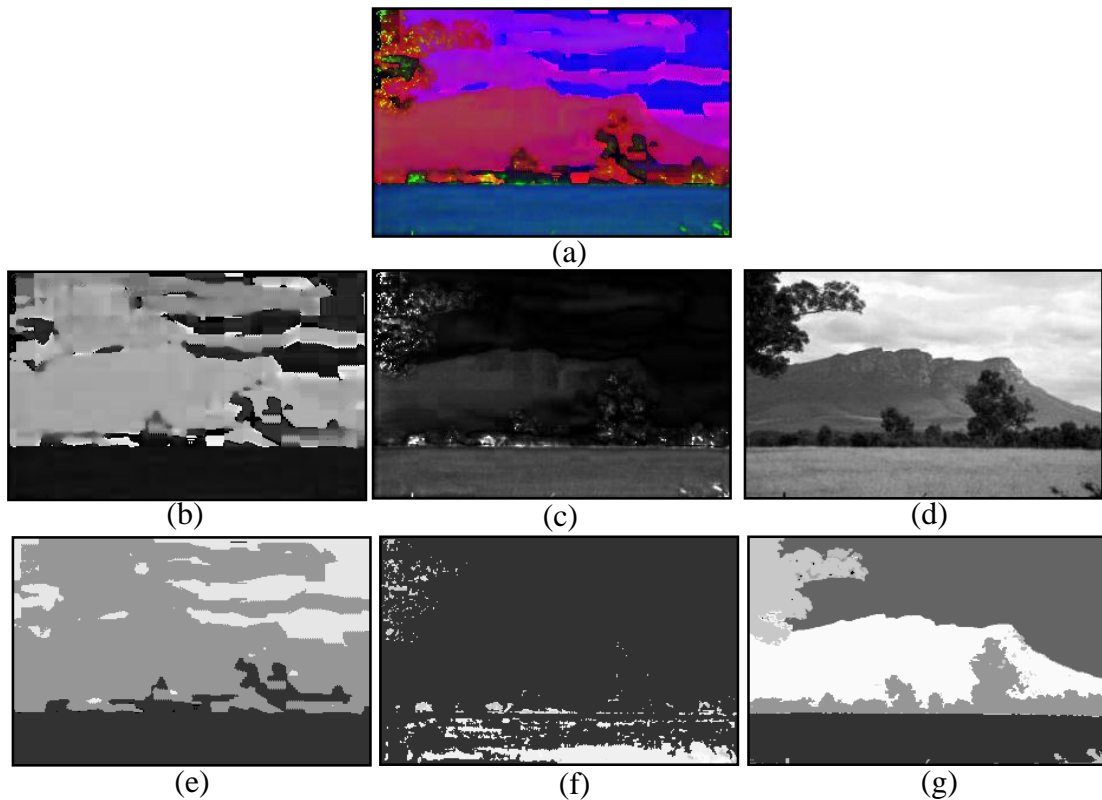
Figure (2.24): The green band regions segmentation of the city map image colored with blue color.

Figure (2.25) shows the similar region in blue band of the city map image grouped together, and are colored with blue color.



2.6.2.HSI Image Segmentation

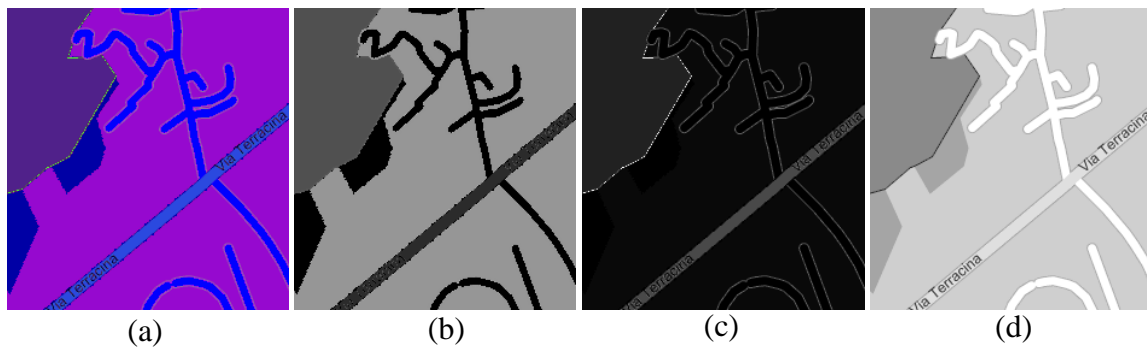
The photo image in figure (2.26) is converted to the HSI model, figures (2.26-b, 2.26-c, and 2.26-d), represent the three bands of HSI model hue, saturation and intensity band respectively, and images in figures (2.26-e, 2.26-f, and 2.26-g), represent the image segmentation to these three bands of the HSI model. The intensity band gave good segmentation, but the hue and saturation gave bad segmentation. This proves that almost all the information can be found in the intensity band. The HSI can be used instead of RGB to reduce the time of processing; we can only process the intensity band to obtain a good result of segmentation.



a- Original image in HSI model. b- Hue band. c- Saturation band. d- Intensity band. e- Segmentation to the Hue band. f- Segmentation to the Saturation band. g- Segmentation to the Intensity band.

Figure (2.26): Segmentation to the HSI model.

The city map image is also converted to the HSI model as shown in figure (2.27-a) and figures (2.27-b, 2.27-c and 2.27-d). The intensity band gave good segmentation compared with the hue and saturation band of HSI model.



(a) City map image in HSI model. (b) Hue band. (c) Saturation Band. (d) Intensity band.

Figure (2.27): Segmentation by the HSI model of the city map image.

Figure (2.28) shows the histogram of the intensity band for the city map image.

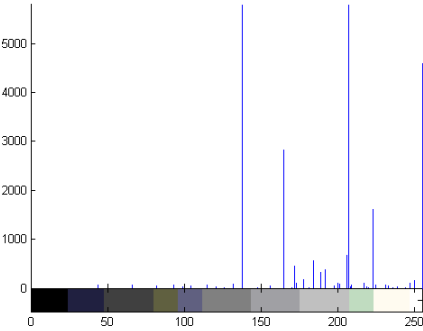
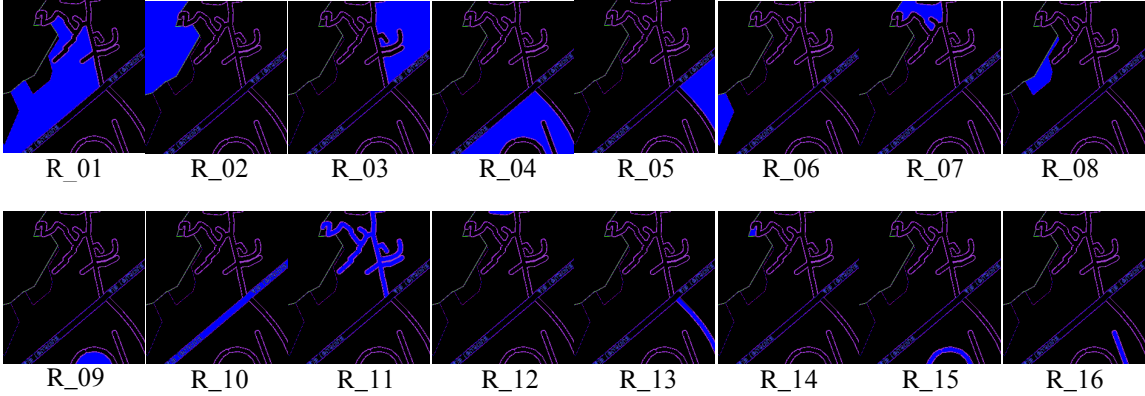


Figure (2.28): Histogram of the intensity band.

Figure (2.29) shows the regions of intensity band of city map image after segmentation.



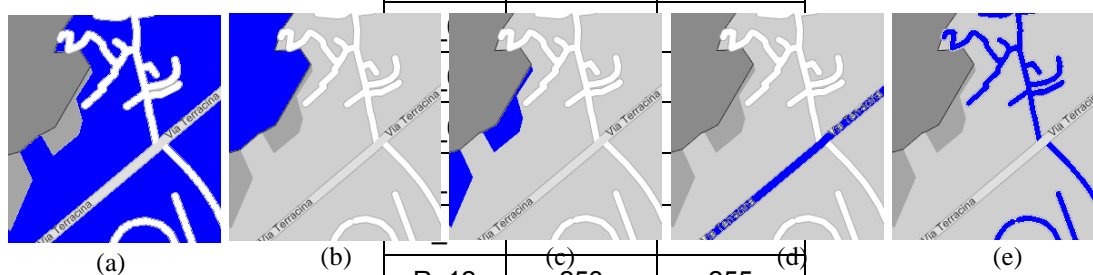
R_01 to R_16: regions of segmented image of blue band of the city map image.

Figure (2.29): Regions Segmentation to the image for intensity band of the city map image.

Table 2.2 shows the intensity range of each segmented region in the intensity band to the HSI model of the city map image.

Table 2.2: Intensity ranges of segmented image to the intensity band of the City Map Image.

Region No	Range of segmented regions for intensity band	
	From	To
R_01	205	209
R_02	136	140
R_03	205	209
R_04	205	209
R_05	205	209
R_06	163	167



(a): Regions whose intensity range is 205 - 209.	R_12	253	255
(b): Region whose intensity range is 136 to 140.	R_13	253	255
(c): Regions whose intensity range is 163 to 167.	R_14	205	209
(d): Regions whose intensity range is 221 to 225.	R_15	253	255
(e): Region whose intensity range is 253 to 255.	R_16	253	255

Figure (2.30): Regions segmentation to the intensity band of the map image colored with blue color.

Figure (2.30) shows the similar region in intensity band of the city map image grouped together and colored with blue color.

2.7. Conclusions and Discussions

Table (2.3) shows the relationship between the number of dilation operation (step 3 of the algorithm) and elapsed time for applying the proposed algorithm, and the number of initial seed regions, and the number of colored regions in the image segmentation. The values in table (2.3) are gathered through applying the proposed first technique to the image in figure (2.14 – a), the number of dilation operation in column one (number of dilation) is changed from 1 to 5, because the dilation operation

is applied to the image (for closed border line and join the border together) at least one time and at most five times. If it is applied more than five times, then most of the initial seed regions will disappear.

Table 2.3: The relationship between the number of dilation operations, number of seed regions and the number of colored regions based on the RGB model.

Number of dilation	Seed regions in R band	Seed regions in G band	Seed regions in B band	Color regions R	Color regions G	Color regions B
1	103	121	148	11	12	10
2	105	122	103	20	28	23
3	66	73	56	22	23	15
4	55	57	37	21	19	11
5	38	42	29	18	16	10

The number of the colored regions in the three bands of the RGB model depends on the number of dilation, These regions are increased until they reach a suitable value, which produces the maximum number of color regions. After that these regions are decreased, because when the number of dilation is small, the border of the regions are still disconnected, and they have gaps between them. when the number of dilations increases, the borders of the regions are connected together and the regions are split into color regions. But when the number of dilation operations increases, then the number of colored regions is decreased, because some of the regions are connected with the other regions. From table (2.3), where the number of dilation equals (2), it will be given the maximum value of the colored (segments) regions, which gives the best results.

Table 2.4 shows the relationship between the value of the expand interval and, the number of initial seed regions, and the number of colored regions in the segmented image.

Table 2.4: The relationship between the values of expand interval, the number of seed regions, the number of color regions based on the RGB model.

Expand interval Value	Seed regions in R band	Seed regions in G band	Seed regions in B band	Color Regions R	Color regions G	Color regions B
0	105	122	103	30	35	24
1	105	122	103	25	33	23
2	105	122	103	20	28	23
3	105	122	103	18	25	23
4	105	122	103	17	25	22
5	105	122	103	17	25	21

The expanded interval (in pixel) in table (2.4) is from 0 to 5, where 0 means the interval is not expanded and 1 means the interval is expanded from the right by 1 and from left by 1, and so on. Table (2.4) is obtained when the dilation operation is fixed by 2 and applied to the photo image in figure (2.14). Table (2.4) shows that when the expanded interval increases the colored regions (segment regions) are decreased, which means that it eliminates some regions, which cause the degradation to the result of segmentation, because some of the neighbor regions are merged together and cause this degradation.

After registration of the result and previewing the segmented image, the best quality of segmented image is set between 1 and 4 for the value of expanded interval.

Table (2.5) shows the relationship between the number of dilation operations, the number of seed regions, and the number of colored regions in the segmented image based on HSI model. The values in table (2.5) are gathered from the images in figure (2.26).

Table 2.5: Relationship between the number of dilation operations, the number of seed regions, and the number of color regions based on HSI model.

Number of dilation	Seed regions in H band	Seed regions in S band	Seed regions in I band	Color Regions H	Color Regions S	Color Regions I
1	86	148	130	3	7	13
2	72	75	130	38	4	27
3	41	43	68	21	5	23
4	40	30	50	21	5	23
5	26	20	42	13	6	18

Figure (2.31) shows that the line of Intensity band is near the lines of Red band, Green band and Blue band of RGB model, but the line of Hue band and Saturation band of HSI model are too far from the lines of the RGB model, therefore the hue and saturation bands were discarded.

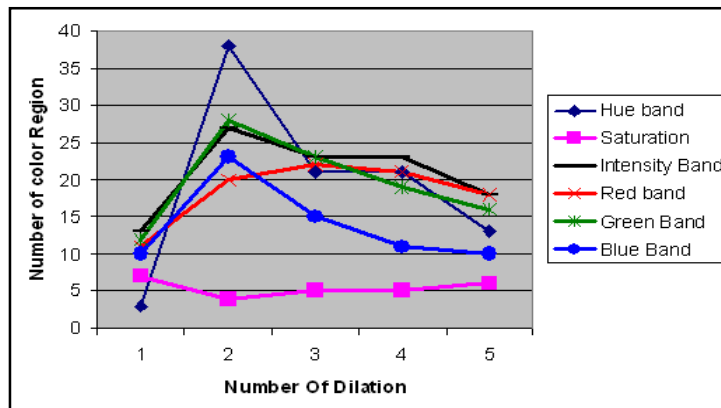


Figure (2.31): The relationship between the number of dilation operations and number of color regions in the three band of RGB model and HSI model

Figure (2.32) shows that the line of Intensity band is near the lines of Red band, Green band and Blue band of RGB model, but the line of Hue band and saturation band of HSI model are too far from the other lines. So if the value of expand interval is changed from 0 to 5, then the results of segmentation of image on HSI model (except Hue band and saturation band) will be similar to the result of segmentation of image on RGB

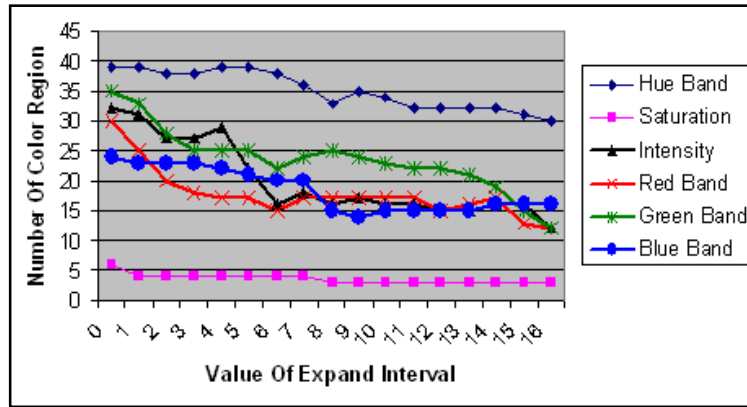


Figure (2.32): The relationship between the values of the expand intervals, and the number of the color regions in the three bands of RGB model and HSI model.

model, and the relationship between quality and number of dilation on HSI model is similar to the relationship between the number of dilation and quality on RGB model except the Hue band and Saturation band.

At last we can conclude that we can use the intensity band of the HSI, in segmentation which reduces the time of processing instead of processing the three bands of the RGB model.

Chapter Three

Image Segmentation by Wavelets

3.1.Introduction

Wavelets were first introduced to medical imaging research in 1991 in a journal paper describing the application of wavelet transforms for noise reduction in MRI images. Wavelet transforms have been successfully applied to many topics including tomographic reconstruction, image compression, noise reduction, image enhancement, texture analysis/segmentation and multi-scale registration. One important feature of wavelet transform is its ability to provide a representation of the image data in a multi-resolution fashion (Fan and Xia,2003).

Edge detection is by far the most common approach for detecting meaningful discontinuities in intensity values, such discontinuities are detected by using first- and second-order derivatives. Edge detection plays an important role in image segmentation. In many cases, boundary delineation is the ultimate goal for the image segmentation and a good edge detector itself can then fulfill the requirement of segmentation. On the other hand, many segmentation techniques require an estimation of object edges for their initialization. So the final result of the segmentation method depends heavily on the accuracy and completeness of the initial edge map (Lei and Bao, 2002).

3.2. Image Representation in Multi-Resolution

When we look at images generally, we see connected regions of similar texture and gray level that combines to form objects. If the objects are small in size or low in contrast, we normally examine them at high resolutions; if they are large in size or high

in contrast. a coarse view is all that is required. If both small and large objects or low and high contrast objects - are present simultaneously, it can be advantageous to study them at several resolutions. This, course, is the fundamental motivation for multiresolution processing (Rafael et al, 2002).

There are many methods to represent image in multi-resolution, such as image Pyramids and the Haar transform.

3.2.1. Image Pyramids.

An image pyramid is a collection of decreasing resolution image arranged in the shape of the pyramid. The base of the pyramid contains a high resolution representation of the image being processed; the apex contains a low-resolution approximation. As you move up the pyramid both size and resolution decrease (Rafael et al, 2002) .As can be seen in Figure (3.1).

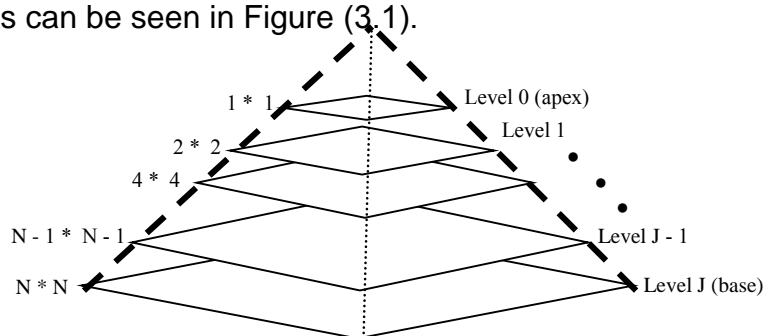


Fig (3.1): Pyramidal image structure

3.2.2. Haar Transform

The Haar Function was proposed in 1990 by Alfred Haar, and its basic functions are the oldest and simplest known orthonormal wavelets. For the haar transform, transformation matrix \mathbf{H} is used to represent image in multi-resolution. It contains the

Haar basic functions, $h_k(z)$ which is defined over the continuous closed interval $z \in [0, 1]$ for $k = 0, 1, 2, \dots, N-1$ where $N = 2^n$. So, to generate \mathbf{H} , you should define the integer k such that $k = 2^p + q - 1$, where $0 \leq p \leq n-1$, $q = 0$ or 1 for $p = 0$, and $1 \leq q \leq 2^p$ for $p \neq 0$. Then the Haar basic functions are (Rafael et al, 2002):

$$h_0(z) = h_{00}(z) = \frac{1}{\sqrt{N}}, z \in [0,1] \quad \dots (3.1)$$

And

$$h_k(z) = h_{pq}(z) = \frac{1}{\sqrt{N}} \begin{cases} 2^{p/2} & (q-1)/2^p \leq z < (q-0.5)/2^p \\ -2^{p/2} & (q-0.5)/2^p \leq z < q/2^p \\ 0 & \text{otherwise, } z \in [0,1] \end{cases} \quad \dots (3.2)$$

The i th row of an $N * N$ Haar transformation matrix contains the elements of $h_i(z)$, for $z = 0/N, 1/N, 2/N, \dots, (N-1) / N$.

If we assume $N = 2$. then the values of k, q and p based on the relation in the above paragraph will be as the values in the following table (3.1)

Table (3.1). Values of k, p and q

k	p	q
0	0	0
1	0	1

The $2 * 2$ transformation matrix \mathbf{H}_2 is

$$H_2 = \frac{1}{\sqrt{2}} \begin{bmatrix} 1 & 1 \\ 1 & -1 \end{bmatrix} \quad \dots (3.3)$$

3.3. Multiresolutions Expansion

In Multiresolution analysis, there are two functions that play an important role; a scaling function and wavelet function. Scaling function is used to create a series of approximation of a function or image, each differing by a factor of 2 from its nearest neighboring approximation. Wavelet functions are used to encode the difference in information between adjacent approximations (Rafael et al, 2002).

3.3.1. Scaling function

The set of expansion functions composed of integer translations and binary scaling of the real, square-integrable function $\varphi(x)$; that is, the $\{\varphi_{j,k}(x)\}$ where:

$$\varphi_{j,k}(x) = 2^{j/2} \varphi(2^j x - k) \quad \dots (3.4)$$

For all $j,k \in \mathbf{Z}$ and $\varphi(x) \in L^2(\mathbf{R})$

Where:

\mathbf{R} is the set of real numbers, denote the set of measurable, square-integrable one-dimensional functions.

\mathbf{Z} : is the set of integer.

Figure (3.2) shows the basic Haar scaling Function.

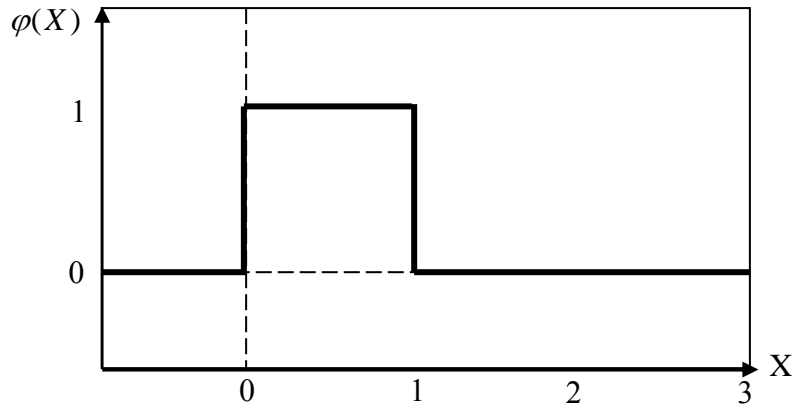


Figure (3.2). The basic Haar scaling function.

Figure (3.2) represent the Haar scaling function when $j = 0$ and $k = 0$. So based on the equation (3.4),

$$\varphi_{0,0}(x) = \varphi(x) \quad \dots (3.5)$$

And based on figure (3.2)

$$\varphi(x) = \begin{cases} 1 & 0 \leq x < 1 \\ 0 & \text{otherwise} \end{cases} \quad \dots (3.6)$$

The scaling function coefficients for the Haar function of the equation (3.6) are;

$$h_\varphi(0) = h_\varphi(1) = 1/\sqrt{2} \text{ that is the first row of matrix } \mathbf{H}_2.$$

3.3.2. Wavelet Function

The wavelet function $\psi(x)$ that, together with its integer translates to binary scaling.

The set $\{\psi_{i,j}(x)\}$ of wavelets are:

$$\psi_{i,j}(x) = 2^{j/2} \psi(2^j x - k) \quad \dots (3.7)$$

For all $j, k \in \mathbf{Z}$ and $\psi(x) \in L^2(\mathbf{R})$

Figure (3.2) shows the basic Haar wavelet function. When $j = 0$ and $k = 0$, So based on the equation (3.7).

$$\psi_{0,0} = \psi(x) \quad \dots (3.8)$$

And based on figure (3.3)

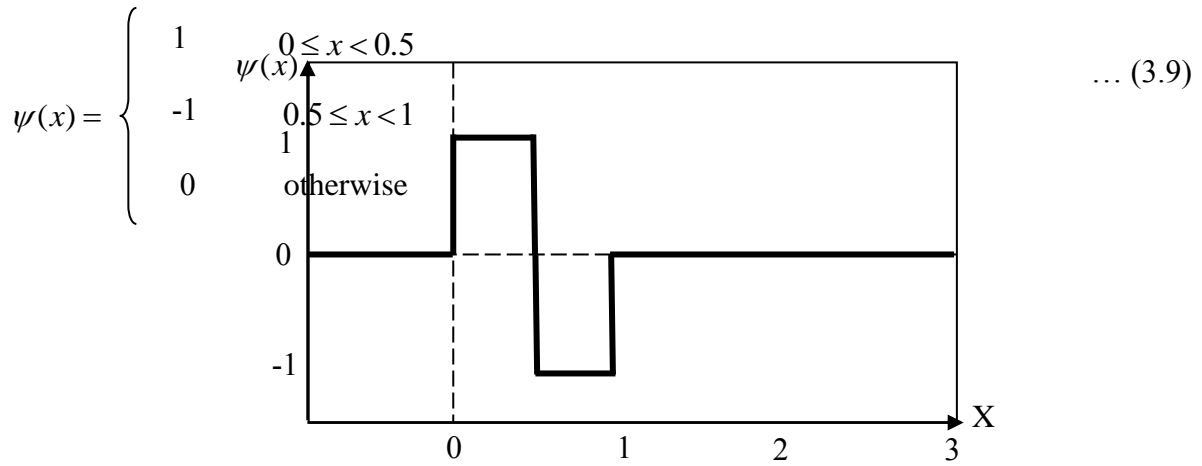


Figure (3.3). The basic Haar wavelet function.

The relationship between scaling function and wavelet function is defined as follows:

$$h_\psi(n) = (-1)^n h_\phi(1-n) \quad \dots (3.10)$$

The Haar scaling vector was defined as $h_\phi(0) = h_\phi(1) = 1/\sqrt{2}$ by using the equation (3.10).

The corresponding wavelet vector is

$$h_\psi(0) = (-1)^0 h_\phi(1-0) = 1/\sqrt{2} \quad \text{And} \quad h_\psi(1) = (-1)^1 h_\phi(1-1) = -1/\sqrt{2}$$

These coefficients are corresponding to the second row of matrix \mathbf{H}_2 in equation (3.3).

In other words, the coefficients of any wavelet family may be calculated either by using Multiresolutions expansion or by finding the transformation matrix for this wavelet family.

3.4. Wavelet Transform in One Dimension Based on the Discrete Wavelet Transform.

If we want to expand transform function $f(x)$ that represents the sequence of number, then the resulting coefficients are called the *discrete wavelet transform* of $f(x)$. So the equations that are used to transform function $f(x)$ into many coefficients are:

For $j \geq j_0$ and

$$W_\varphi(j_0, k) = \frac{1}{\sqrt{M}} \sum_x f(x) \varphi_{j_0, k}(x) \quad \dots (3.11)$$

$$W_\psi(j, k) = \frac{1}{\sqrt{M}} \sum_x f(x) \psi_{j, k}(x) \quad \dots (3.12)$$

$$f(x) = \frac{1}{\sqrt{M}} \sum_k W_\varphi(j_0, k) \varphi_{j_0, k}(x) + \frac{1}{\sqrt{M}} \sum_{j=j_0}^{\infty} \sum_k W_\psi(j, k) \psi_{j, k}(x) \quad \dots (3.13)$$

3.5. Wavelet Transform in Two Dimensions

In wavelet transform in two dimensions, there are two variables that determine the scaling function and wavelet function; x, y and there are three two-dimension wavelets required, $\psi^H(x, y), \psi^V(x, y)$ and $\psi^D(x, y)$; these are horizontal wavelet, vertical wavelet and diagonal wavelet respectively. The scaling function and wavelet function are based on just one variable which does not distinguish between wavelet functions, so based on the following equations the problem would be solved.

$$\varphi(x, y) = \varphi(x)\varphi(y) \quad \dots (3.14)$$

$$\psi^H(x, y) = \psi(x)\varphi(y) \quad \dots (3.15)$$

$$\psi^V(x, y) = \varphi(x)\psi(y) \quad \dots (3.16)$$

$$\psi^D(x, y) = \psi(x)\psi(y) \quad \dots (3.17)$$

Consequently, the basic function of the scaling and wavelet functions based on equation (3.4) and equation (3.7) respectively, are converted to be based on two variables (x,y). As seen in equation (3.18) for the basic scaling function and equation (3.19) for the basic wavelet function.

$$\varphi_{j,m,n}(x, y) = 2^{j/2} \varphi(2^j x - m, 2^j y - n) \quad \dots (3.18)$$

Where:

$$\psi^i_{j,m,n}(x, y) = 2^{j/2} \psi^i(2^j x - m, 2^j y - n) \quad i = \{H, V, D\} \quad \dots (3.19)$$

H: is horizontal coefficient.

V: is vertical coefficient.

D: is diagonal coefficient.

The equations (3.11, 3.12, 3.13) also are changed based on two dimension function $f(x, y)$, where the starting scale is calculated based on the following equation:

$$W_\varphi(j_0, m, n) = \frac{1}{\sqrt{MN}} \sum_{x=0}^{M-1} \sum_{y=0}^{N-1} f(x, y) \varphi_{j_0, m, n}(x, y) \quad \dots (3.20)$$

$$W_\psi^i(j, m, n) = \frac{1}{\sqrt{MN}} \sum_{x=0}^{M-1} \sum_{y=0}^{N-1} f(x, y) \psi^i_{j, m, n}(x, y) \quad \dots (3.21)$$

Also, the equation (3.13) is changed as:

$$f(x, y) = \frac{1}{\sqrt{MN}} \sum_m \sum_n W_\varphi(j_0, m, n) \varphi_{j_0, m, n}(x, y) + \dots \quad (3.22)$$

$$\frac{1}{\sqrt{MN}} \sum_{i=H,V,D} \sum_{j=j_0}^{\infty} \sum_m \sum_n W_\psi^i(j, m, n) \psi_{j, m, n}^i(x, y)$$

Figure (3.4) shows the scale $j + 1$ approximation coefficient to construct the scale j approximation and detail coefficients. The image $f(x,y)$ is used as the $W_\varphi(J, m, n)$ input convolving its rows with $h_\varphi(-n)$ and $h_\psi(-n)$ and down sampling its columns. The two sub images result whose horizontal resolution is reduced by factor of 2, the high pass or detail component characterizes the high image with vertical orientation; the low pass, approximation component contains its low-frequency vertical information.

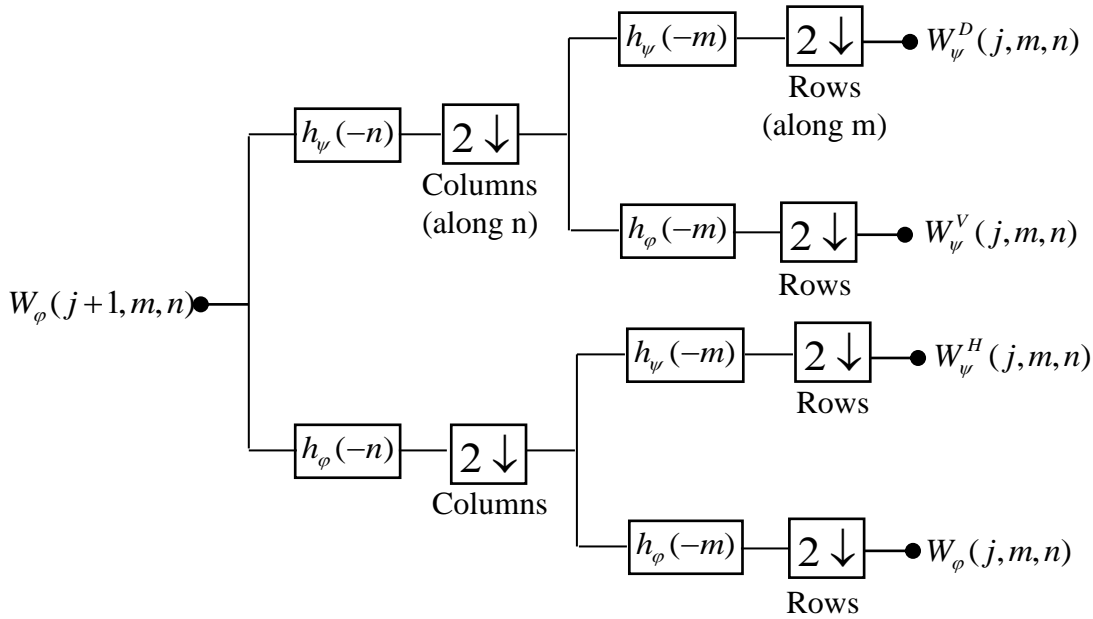
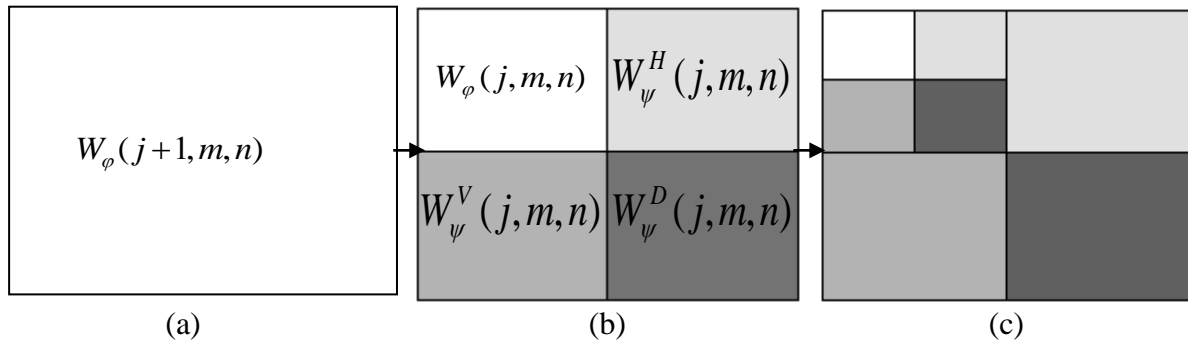


Figure (3.4). The process of transform $j+1$ scale to j approximation and detail coefficient

Both sub images are then filtered column wise and down-sampled to yield four quarter-size output sub images; $W_\varphi, W_\psi^H, W_\psi^V,$ and W_ψ^D . (Rafael et al, 2002)

Figure (3.5) shows two iterations of the filtering process which produces the two-scale decomposition at far right.



(a) : image $f(x,y)$ is used as the $W_\phi(J, m, n)$ input.

(b) : the result of decomposition at scale j .

(c) : the result of decomposition at scale $j-1$.

Figure (3.5). Decomposition process at two scales.

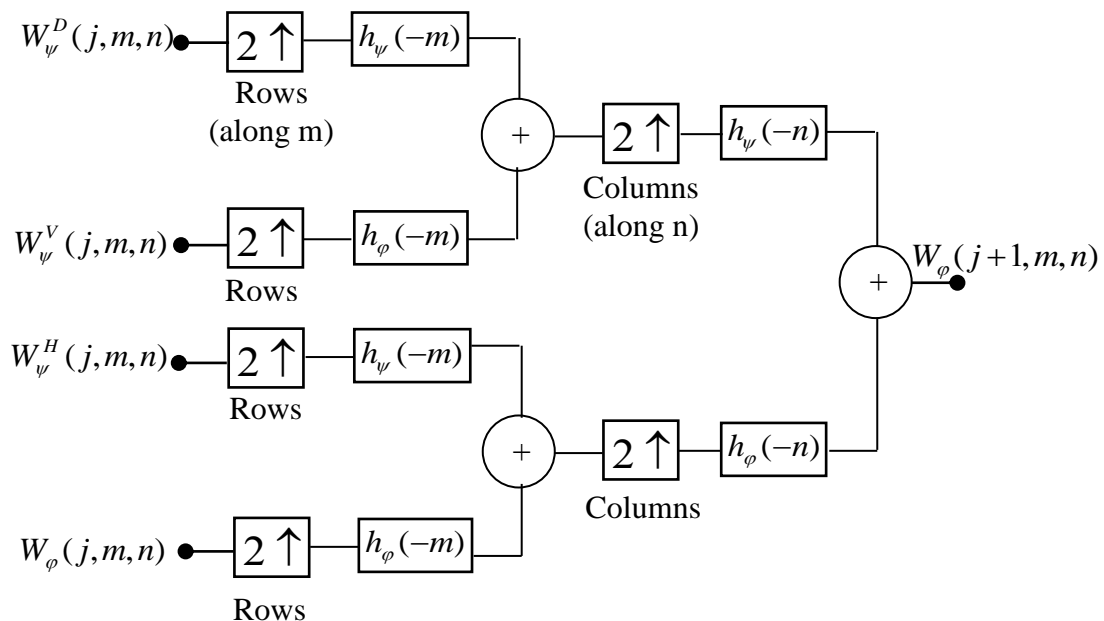


Figure (3.6). Diagram shows the process of reconstruct j approximation and detail coefficients to scale $j+1$

Figure (3.6) shows the inverse process of decomposition that is reconstruction. In the reconstruction algorithm four scale j approximation and detail sub images are

upsampled and convolved with two one-dimensional filters on its columns and the other on its rows, addition of the results yields the scale $j + 1$ approximation. This process is repeated until the original image is reconstructed (Rafael et al, 2002).

3.6. Two-Dimensional Wavelet Transform by Averaging and Differencing Method

Since the scaling and wavelet functions are separable, each convolution breaks down image into one-dimensional convolutions on the rows and columns of an image $f(i,j)$ of $N \times N$ dimension. At stage one, the rows of the image $f(i,j)$ first convolve with low-pass filter and high-pass filter. The columns of each of the $N/2 \times N$ array then convolved with low-pass filter and with high-pass filter. The result is the four $N/2 \times N/2$ arrays required for that stage of the transform. The transform process can be carried to m stages.

The algorithm of the averaging and differencing which apply the low-pass and high-pass filter function is as follows;

1. Take a vector row from image f of $N \times N$ dimension:

$$Y = \{f(1,1), f(1,2), f(1,3) \dots f(1,j)\} \quad \dots (3.23)$$

Where;

$$j = 1, 2, \dots, N$$

Y : vector of $1 \times N$ dimension.

2. Add two neighbor pixel and divide them by 2:

$$B = \{ \{f(1,1) + f(1,2)\}/2, \{f(1,3) + f(1,4)\}/2, \dots, \{f(1,j-1) + f(1,j)\}/2 \} \quad \dots (3.24)$$

Where;

$$j = 1, 2, \dots, N$$

B: vector of $1 \times N/2$ dimension.

3. Extract the first number of each pair from Y and subtract them from B ;

$$C = \{ f(1,1), f(1,3), f(1,5), \dots, f(1,j-1) \} \quad \dots$$

(3.25)

$$D = C - B$$

Where:

$$j = 1, 3, 5 \dots N-1$$

C: vector of $1 \times N/2$ dimension.

D: vector of $1 \times N/2$ dimension.

4. Let $Y_1 = [B, D]$, and replace the vector row Y in an image by Y_1 .

Where:

Y_1 : vector of $1 \times N$ dimension.

Now, the one half of the output is produced by the low-pass filter function:

$$a_i = \frac{1}{2} \sum_{j=1}^N c_{j+1-2i} f_j \quad i=1, 2, \dots, N/2 \quad \dots (3.26)$$

While the other half is produced by the high-pass filter function:

$$b_i = \frac{1}{2} \sum_{j=1}^N (-1)^{j+1} c_{2i-j} f_j, \quad i = 1, 2, \dots, N/2 \quad \dots (3.27)$$

Where:

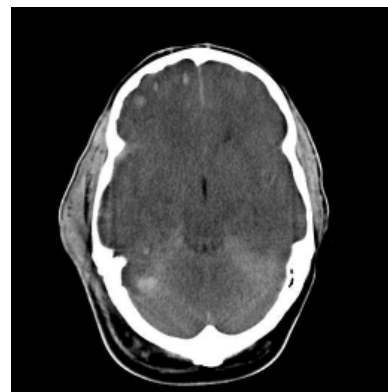
c's: are the coefficients (in this example $c_0 = c_1 = 1$).

a,b: the output functions.

Similarly, we can calculate the remaining rows to obtain the new matrix of $N/2 \times N$ dimension. The same operation could be applied to the columns of the new matrix, and the results are four bands LL_1, LH_1, HL_1, HH_1 each one with $N/2 \times N/2$ dimension. The wavelet transform have been applied on medical images shown in figures (3.7 – a, 3.7 - b).



(a)



(b)

(a) Front view of the human head. (b) Back view of the human head.

Figure (3.7): Medical images that are used to extract their edges by using wavelet

3.7. The Proposed Second Technique for medical image segmentation.

The proposed second technique consist of three parts, each of them segment a certain kind of medical images. The first part is concerned with edge detection and

image segmentation for front view and back view of human head. The second part is concerned with extracting pupil and iris region for human eye image. The third part is concerned with extracting high light regions using wavelets.

3.7.1. The Proposed Second Technique (Part a) for Edge Detection and Medical Image Segmentation by Using Wavelet.

Segmentation is one of the most important applications in medical image analysis. In this proposed technique, wavelet was applied to determine the image edges. The results showed that the first level of transformation is very enough to give good results. The obtained edges of the image are enhanced, by using threshold technique, followed by dilation operation to determine the closed segment regions. The segments are colored with any color to discriminate these regions from the other regions of the image.

The block diagram of the proposed second technique (Part a) is as shown in figure (3.8).

Step 1	Wavelet Transform to the first Level.
Step 2	Merge LH & HL bands
Step 3	Converting image to black and white by selecting threshold
Step 4	Apply Median filter to remove noise
Step 5	Apply dilation operation
Step 6	Coloring the closed edges (segments) regions

Figure (3.8): steps for proposed second technique (part a) to the edge detection and medical image segmentation by using wavelet.

The proposed second technique (Part a) applied on the medical images is shown in figures (3.7 – a, 3.7 - b).

To extract the image edges by using wavelet transform using this technique, we apply the following detailed steps:

Step 1: Apply the wavelet transform algorithm to the images in figures (3.7 – a, 3.7 - b).

Step 2: Merge the LH and HL bands in figure (3.9) and figure (3.11) to the image in figure (3.10 -b) and figure (3.12-b) together by using the following equation:

$$g(i,j) = \begin{cases} LH(i,j) & \text{if } LH(i,j) \geq HL(i,j) \\ HL(i,j) & \text{if } LH(i,j) < HL(i,j) \end{cases} \quad \dots (3.28)$$

Where:

$$i, j = 1, 2, \dots, N/2$$

g : the output image of $N/2 \times N/2$ dimension.

Step 3: Convert the new image into black and white image by applying threshold technique to the new image, the threshold value determined experimentally to get the best result as shown in figure (3.10-c) and figure (3.12-c).

Step 4: Apply the median filter to the new image to remove the noise.

Step 5: Apply the dilation operation to enclose the open edges.

Step 6: Set the required color to the closed regions (selected segments) to discriminate each region from others, as shown in figure (3.10 - d) and figure (3.12 - d).

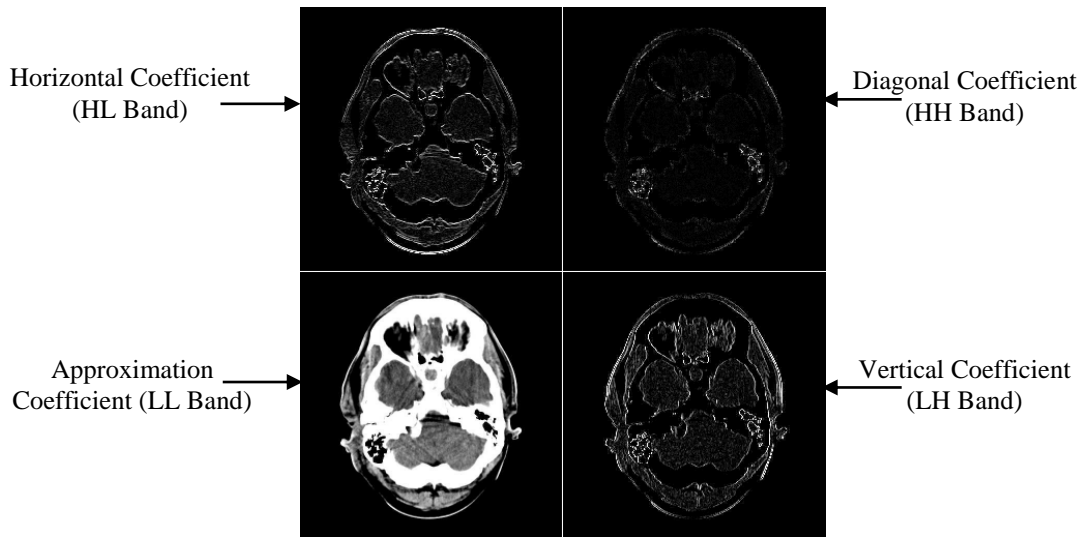
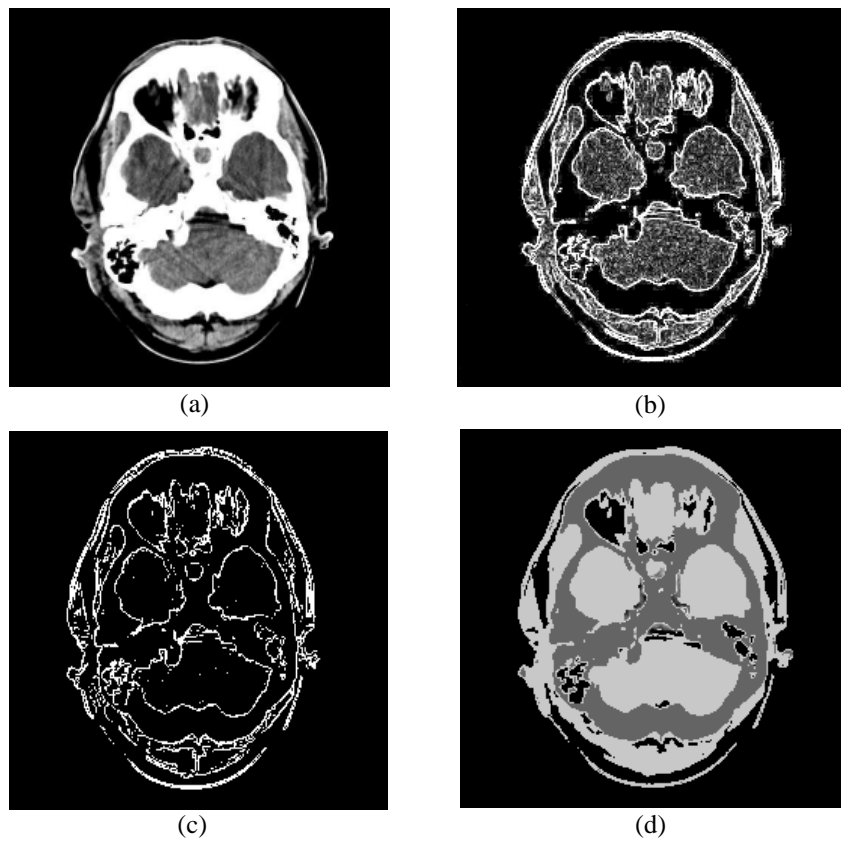


Figure (3.9): First scale of wavelet transform of the front view of the human head



(a): The original image.

(b): Applying the wavelet transform to the image in figure (a), followed by merging the HL & LH bands of the image.

(c): Edge detection to the image in figure (b).

(d): Color filling to the image segmentation in figure (c)

Figure (3.10): Edge detection and image segmentation by using wavelet to the front view of the human head

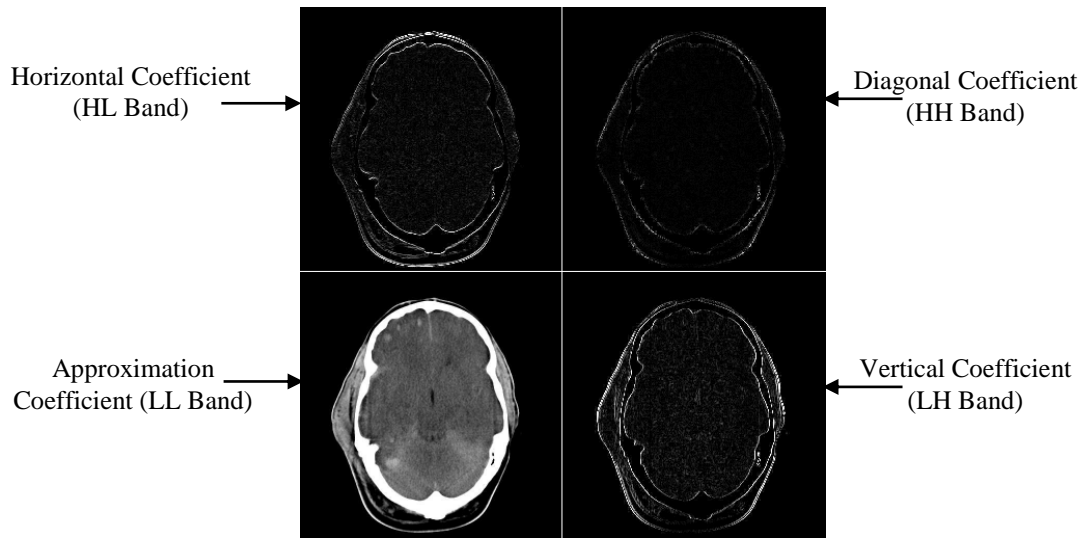
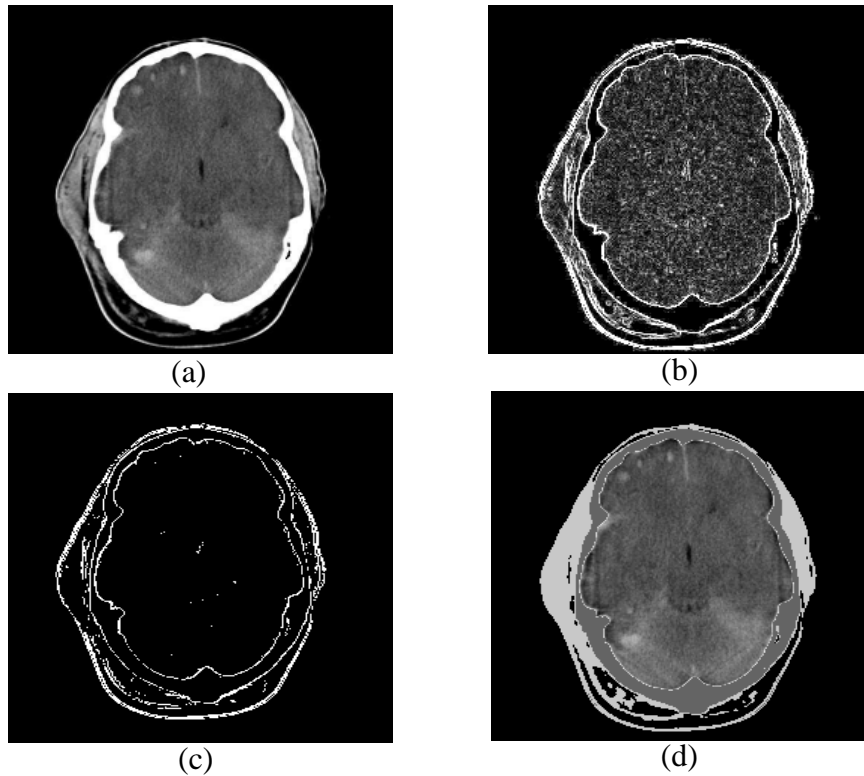


Figure (3.11): First scale of wavelet transform to the back view of the human head



(a) The original medical image.

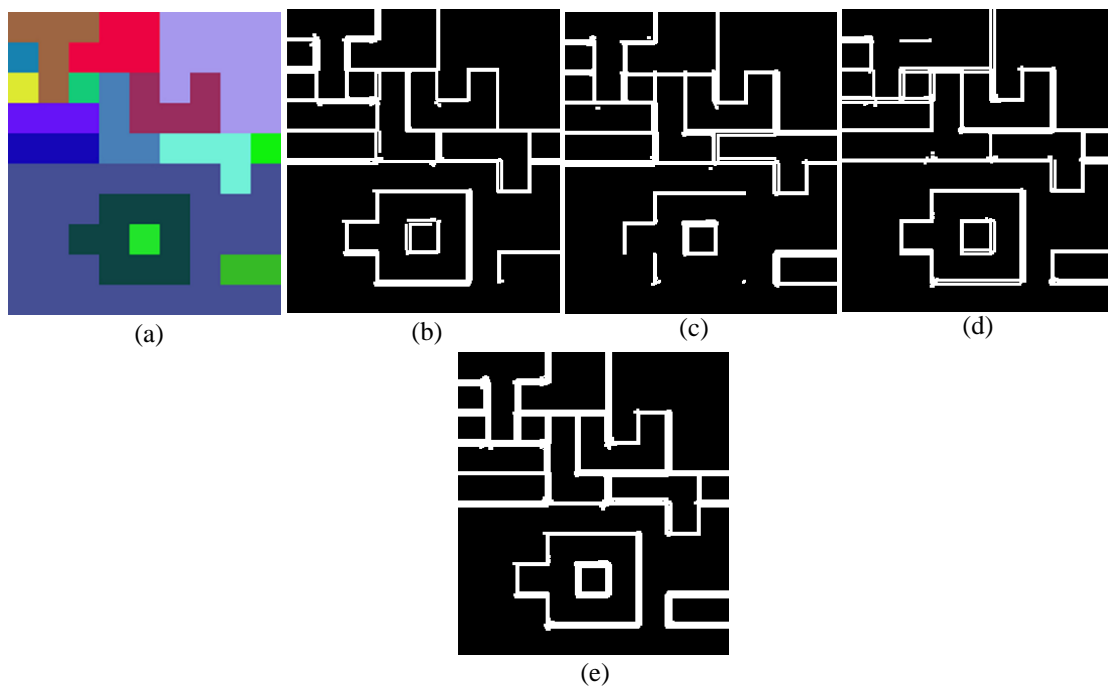
(b) Applying the wavelet transform to the image in figure (a), followed by merging the HL & LH bands of the image.

(c) Edge detection to the image in figure (b).

(d) Color filling to the image segmentation in figure (c)

Figure (3.12): Edge detection and image segmentation using wavelet to the back view of the human head

The image of figure (3.5) in chapter two is also used to test the proposed second technique (Part a) to extract its edges and the algorithm gave us good result. The proposed technique was applied on each of three bands of the image, the result of each band is grouped together as shown in figure (3.13).



(a) Original image. (b) Edges for red band. (c) Edges for green band.
 (d) Edges for blue band. (e) Edges for three bands grouped together
 Figure (3.13): Edges for image that was tested using proposed algorithm.

3.7.2. The Proposed Second technique (Part b) for Medical Eye Images Segmentation by Canny Edge Detector

Segmentation is one of the most important applications in medical image analysis. The proposed second technique (Part b) is applied on iris image to determine edge of iris, pupil and extract any different color region on it. It is based on drawing a circle by using the center of pupil and its radius is the distance between the center of pupil and the closest edge for the iris, the technique is applied on two different sources of images and shows good results. This technique is useful when we want to detect the white water inside the eyes (Alsultanny and Al-Fraheed, 2007).

The Canny mask gave the best results of edge detection compared with the other methods of edge detection especially for the medical images. When we want to detect

a very small segment, sometimes the Canny mask can not detect the border completely, in this case we apply the dilation process (Rafael et al, 2002) to complete the border of regions, to obtain a closed regions. Figure (3.14) shows the block diagram of the proposed second technique (part b).

- | | |
|--------|---|
| Step 1 | Detect the pupil area by using histogram process |
| Step 2 | Determine the pupil center |
| Step 3 | Apply canny mask to detect the iris edge |
| Step 4 | Apply Dilation to close the open boundaries |
| Step 5 | Determine the closest iris edge to the pupil center |
| Step 6 | Draw circle based on pupil center and its distance from iris edge |

Figure (3.14): steps for proposed second technique (part b) for medical eye image segmentation using canny edge detector.

The proposed second technique (part b) is applied on the eye for medical application. Figure (3.15) shows a sketch, how to determine the iris from the eye image, by applying the following detailed steps:

Step 1: Use histogram: we search the gray value for the pixels that set in pupil area. From the study, we found them lie between (0 – 25) between (0 – 50).

Step 2: Center of iris: determine the coordinate of the center of pupil area $P_1(x_1, y_1)$.

Step 3: Edge detection: apply the Canny mask to edges of iris. But it does not detect the border of iris completely.

Step 4: Find the closest edge of iris to center of pupil and mark it as $P_2(x_2, y_2)$.

Step 5: Calculate the distance between P_1 and P_2 by using;

$$R = \sqrt{(x_2 - x_1)^2 + (y_2 - y_1)^2} \quad \dots (3.29)$$

Where;

R: is the distance (radius) between P_1 and P_2 .

Step 6: Draw the circle whose radius is R and its center is $P_1(x_1, y_1)$ by using the following:

$$X_2 = R * \text{Cos}(\theta) \quad \dots$$

(3.30)

$$Y_2 = R * \text{Sin}(\theta) \quad \dots$$

(3.31)

Where;

θ : is the angle 1,2,3,.....360.

R: is the radius of the circle.

x_1, x_2 : the x-coordinates.

y_1, y_2 : the y-coordinates.

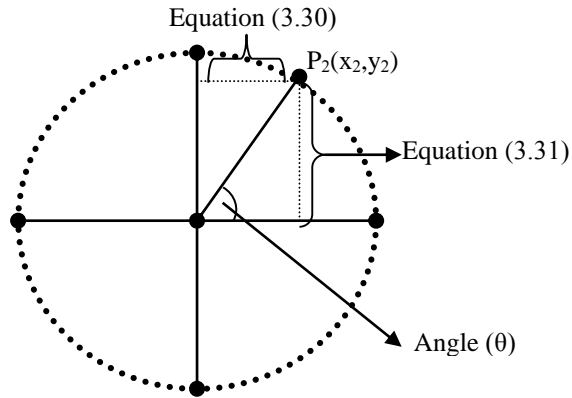
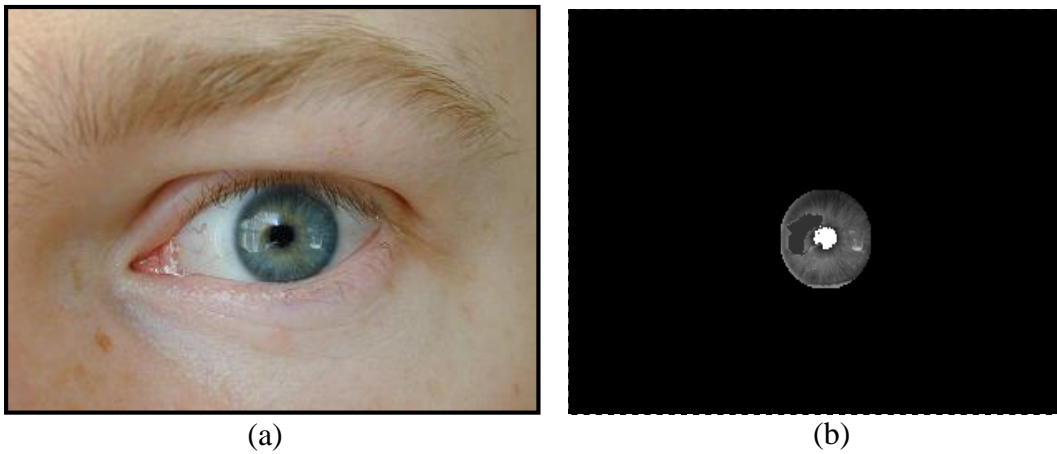


Figure (3.15): Sketch to determine the iris dimension

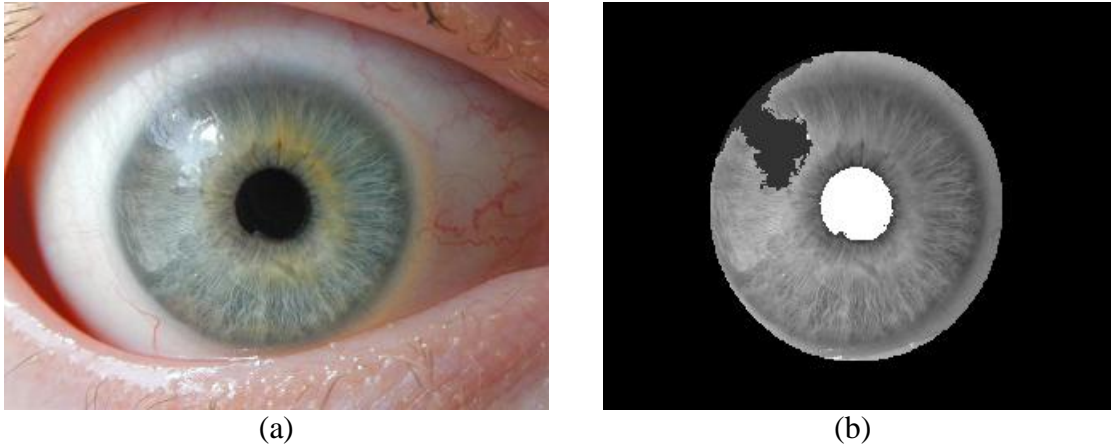
Figures (3.16) and (3.17) show the processing of the ill eyes image, to segment the ill regions in the iris.



(a) Original medical eye image.

(b) Color filling Image after applying the proposed second technique (part b).

Figure (3.16). Applying segmentation by using proposed second technique (part b)



(a) Original medical eye image.
 (b) Color filling after applying the proposed second technique (part b)
 Figure (3.17): Applying segmentation to another image, by using the proposed second technique (part b)

The discrete wavelet frame (DWF) decomposition, a variation of the discrete wavelet transform, is used. Unlike other decomposition, DWF is computationally inexpensive for the evaluation of low frequency components, because its computation is simple and it needs a very short time to obtain the low frequency component of DWF. The DWF decomposition can be calculated by successive 1-D processing along the rows and columns of the image. A block diagram of one-level DWF decomposition of an image is presented in figure (3.18), where L and H correspond to low-pass and high-pass filters respectively.

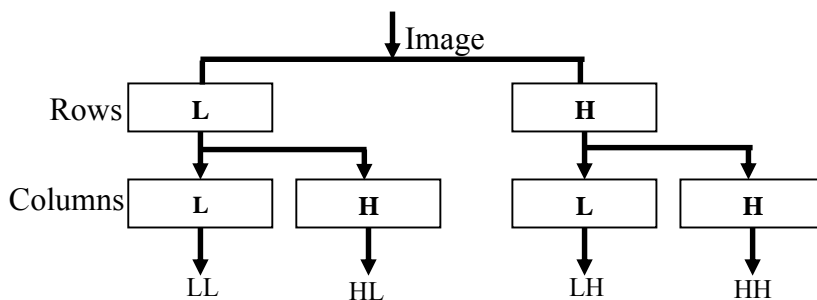


Figure (3.18). The discrete wavelet frame decomposition with low pass (L), and high pass (H) filters, the input image decomposed into four sub bands.

3.7.3. The Proposed Second Technique (Part c) for extracting high light region using wavelet.

This technique consists of two stages, the first stage uses the proposed second technique (part a) to determine the highlight region, and the second stage based on drawing a circle to determine object and it showed good results to the two different sources of medical images. The background must be selected to obtain good results, by using background of high level of darkness (Alsultanny and Al-Fraheed, 2007).

The steps of the first stage of the technique is shown in figure (3.8) and the steps for second stage is shown in figure (3.19).

Step 1	Right-Top Part
Step 2	Find region that has the greatest intensity value
Step 3	Find region that has the greatest intensity value
Step 4	Draw circle whose center is the position of the greatest value.
Step 5	Distribute the intensity value of circle into group, and fill each group with specific color
Step 6	Merge all neighboring groups without background group
Step 7	Delete smallest regions
Step 8	Apply morphological operations

Figure (3.19): steps for second stage of the proposed second technique (part c) for extracting high light region.

By applying the first stage of the proposed technique on the image shown in figure (3.20 - a), we will get the result image as shown in figure (3.20 - b). This image is obtained by applying the first level of wavelet transform, and then merging LH and HL bands to obtain the image in the right-bottom of figure (3.20 - b). Then we convert the image to binary image by selecting a threshold level to select only the required regions in the image as shown in the left-top of image in figure (3.20 - b), then we match the selected region with the original image to obtain the highlighted segments of the image as shown in the right-top image in figure (3.20 - b). The sequences in figure (3.20 - b) were applied to the image in the right-top of figure (3.20 - b), which is also shown in figure (3.20 - c) to obtain the image shown in figure (3.20 - d).

The detailed steps for the Second stage of the proposed technique is shown in figure (3.20 - b).

Step 1: Find region that has the greatest intensity value.

Step 2: Draw circle whose center is the position of the greatest intensity value. The diameter of the circle is set between 15 and 20.

Step 3: Distribute the intensity value of the circle into groups, the size of group set between 20 and 25.

Step 4: Fill each group with specific color.

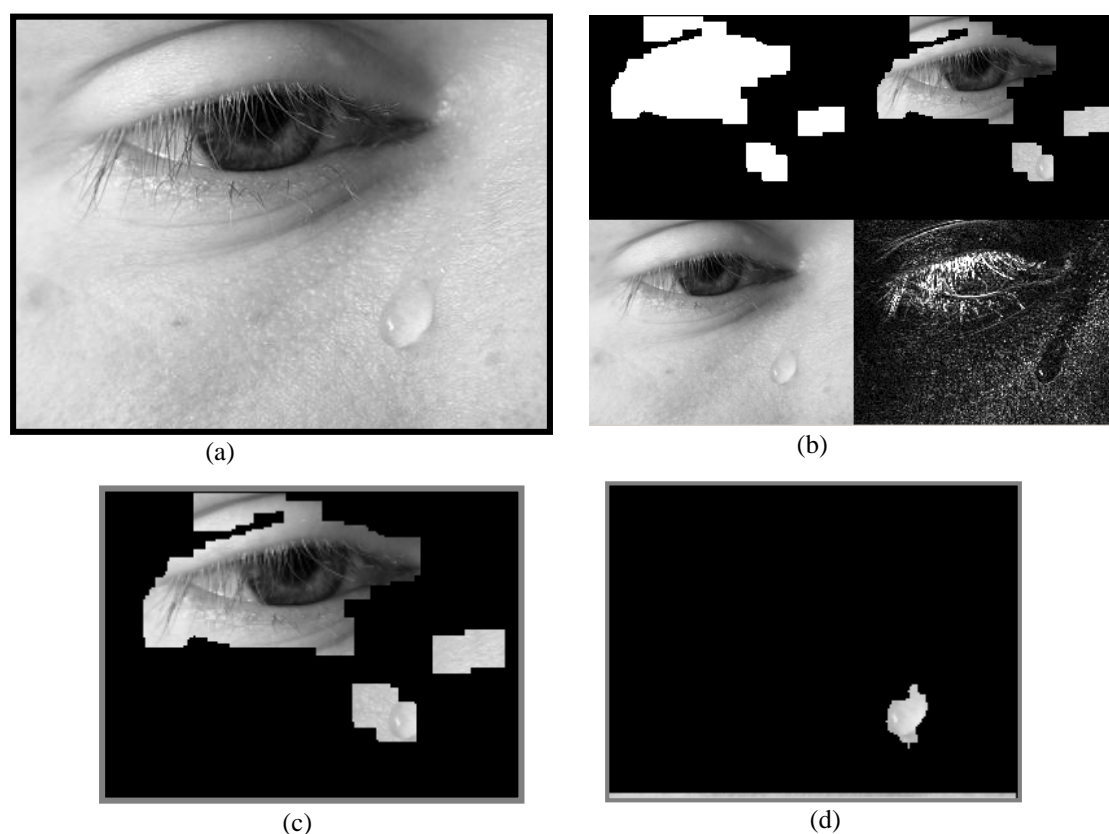
Step 5: Merge all neighboring groups without background group and convert them into binary image.

Step 6: Search the smallest regions that are not connected with other groups in order to delete them.

Step 7: Apply morphological algorithm on the binary image in order to close all spaces between groups and make them closed area.

Step 8: Replace the white points with the original gray from the original image otherwise set them with the black color.

Figure (3.21) shows the result of applying algorithm 2 to an image that contains soft lens, and we try to segment the region that contains only soft lens.



(a): Original image

(b): Image after applying the first stage of the algorithm 2

*Left - Bottom: Original Image which is size $N/2 * N/2$.*

Right - Bottom: LH & HL Bands after merge.

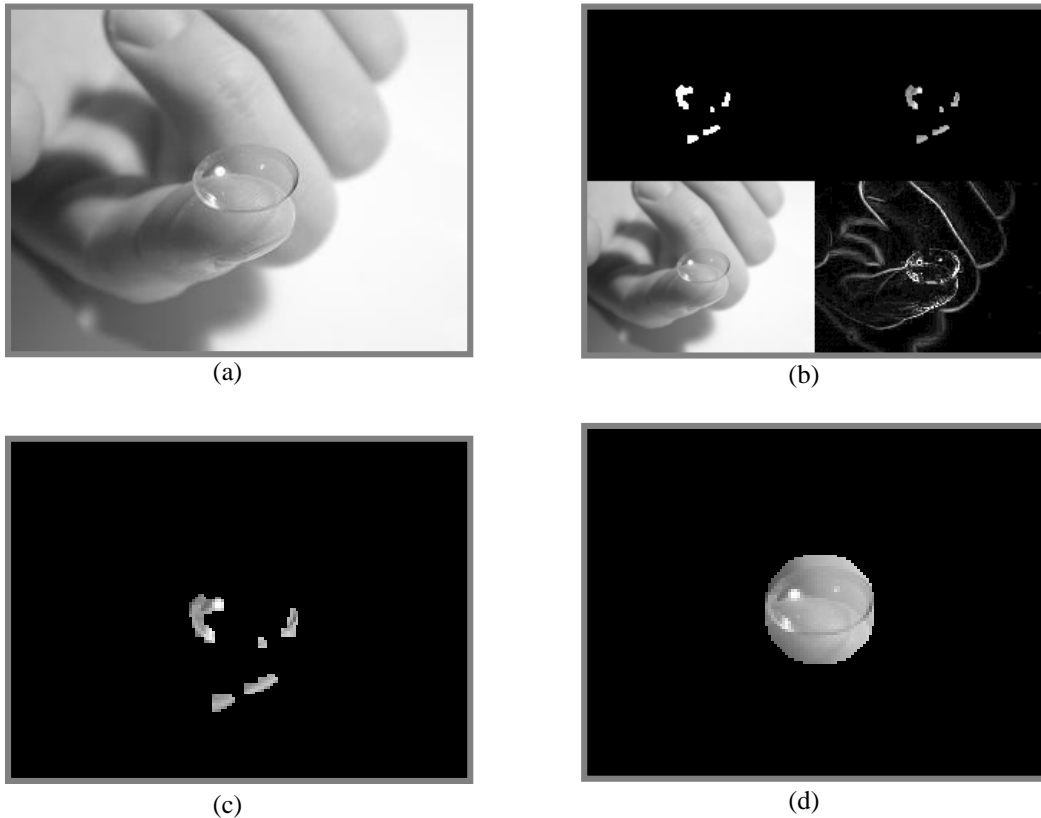
Left - Top: Image that has highlighted area.

Right - Top: Original Image with Highlighted area.

(c): Right - Top Part of the figure (6-b).

(d): The result of the second stage of the proposed technique.

Figure (3.20): Applying segmentation by using wavelet algorithm to determine the ill



(a): The original image in gray level.

(b): The result of the first stage of the algorithm.

Left - Bottom: Original Image which is size $N/2 * N/2$.

Right - Bottom: LH & HL Bands after merge.

Left - Top: Image that has highlighted area.

Right - Top: Original Image with Highlighted area .

(c): Right - Top Part of figure (17-b).

(d): The result of the Second stage of the algorithm 2.

Figure (3.21) Applying segmentation by using wavelet algorithm to determine soft lens.

3.8. Conclusions and Discussions

In the proposed second technique (part a), the images are transformed at just first scale and it gave us the best results, but if the images were transformed to more than one scale then the edges in images may be become hidden. Figure (3.22) shows the relation between the scale and number of closed regions to the image in figure (3.13). The black line in figure (3.22) represents the actual number of regions in the image. Consequently, it can be seen that the number of regions decreases whereas

the number of scales increases.

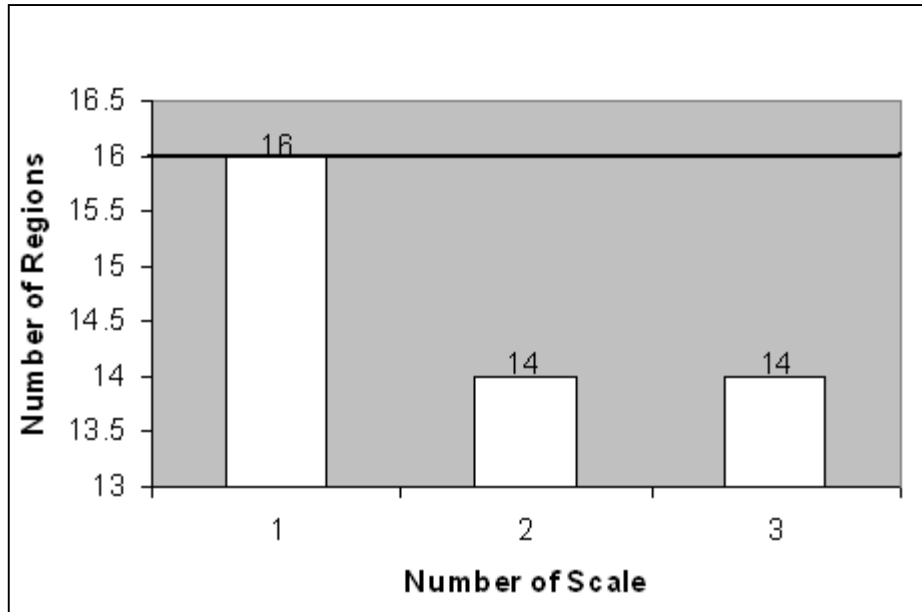
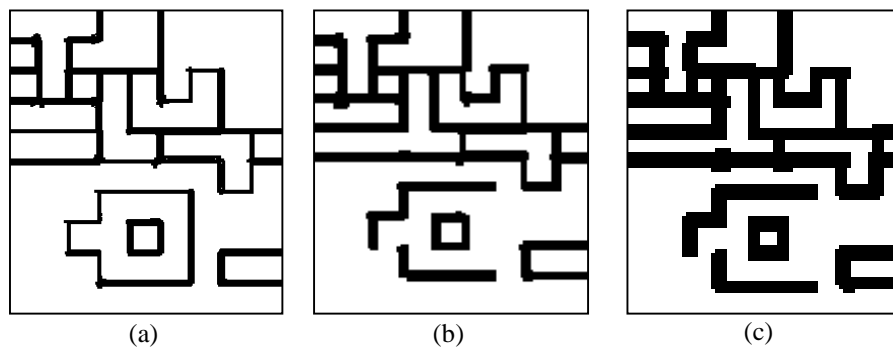


Figure (3.22): Relationship between the scale and number of regions.

Figures (3.23-a, 3.23-b, 3.23-c) show the edges to the image at the first, second and third scale respectively.

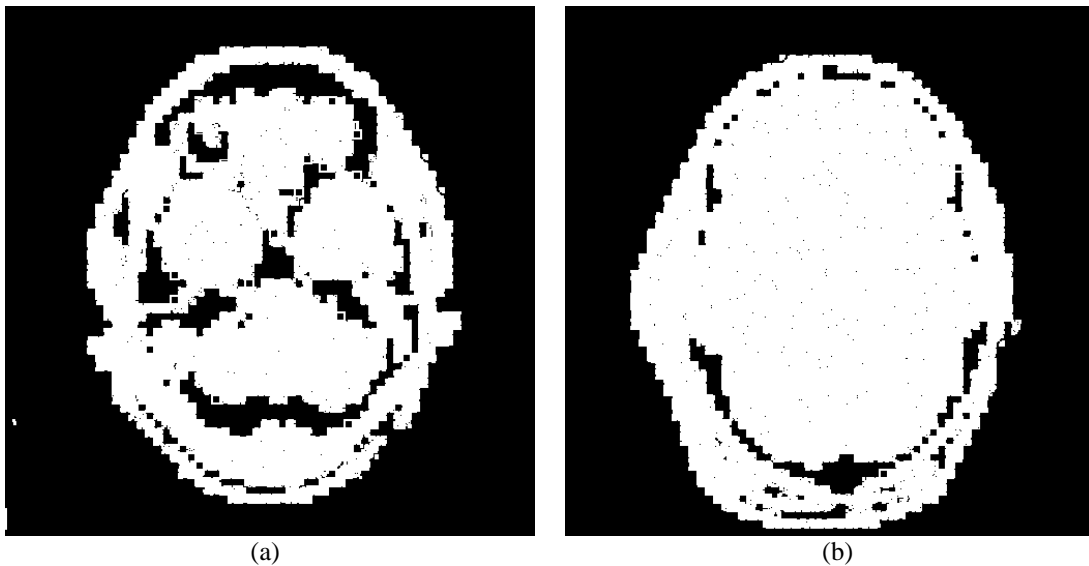


- (a) Edges detections at first scale.
- (b) Edges detections at Second scale.
- (c) Edges detections at Third scale.

Figure (3.23): image of edges at different scale.

By comparison the proposed second technique (part a) with the methods that detect horizontal lines and vertical lines in an image using horizontal mask and vertical mask

respectively in chapter two, we find that: The proposed second technique (part a) gave better results than horizontal and vertical masks method. The medical images of the front and back view of the human head were tested previously and gave us results as shown in figure (3.10) and figure (3.12). But the same images were tested by the horizontal and vertical masks method and gave us bad results as shown in figures (3.24-a, 3.24-c) (which show edges for medical images tested by merging horizontal and vertical lines that are detected by horizontal and vertical masks) because the edges of the images are degraded by comparing the result in figure (3.24) with results in figures (3.10, 3.12).



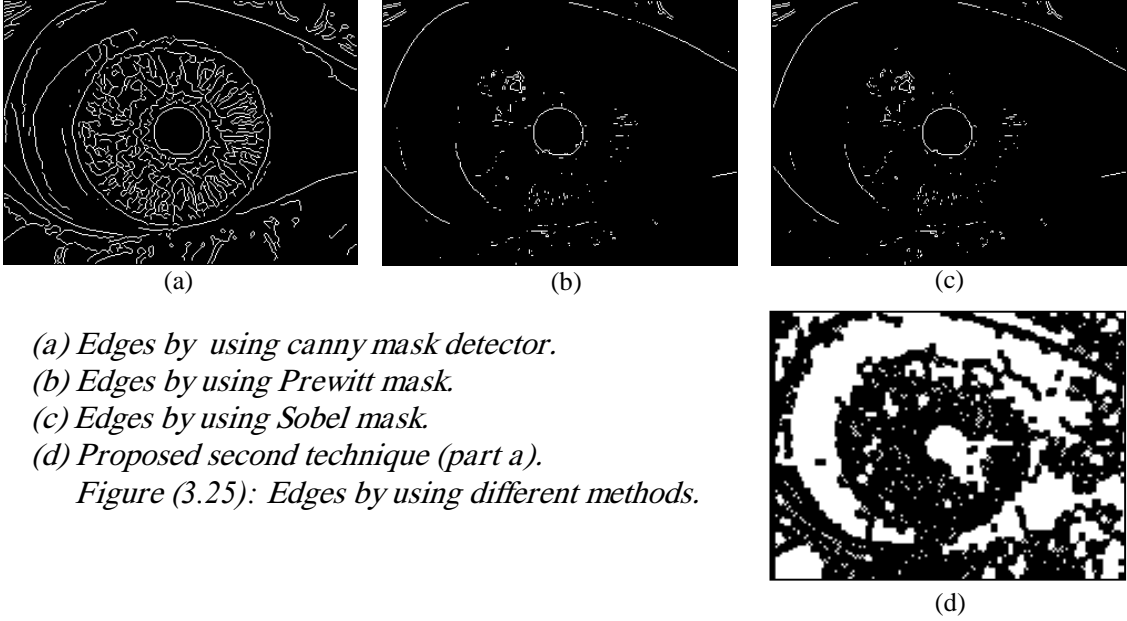
(a) Edges to the front view of the human head.

(b) Edges of the back view of the human head.

Figure (3.24): Edges to the human head.

The proposed second technique (part b) uses the canny mask detector to extract edge of iris and it gave the best result compared with other methods to detect edges such as Sobel, Prewitt and proposed second technique (part a). Figure (3.25) shows the

edges of eye image in figure (3.17 – a) using other methods.



(a) Edges by using canny mask detector.
(b) Edges by using Prewitt mask.
(c) Edges by using Sobel mask.
(d) Proposed second technique (part a).
Figure (3.25): Edges by using different methods.

Chapter Four

Segmentation Based on 2D Wavelet

4.1.Introduction

Various techniques and algorithms have been proposed for image segmentation and are classified into three categories: clustering, edge detection and region extraction. However, most segmentation techniques are based on the third category (Haihua et al, 2005).

The fundamental idea behind wavelets is analyzing according to scale, each scale has four coefficients; the first is approximation coefficient and it is set at left-above corner of transformation image, the second is horizontal coefficient and it is set at right-above corner of transformation image, the third is vertical coefficient and it is set at left-bottom corner of transformation, the last is diagonal coefficient and it is set at right-bottom coefficient (Rafael et al, 2002).

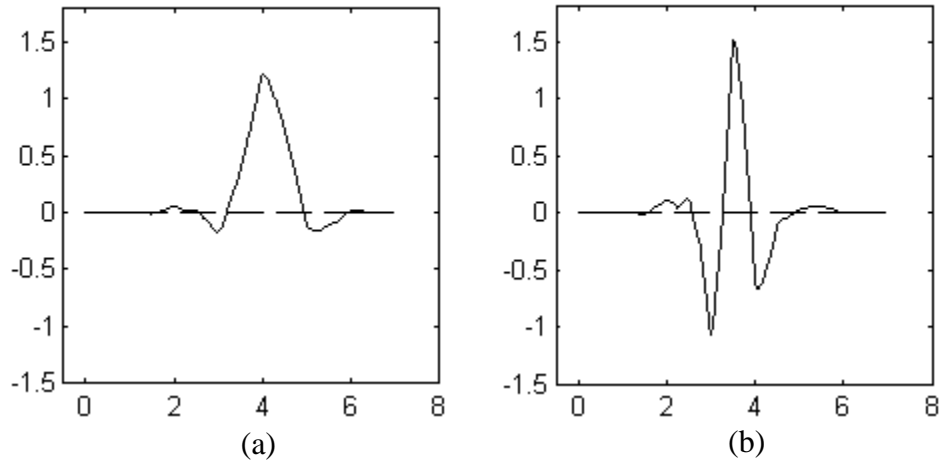
4.2.The Proposed Third Technique for Colored Image Segmentation Based on Region Growing Algorithm and 2DWT.

The proposed third technique consists of three stages; the first stage is concerned with extract edges from RGB image based on 2DWT. The second stage prepares the seed regions in an image. The third stage applies the region growing algorithm based on seed regions that are determined in second stage.

4.2.1.The first stage to the proposed third technique for Extracting Edges of RGB images.

There are many wavelet families that are used to transform image, such as: haar, daubechies, coiflets, symlets ... etc. (Mei, 2002). For each of them; there are wavelet

function and scaling function that are required in transform processing. Figure (4.1 – a, b) shows the basic functions of scaling function and wavelets function respectively for symlets wavelet family.



a- the basic symlets scaling function.

b- the basic symlets wavelet function.

Figure (4.1). The basic scaling and wavelet function of symlets wavelet family.

The following figure (4.2) represents the first stage of the proposed third technique which is concerned with extract edges from RGB images based on Two-Dimension wavelet transform.

- Step 1 Split the three bands of the (RGB) image
- Step 2 Enhance image by using Gaussian filter.
- Step 3 Transform image into appropriate scale based on symlets wavelet family.
- Step 4 Replace every pixel in approximation band with 0 intensity value (black color)
- Step 5 Merge the LH, HL, LL band together at scale J. Where J is the last scale.
- Step 6 Replace every band of scale J with band that is produced in the previous step.
- Step 7 Up to next scale $J = J - 1$.
- Step 8 Reconstruct the decomposition image based on the same wavelet family (symlets)
- Step 9 Repeat the previous step for other bands of image (RGB)

Figure (4.2). steps of the first stage to the proposed third technique for extract edges of RGB image.

Following are the detailed steps for edge detection by using two-dimension wavelet transform:

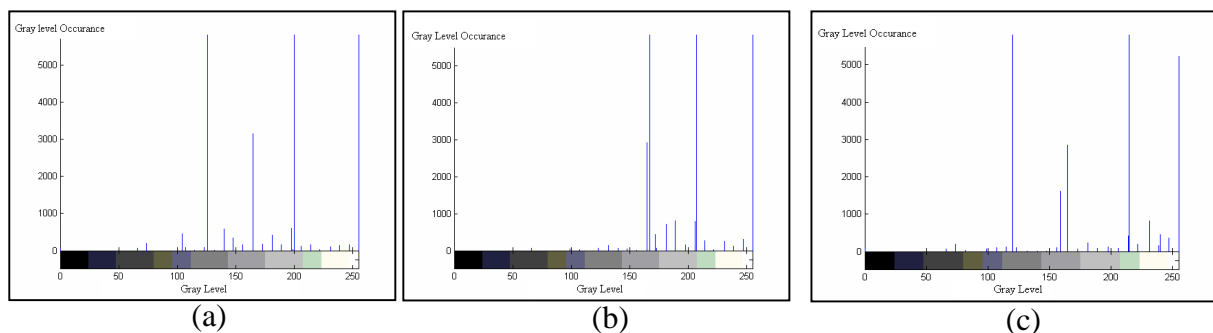
Step 1: Split the RGB band of the image as shown in figure (4.3). The map image represents the map of city and it will be used to test the proposed algorithm.



a- original image. b- Red band. c- Green band. d- Blue band

Figure (4.3): Splitting the three band of the RGB image.

The histograms of the three bands of map image is as shown in figure (4.4).



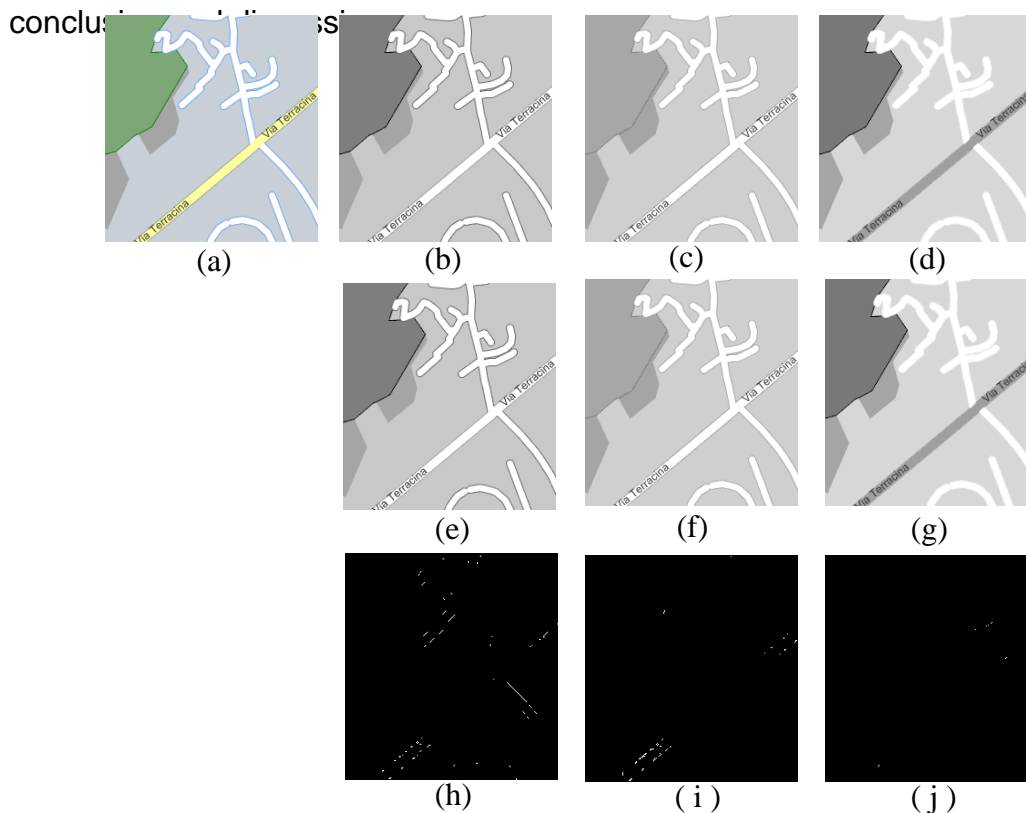
(a) Histogram of red band. (b) Histogram of green band.
(c) Histogram of blue band.

Figure (4.4).Histograms of three bands of map image in figure (4.3).

Step 2: Enhance the image by using Gaussian filter in order to remove any noise pixels and group pixels that are neighboring and closest to its intensity. Figure (4.5) shows the city map image. In this image, the enhancement process did not change a lot of intensity pixels into the three bands of RGB image as shown in figure (4.5 – h, i, j)

because their regions are clear.

Step 3: The image decomposition based on wavelet transform equations and symlets wavelet family. There are many wavelet families but the suitable one is the symlets family because it can show the small details in an image with less number of scales. Figure (4.6) shows the red band of the image after decomposition, it is based on the symlets wavelet family at scale one. The number of the scale is based on the wavelet family that is used in the decomposition processing, consequently, the details that are shown in each of horizontal, vertical and diagonal coefficients of transformed image based on the used wavelets family. This hypothesis will be discussed later in the



(a) original image. (b) Red band. (c) Green band. (d) Blue band. (e) red band after enhancement by Gaussian filter. (f) green band after enhancement by Gaussian filter. (g) blue band after enhancement by Gaussian filter. (h) pixels that are merged with neighboring by enhancement in red band. (i) pixels that are merged with neighboring by enhancement in green band. (j) pixels that are merged with neighboring by enhancement in blue band.

Figure (4.5): Image of the city map before and after enhancement.

Step 4: delete the approximation coefficient of transformed image by replacing every pixel with 0 intensity value (black color). This step is necessary to extract edges because the approximation coefficient always contains the same original image but its size is a half of size of the original image. The figure (4.7) shows the transformed image after removing the approximation coefficient from it.

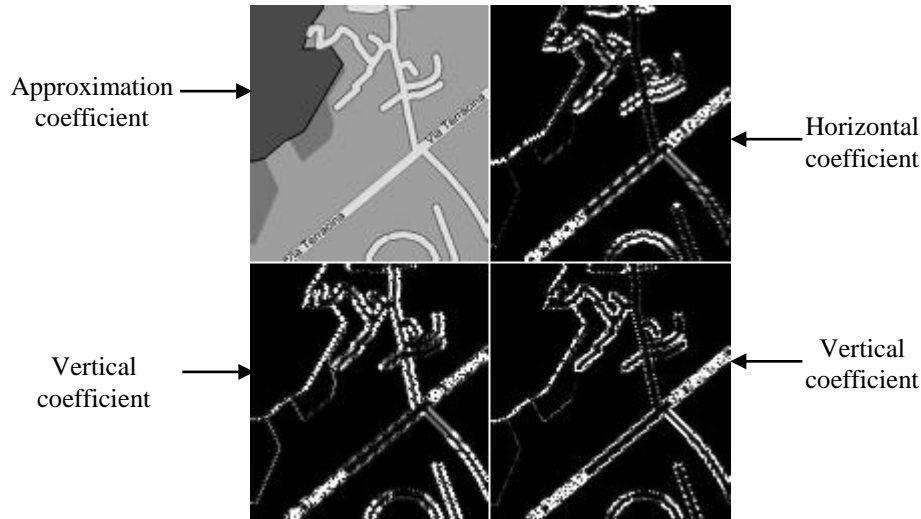


Figure (4.6): Transformed red band of the image based on symlets wavelet family and its contents; approximation, horizontal, vertical and diagonal coefficients.

Step 5: Merge each of the horizontal coefficient (LH), vertical coefficient (HL) and diagonal coefficient (HH) together based on the following equation (4.1):

$$X(i, j) = \begin{cases} HH(i, j) & HH(i, j) \geq LH(i, j) \ \& \ HH(i, j) \geq HL(i, j) \\ LH(i, j) & LH(i, j) \geq HH(i, j) \ \& \ LH(i, j) \geq HL(i, j) \\ HL(i, j) & HL(i, j) \geq HH(i, j) \ \& \ HL(i, j) \geq LH(i, j) \end{cases} \quad \dots (4.1)$$

Where :

$i: 1, 2, 3, \dots N / 2^J$; N is the height of the original image and J is the number of current scale.

$j: 1, 2, 3, \dots M / 2^J$; M is the width of original image.

X : the result band that has the maximum intensity value among LH, HL and HH bands. Which its size is $N / 2^J * M / 2^J$.

HH: The diagonal coefficient.

LH: The horizontal coefficient.

HL: The vertical coefficient.

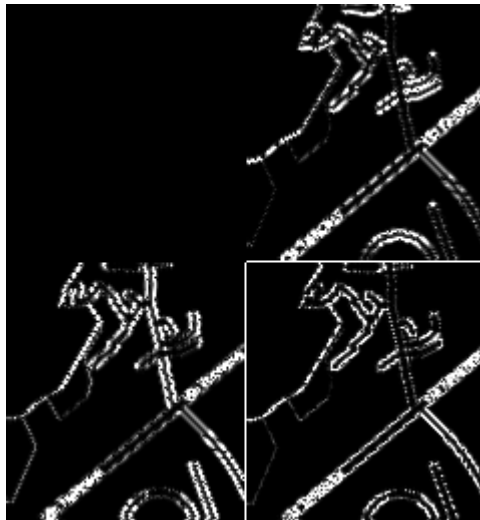
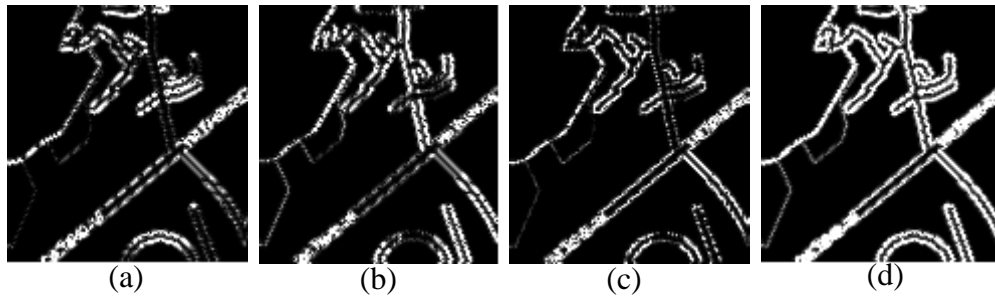


Figure (4.7): The transformed red band of the image after removing approximation coefficient from it.

Figure (4.8 – a, b, c) shows each of the three bands LH, HL and HH respectively. And it shows the result of process (X) in figure (4.8 – d).



(a) Horizontal coefficient (LH) of transformed red band image.
 (b) Vertical coefficient (HL) of transformed red band image.
 (c) Diagonal coefficient (HH) of transformed red band image.
 (d) The result of merging process for three coefficients.

Figure (4.8): The three coefficients of the transformed image and the result of merging.

Step 6 : Replace the result coefficient X with horizontal coefficient, vertical coefficient and diagonal coefficient at scale J. Figure (4.9) shows the transformed image after replacing horizontal, vertical and diagonal coefficients with coefficient X.



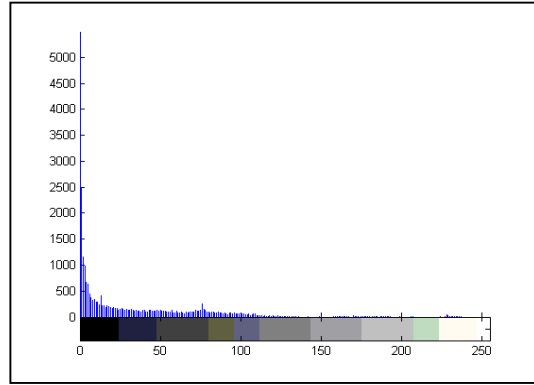
Figure (4.9): Shows the image transformed after replacing each of the three coefficients with coefficient X that is produced from step 5.

Step 7: If there are remaining scales then up to next scale and repeat steps 5, 6, 7. otherwise go to next step.

Step 8 : Reconstruct the decomposition image based on the reverse wavelets transform equation and the same wavelet family *symlets* that are used in decomposition step. Figure (4.10) shows the edges of the red band of the image and



(a)



(b)

(a) edges of red band of map image

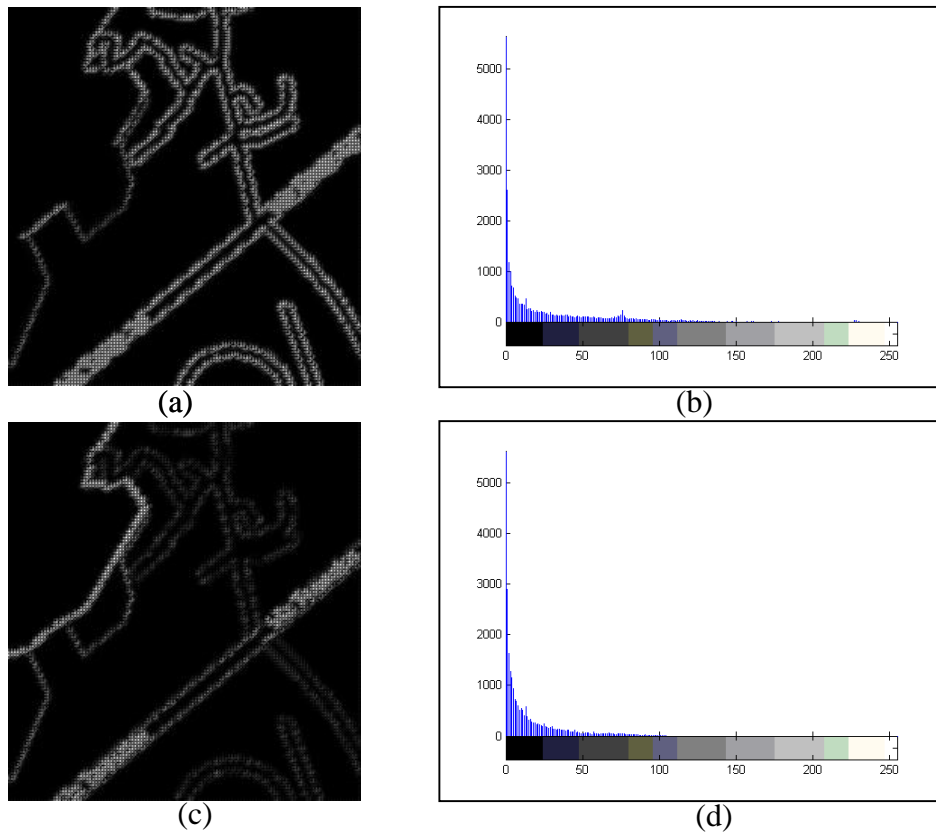
(b) Histogram of edge image of red band of map image

Figure (4.10): Edge image of red band of map image and its histogram.

its histogram after reconstructing the transformed image in figure (4.9).

Step 9: Repeat the steps from 1 to 9 on other band of RGB image. Figure (4.11 – a , c) shows the edges of Green band and Blue band of image in figure (4.3) respectively.

And its histograms in figure (4.11).



(a) Edges of the green band.
(b) Histogram of green band of map image
(c) Edges of the blue band.
(d) Histogram of blue band of map image

Figure (4.11): Edges of the green and blue band of the image in figure (4.3).

4.2.2. The Second Stage of The Proposed Third Technique for Determining Seed Regions

The important step in region growing algorithm is determining the seed points that are used as initial point for growing process. In the proposed algorithm the seed points will

be replaced with seed regions. Figure (4.12) shows the block diagram of proposed algorithm that determines the seed regions based on the edges of the three bands of the RGB image which are produced by the first stage of the proposed third technique in previous section.

- Step 1 Convert each edge of image of RGB bands into black-white image.
- Step 2 Remove any gap in black-white image by using morphological closing operation.
- Step 3 Clean a black-white image from any noise pixels by using morphological clean operation.
- Step 4 Merge the three black-white images of RGB image together.
- Step 5 Connect any one-pixel gap between two pixels by using morphological bridge operation.
- Step 6 Set every black region a seed region for region growing algorithm.

Figure (4.12): Steps to second stage of the proposed third technique for determining seed regions.

Following are the steps of the proposed algorithm in figure(4.11) that determine the seed regions of the RGB image:

Step 1: Convert the image of RGB bands that are produced at final step in the proposed algorithm in the previous section to binary image based on the threshold value that is

selected from the histogram, we can test more than one value. Equation (4.2) is used to convert edges into binary image.

$$BW(i, j) = \begin{cases} 1 & edge_image(i, j) \geq T \\ 0 & edge_image(i, j) < T \end{cases} \quad \dots (4.2)$$

Where:

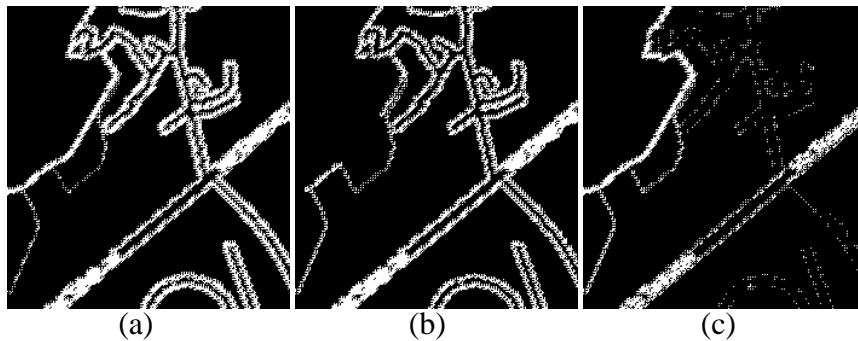
T : threshold value.

Edge_image: edge image of the RGB image.

i: height index.

j: width index.

Figure (4.13) shows the binary image to the bands.



(a) The binary image to the red band.

(b) The binary image to the Green band.

(c) The binary image to the Blue band.

Figure (4.13): The binary image to the three bands of RGB image.

Step 2: Remove any gaps in binary image in order to close its edges. Equation (4.3) represents the morphological closing operation that is applied.

$$A \bullet B = (A \oplus B) \ominus B \quad \dots (4.3)$$

Where:

A: The binary image.

B: The mask.

\oplus : The dilation operation.

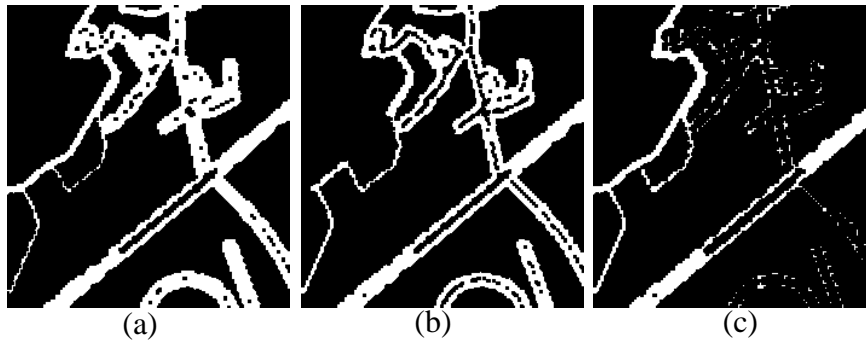
\ominus : The erosion operation.

Figure (4.14) shows the mask that represents the operand B in equation (4.3).

1	1	1
1	1	1
1	1	1

Figure (4.14): The mask that represents the operand B.

Figure (4.15) shows the binary image of RGB image after removing the gaps from them.



(a) The binary image of the red band after removing its gaps.

(b) The binary image of the green band after removing its gaps.

(c) The binary image of the blue band after removing its gaps.

Figure (4.15): The binary image of the RGB image.

Step 3: clean the binary image from any noisy pixel (isolated foreground pixels) by using clean operation of `bwmorph` function. The clean operation is supported by function `bwmorph` in *MatLab* software and it is performed by using lookup table operations. Figure (4.16) shows the image after removing the noisy pixels.

Step 4: Merge edges in figure (4.15) together based on the following equation:

$$\text{Res}(i, j) = \begin{cases} 1 & \text{ER}(i, j) = 1 \text{ OR } \text{EG}(i, j) = 1 \text{ OR } \text{EB}(i, j) = 1 \\ 0 & \text{Otherwise} \end{cases} \quad \dots (4.4)$$

Where:

i: Height index.

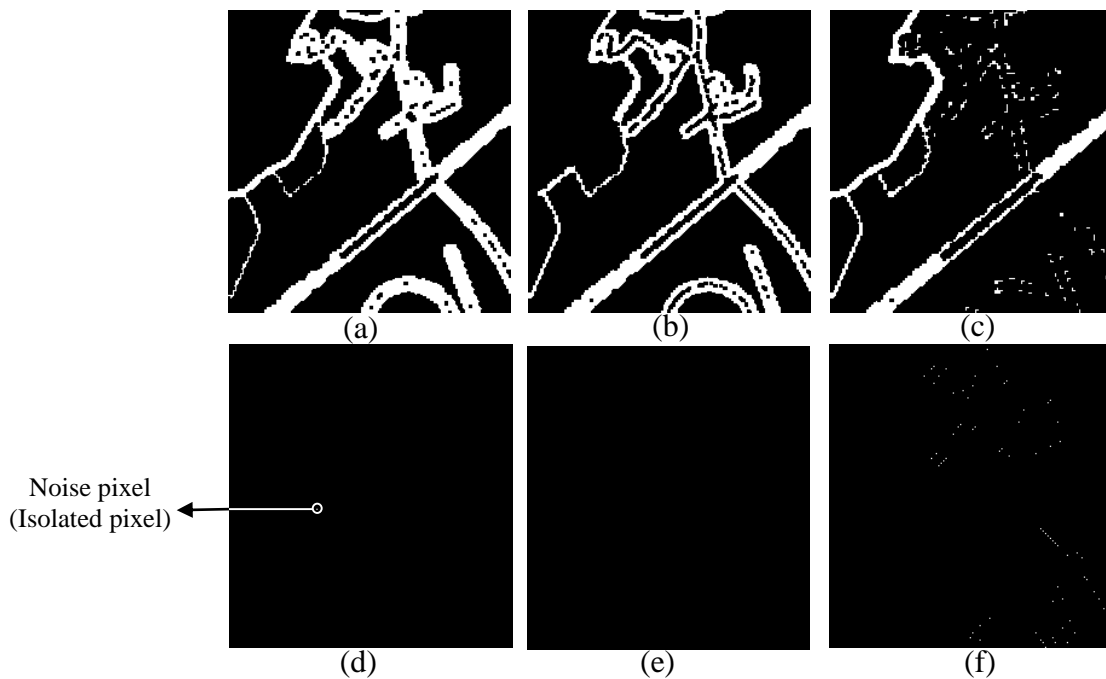
j: Width index.

ER: Red band edge (figure 15 – a).

EG: Green band edge (figure 15 – b).

EB: Blue band edge (figure 15 – c)

Res: Merged image.



(a) The binary image of edge image of red band figure (4.14 – a) after removing isolated pixels. (b) The binary image of edge image of green band figure (4.14 – b) after removing isolated pixels. (c) The binary image of edge image of green band figure (4.14 – b) after removing isolated pixels. (d) Noise pixels to figure (4.15 - a). (e) Noise pixels to figure (4.15 - b). (f) Noise pixels to figure (4.15 - c).

Figure (4.16): The binary image after removing isolated pixels with their isolated pixels that are removed from them.

Figure (4.17) shows the result of merging process.



Figure (4.17): Merging image

Step 5: connect any one-pixel gap in merging image by using bridge operation of `bwmorph` function. The bridge operation is supported by function `bwmorph` in MatLab and it is performed by using lookup table operation. The figure (4.18) shows the merging image after removing one-pixel gaps.

Step 6: Every binary region represents the seed regions that are used as initial region for region growing algorithm as shown in figure (4.18).



Figure (4.18): Merged image after removing one-pixel gaps.

4.2.3. The Third Stage of the Proposed Third Technique for Region Growing Algorithm

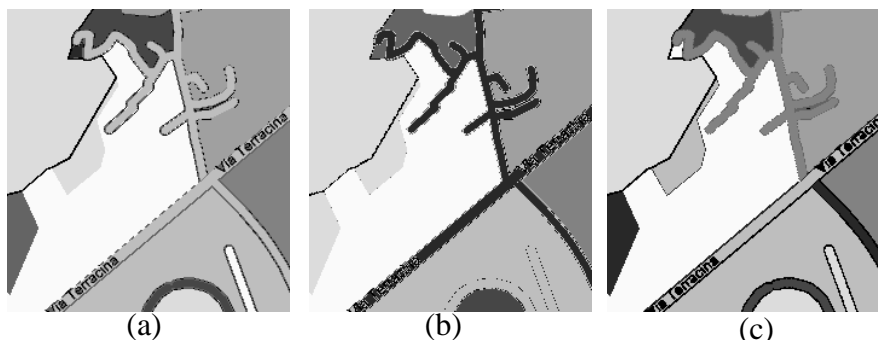
Figure (4.19) shows the process that perform region growing algorithm to the three bands of the RGB image based on the seed regions.

- | | |
|--------|--|
| Step 1 | Split the three bands of the (RGB) image |
| Step 2 | Determine the maximum and the minimum intensity values for every seed region |
| Step 3 | Re-arrange seed regions from the largest to the smallest seed regions |
| Step 4 | Merge seed region with the neighbor pixels region. |
| Step 5 | Delete pixels which are found in more than one region from the smallest regions. |
| Step 6 | Color the regions |
| Step 7 | Repeat the previous steps to the other bands |

Figure (4.19): steps to third stage of the proposed third technique for region growing algorithm
As shown in figure (4.19) the steps of region growing algorithm are applied three times

in red, green and blue band of RGB image respectively.

Figure (4.20) shows image segmentation of city map image.



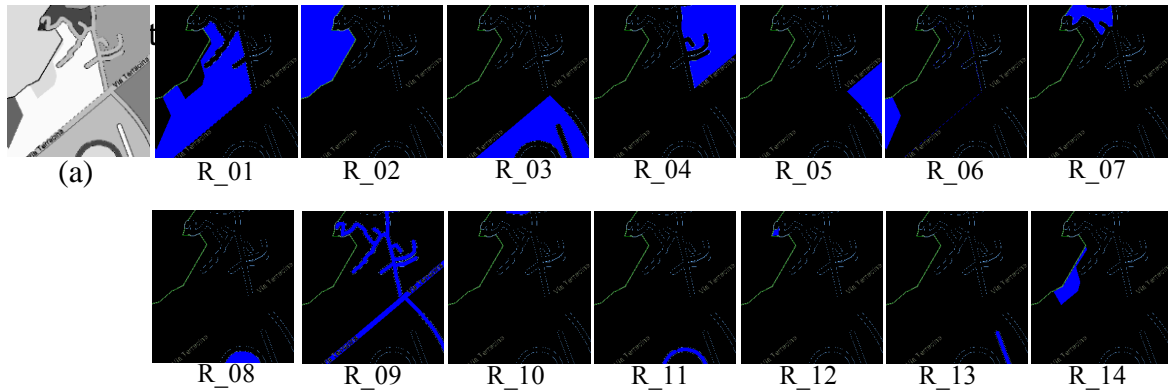
(a) Segmented image of Red Band. (b) Segmented image of Green Band.
(c) Segmented image of Blue Band.

Figure (4.20): RGB image segmentation to the city map image

4.3.Implementation and Results

The proposed technique is tested by different images. The first image is as shown in figure (4.20). The three bands of the segmentation image are different because the original three bands of the city map image in figure (4.3) are also different.

Figure (4.21) shows the regions to the red band of the city map image after

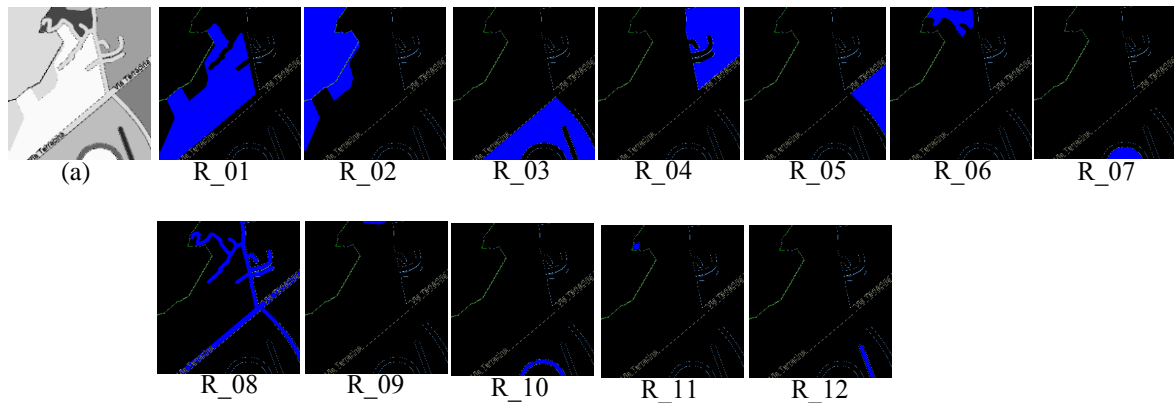


(a) Red band Segmentation.

R_01 to R_14: regions of the red band segmentation.

Figure (4.21): Red band segmentation to the city map with their regions.

Figure (4.22) shows the regions of the green band of the city map after segmentation.

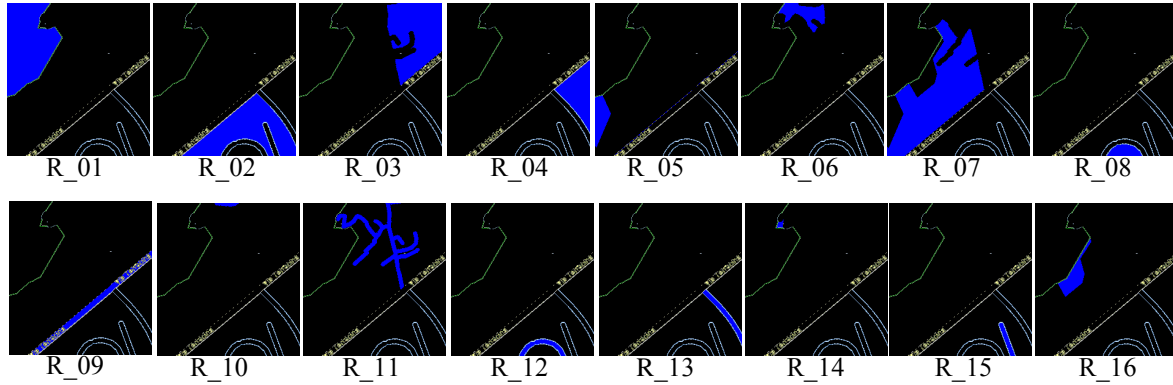


(a) Green band segmentation.

R_01 to R_12: Regions of the green band segmentation.

Figure (4.22): Green band segmentation to the city map with their regions.

Figure (4.23) shows the regions of the blue band of the city map image after segmentation.



(a) Blue band segmentation.

R_01 to R_16: regions of the blue band segmentation.

Figure (4.23): Blue band segmentation to the city map image with their regions.

Table (4.1) shows the intensity range to each region in three bands.

Table (4.1): Intensity Ranges to the regions of city map image.

Region No	Range of segmented red band		Range of segmented green band		Range of segmented blue band	
	From	To	From	To	From	To
R_01	171	202	179	209	118	122
R_02	124	128	165	169	213	217
R_03	198	202	205	209	187	233
R_04	138	202	179	209	213	217
R_05	198	202	205	209	163	216
R_06	163	200	179	209	212	233
R_07	138	202	205	209	212	233
R_08	198	202	253	255	213	217
R_09	253	255	253	255	157	161
R_10	253	255	253	255	253	255
R_11	253	255	205	209	253	255
R_12	198	202	253	255	253	255

R_13	253	255	-	-	253	255
R_14	163	167	-	-	213	217
R_15	-	-	-	-	253	255
R_16	-	-	-	-	163	167

In the proposed third technique the :

Intensity range of region A is $[L_A \text{ to } R_A]$.

Intensity range of region B is $[L_B \text{ to } R_B]$.

Where:

L_A : is left side of intensity range of region A.

R_A : is right side of intensity range of region A.

L_B : is left side of intensity range of region B.

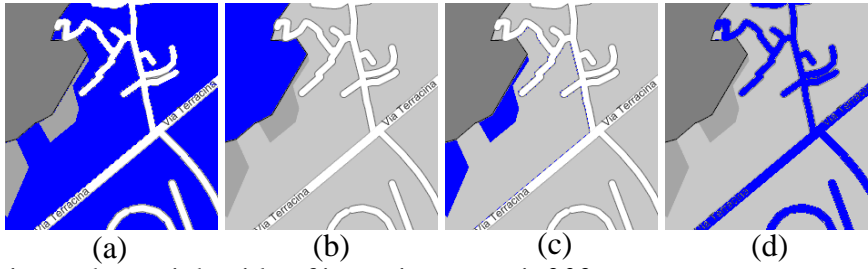
R_B : is right side of intensity range of region B.

Then

Region A is similar to region B if

$$L_A = L_B \quad \text{Or} \quad R_A = R_B$$

Figure (4.24) shows the similar regions in the red band of the map image grouped together and they are colored with blue color.



(a): Regions whose right side of intensity range is 202.

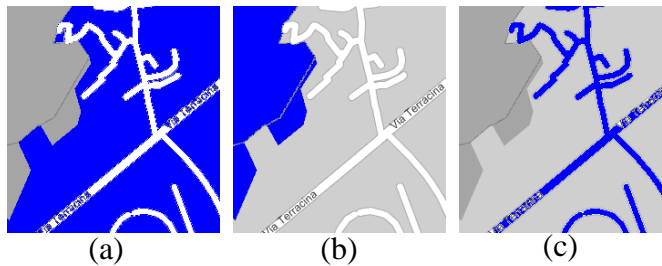
(b): Region whose intensity range is 124 to 128.

(c): Regions whose left side of intensity range is 163.

(d): Region whose intensity range is 253 to 255.

Figure (4.24). Region segmentation to the red band of the map image that is colored with blue color.

Figure (4.25) shows the similar regions in the green band of the map image grouped together and they are colored with blue color.



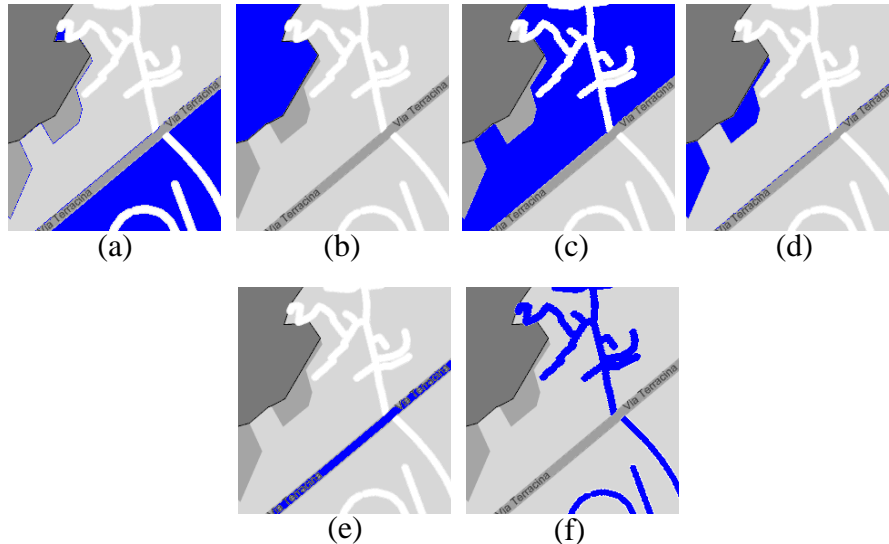
(a): Regions whose right side of intensity range is 209.

(b): Region whose intensity range is 165 to 169.

(c): Regions whose left side of intensity range is 163.

Figure (25). Region segmentation to the green band of the map image that is colored with blue color.

Figure (4.26) shows the similar regions in the blue band of the map image grouped together and they are colored with blue color.

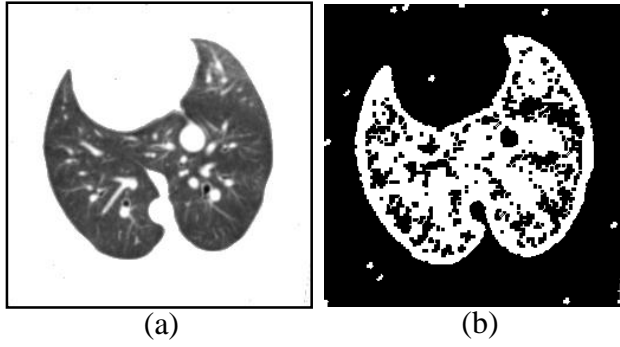


- (a): Regions whose intensity range is 213 - 217.
 (b): Region whose intensity range is 118 to 122.
 (c): Regions whose right side of intensity range is 233.
 (d): Regions whose left side of intensity range is 163.
 (e): Region whose intensity range is 157 to 161.
 (f): Regions whose intensity range is 253 to 255.

Figure (4.26): Regions segmentation to the blue band of map image that is colored with blue color.

The regions in figure (4.26 – a, c) are grouped together compared with region in figure (4.24 – a) and figure (4.25 – a). The regions in figure (4.26 – a) have intensity range in figure (4.26 – c) because they have noise pixels that are not visible and these pixels are set as blue band, so the regions that are grouped together are the segments regions of the red band and green band which are not gathered in the regions of the blue band.

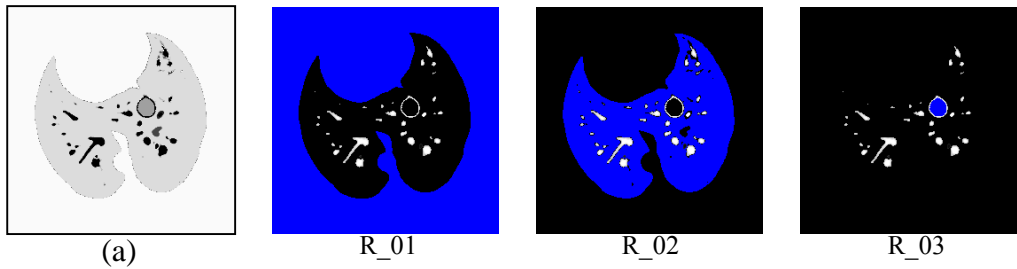
Another image was tested which is lungs image. Figure (4.27 - a) shows its red band and figure (4.27 – b) shows the black seed regions that are used as initial step in the region growing algorithm.



(a) The red band of lungs image.
 (b) The seed regions that are used in region growing algorithm.

Figure (4.27): The lungs image and its seed regions.

The three bands of lungs image are similar so the proposed algorithm was applied in red band. Figure (4.28 – a) shows the segmentation image and figure (4.28 – b, c, d) shows some regions in lungs.



(a) Red band of the red band. (b) background region of lung.
 (c) lung region. (d) circle region in the lung image.

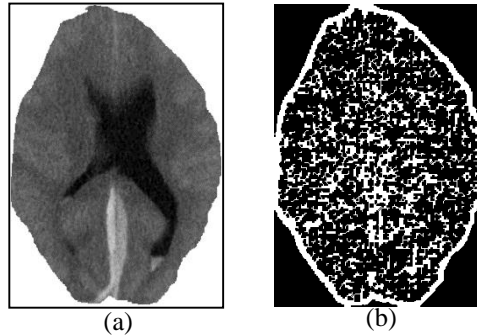
Figure (4.28). Region segmentation to the lungs image and its regions.

Table (4.2) shows the intensity range to each region in the red band.

Table (4.2): Intensity Ranges of the lung Image.

Region No	Ranges of the red band	
	From	To
R_01	180	255
R_02	49	146
R_03	253	255

Figure (4.29 - a) shows the brain image that has the black region. Figure (4.29 – b) shows the black seed region.

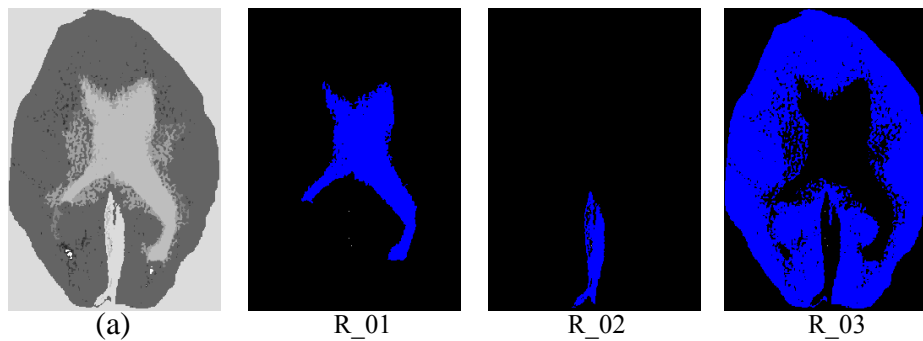


(a) Red band of the brain image.

(b) Black seed region of the red band.

Figure (4.29): Brain image with its seed region.

Figure (4.30 – a) shows the image segmentation. The region was extracted as shown in figure (4.30 – R_01) and its intensity range was 0 – 51, the other regions were shown in figure (4.30 – R_02, R_03). Table (4.3) shows the intensity range of the regions R_01, R_02 and R_03 respectively.



(a) the brain image segmetation.

R_01 to R_03: Regions of the image segmentation.

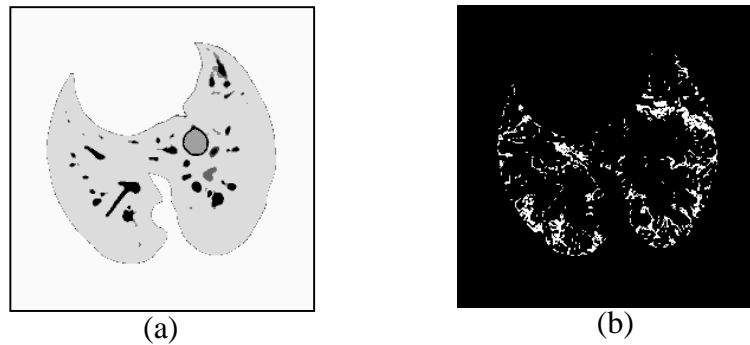
Figure (4.30): Image segmentation with their regions

Table (4.3): Intensity Ranges of Brain Image Segmentation.

Region No	Ranges of the red band	
	From	To
R_01	0	51
R_02	119	189
R_03	69	135

4.4. Conclusions and Discussions

It is important to enhance the band of the RGB image before segmentation which is performed by first stage of the proposed third technique, because some of images have pixels neighboring but their intensity values are different, so in order to group these pixels together with one intensity bands of the RGB images were enhanced by using Gaussian filter. The lung image in figure (4.27 -a) was enhanced as shown in figure (4.28 – a). Figure (4.31 - a) shows the lung image without enhancement and figure (4.31 - b) shows the pixels that are merged by Gaussian filter.



(a) lung image segmentation without enhancement.

(b) pixels merging with other pixels.

Figure (4.31): Lungs image segmentation with their pixels merging.

Figure (4.32) shows the comparison between the enhancement band of image and the non-enhancement based on the number of seed regions, number of colored region and the elapsed time.

The advantage of enhancement step is to reduce the elapsed time of the proposed algorithm and to reduce the non-useful regions by merging them with other regions

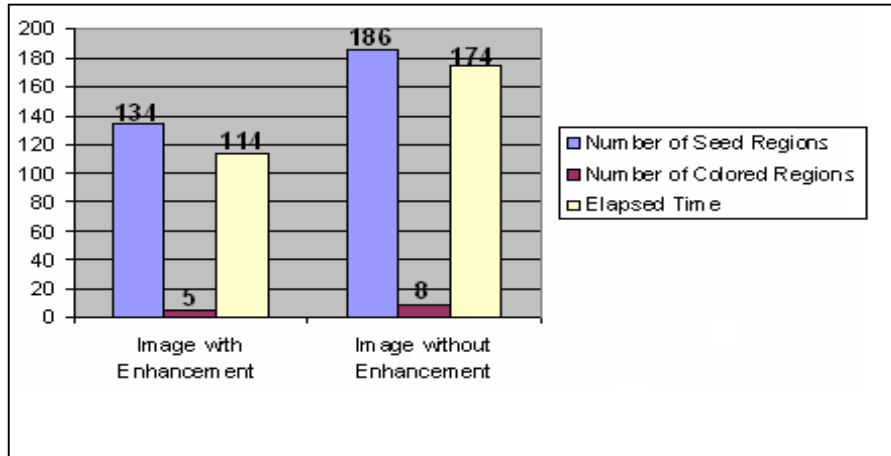


Figure (4.32): Relationship between image segmentation with the enhancement and the non-enhancement

and to reduce the number of seed regions that are used as initial step in the region growing.

The Gaussian filter based on the standard deviation is used to merge the neighboring pixels together. So the value of the standard deviation plays an important role. Table (4.4) shows the number of the seed regions, the number of segmented regions and the elapsed time.

As shown in table (4.4), when the value of standard deviation increases the value of the seed regions decreases, but for another value of standard deviation, the seed regions increase suddenly, and so at this value, the standard deviation gives us the best value for the number of seed regions, number of colored regions and elapsed time. Figure (4.33) shows the relationship between the value of standard deviation, the number of seed regions, the number of colored regions and the elapsed time. Each of them decreases when the value of the standard deviation increases. The

best value of standard deviation is shown in figure

(4.33) – marked by the vertical line. Figure (4.34) shows the pixels that are merged in lung image by using the best value of standard deviation in figure (4.33).

Table (4.4): The relationship between standard deviation and number of seed regions, number of colored regions and elapsed time.

Standard deviation value	Number of seed regions	Number of colored regions	Elapsed time for running
1	149	9	140
1.5	149	13	135
2	138	10	117
2.5	126	10	108
3	123	9	99
3.5	147	10	125
4	134	5	118
4.5	121	5	92
5	70	4	49
5.5	71	4	51
6	65	2	46
6.5	99	2	75
7	109	2	84
7.5	86	2	63
8	107	2	81

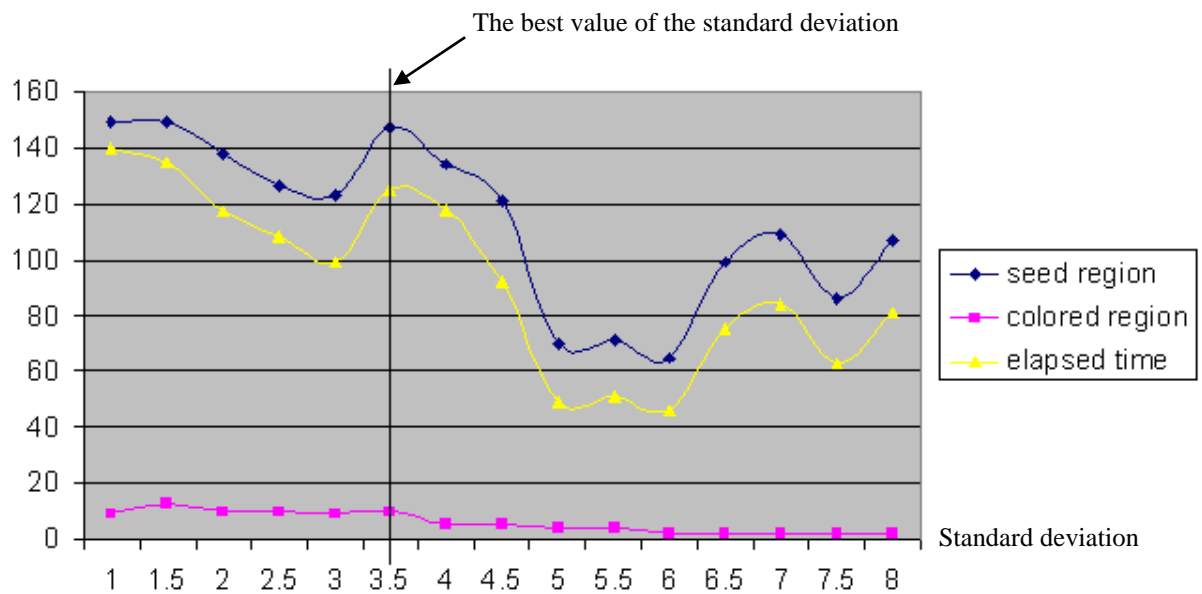


Figure (4.33): Relationship between the standard deviation, number of the seed regions and number of the colored regions.

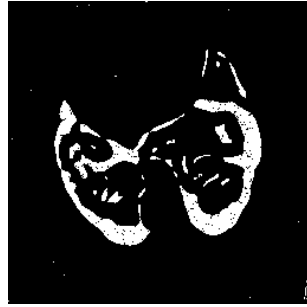


Figure (4.34): Pixels that are merged together by Gaussian filter with the best value of the standard deviation.

There are many wavelet families that are used to perform two-dimension decomposition but the best of them is *Symlet* wavelet family. Figure (4.35), figure (4.36) and figure (4.37) show the difference between db2, haar and sym4 wavelet family respectively, based on the number of pixels that are set between 170 – 255 to the map image in figure (4.3 - a).

As shown in figure (4.35), figure (4.36) and figure (4.37), the number of pixels set between 170 – 255 to the map image are 1655, 1753 and 1508 respectively, So the *Sym4* is the smallest value. But its distribution in figure (4.37) is better than db2 and haar wavelet because every intensity value from 170 to 255 has a number of pixels that belongs to it. There are also intensity values that have few number of occurrences and zero sometimes. Consequently the best wavelet to perform decomposition and reconstruct it in order to extract edges from image is *Sym4* wavelet or *Symlet* wavelet family.

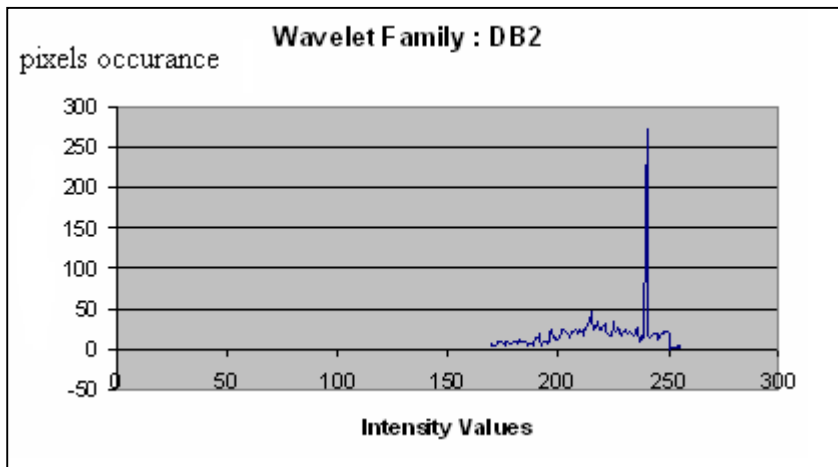


Figure (4.35). The distribution pixels between 170 – 255 based on db2 wavelet family.

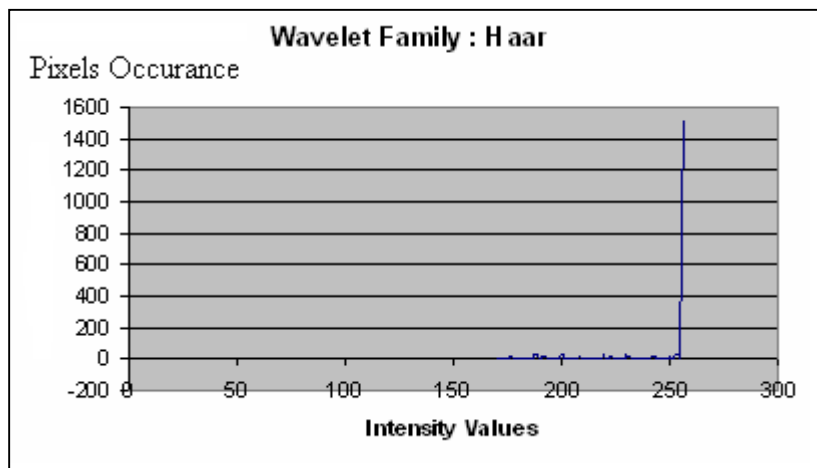


Figure (4.36): The distribution pixels between 170 – 255 based on haar wavelet family.

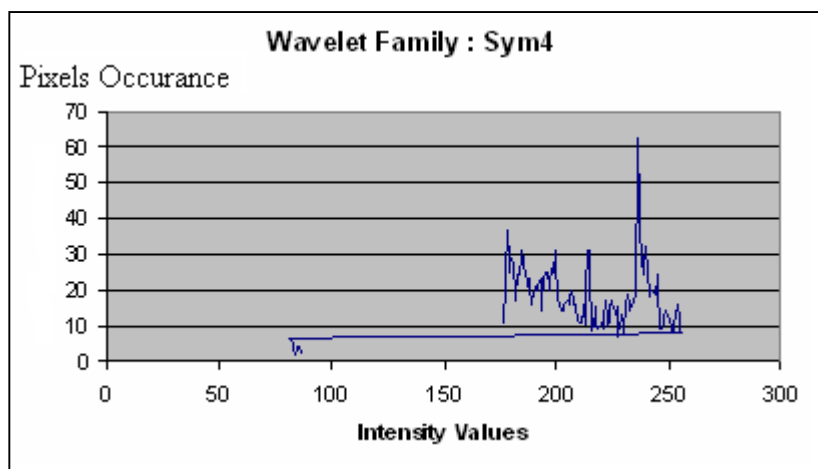
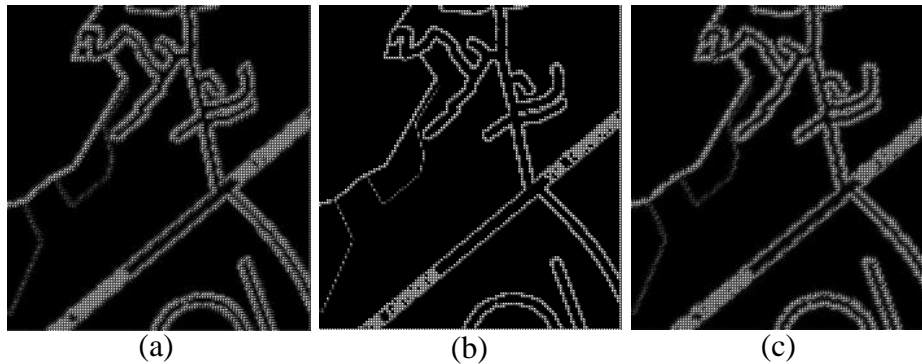


Figure (4.37): The distribution pixels between 170 – 255 based on sym4 wavelet family.

Figure (4.38- a, b, c) shows image edges to the map image based on the db2, haar and sym4 wavelet family respectively.



(a) Image edges to the map image based on db2 wavelet.

(b) Image edge to the map image based on haar wavelet.

(c) Image edge to the map image based on sym4 wavelet.

Figure (4.38): Image edge to the map image based on three types of wavelet.

Finally, wavelet may be used as a tool to extract edges in an image and to segment image. The image must be enhanced before transformation by using Gaussian filter that is based on the value of standard deviation in order to group similar neighboring pixels together.

The Symlet wavelet family gave us the best result in comparison with other wavelet families.

Chapter 5

Conclusions and Future Work

5.1. Introduction

In this thesis the proposed segmentation technique based on region growing algorithm is introduced, which was tested by using two kinds of images; the first is the gray images and the second is the color image in order to verify the performance of the segmentation technique.

The basic region growing algorithm was presented by preparing the parameters that are used to extract certain regions. These parameters are: convert image to gray level image, define the seed point values and the difference values between neighboring pixel values and seed point values. The proposed first technique defined these parameters automatically by replacing the seed points with seed regions and define these regions by using canny edge detector. After that, the maximum and minimum intensity values of these regions were defined in order to merge every neighboring pixel if its intensity value sets between maximum and minimum intensity values for neighboring region. The proposed first technique was applied on each band of the RGB bands for colored images and intensity band of the HSI model for colored images.

The edges detection is an important step in segmentation, the edge detection methods such as; Sobel method, prewitt methods, canny edge detector and the difference-average method was applied on gray scale image in order to check if any of them gives the best results. After that, the proposed second technique (part a) used the difference-average method to extract edges on gray scale image, and using it to segment colored images. The two proposed techniques were developed to be used in image segmentation; the first one was the proposed second technique (part b) for extracting

white-water region from medical eye image by using canny edge detector. And the other was the proposed second technique (part c) for extracting the transparent regions by using the proposed second technique (part a).

The color image was segmented by using two dimensional wavelet transform (2DWT) and region growing algorithm. The symlet wavelet family was used to provide 2DWT with scaling and wavelet function. After that, the morphological algorithm was applied on the extracted edges in order to enhance them by removing any gaps on them. The seed regions were used as the initial step to the region growing algorithm.

5.2. Conclusions

The conclusions of the proposed techniques in this study are:

- ❖ For the proposed first technique, there are many conclusions that were shown by results. These conclusions are:
 - The three bands of RGB model gave different segmentation regions. The intensity band of the HSI model was used to extract regions. The intensity band of the HSI model was processed just to reduce the processing time.
 - The dilation is used to remove gaps between edges and to close border lines together. The results showed that the number of dilation operations that gave the best number of regions was 2.

- The value of the expand interval was necessary to merge the maximum number of neighboring pixels to the regions. The results showed that the suitable value to this parameter was 2.
- ❖ For the proposed second technique, there are many conclusions that were shown by results. These conclusions are:
- The canny edge detector is more suitable to detect edges in the eye image, and the differencing-averaging method is more suitable to the back and front view of the head image.
 - The first scale of differencing-averaging method is enough to extract edges from image.
- ❖ For the proposed third technique, there are many of conclusions that are showed by results. These conclusions are:
- There are many wavelet families such as; Haar wavelet, DB wavelet and Symlet wavelet. The results showed that the symlet wavelet family is the suitable one in the edges detection based on the two-dimension wavelet transform.
 - The enhancement step is necessary to group the values of neighboring pixels together. The results showed that the enhancement by using Gaussian filter reduced the number of the seed regions and the number of colored regions.

- The Gaussian filter is based on the value of standard deviation. The results showed that the suitable value of the standard deviation was 1 and may be set between 1 and 3.5

Finally, there are many conclusions related to region growing algorithm and edge detection. These conclusions are:

- ✓ Determining seed regions is an important step in the region growing algorithm, for region growing could be determined either manually or automatically. The results showed the automatic determination of the seed regions was better and more accurate than manual determination.
- ✓ To determine the seed regions automatically, the canny edge detector and 2D wavelet transform were used. The results showed that the canny edge detector is more suitable to detect edges and define seed regions than 2DWT.
- ✓ The histogram is used to determine the threshold values and the morphological algorithm is used to enhance the edges.

5.3. Suggestions for Future Work

The researcher made the following suggestions for a possible future work:

1. Improving the proposed third technique for segmenting images to be more accurate

2. Developing a technique for the color image segmentation by using neural networks and developing a new technique in order to merge the neural networks and region growing algorithm.
3. Using the proposed first technique in a system which identifies the regions in imported images from database Google Earth and find the area for these regions based on the geographical measurements.
4. Developing the proposed second technique (part b) to determine the edge of pupil and iris region in medical eye image to identify persons based on iris recognition.

References

Alsultanny. Yas and Al-Fraheed. Mohammad, 2007, "**Image Segmentation Applied on Medical Images using Wavelet** ", the first international conference on digital communication and computer application, Jordan. Irbid. Jordan university science and technology (Just), pp: 688 – 694.

Amira. A and Farrell. P, 2005, "**An Automatic Face Recognition System Based On Wavelet Transforms**", Circuits and Systems, 2005. ISCAS 2005. IEEE International Symposium, Vol. 6, pp. 6252 - 6255.

Araujo. R.T.S, Medeiros. F.N.S, Costa. R.C.S, Marques. R.C.P, Moreira. R.B and Silva. J.L, 2004, "**Spots Segmentation In SAR Images For Remote Sensing Of Environment**", Image Analysis and Interpretation, 2004. 6th IEEE Southwest Symposium, pp: 95 – 99.

Bogdan Cramariuc, Moncef Gabbouj and Jaakko Astola, 1997, "**Clustering Based Region Growing Algorithm for Color Image Segmentation**", DSP 97: pp. 857 – 860, IEEE.

C. C. Chu and I. K. Aggarwal, 1993, "**The Integration of Image Segmentation Maps using Region and Edge information**", IEEE Trans. Pattern Anal. Mach. Intell., vol. 15, no. 12, pp. 1241-1252.

Camapum. J.F, Silva. A.O, Freitas. A.N, Bassani. H.F and Freitas. F.M.O, 2004, "**Segmentation Of Clinical Structures From Images Of The Human Pelvic Area**", Computer Graphics and Image Processing, 2004. Proceedings. 17th Brazilian Symposium, pp. 10 – 16.

Chen Jia-xin and Liu Sen, 2005, "**A Medical Image Segmentation Method Based On Watershed Transform**", Computer and Information Technology, 2005. CIT 2005. The Fifth International Conference, pp.634 – 638.

Cheng. S.-C, 2003, "**Region-Growing Approach To Colour Segmentation Using 3-D Clustering And Relaxation Labelling**", Vision, Image and Signal Processing, IEEE Proceedings, vol 150, Issue 4, pp. 270 – 276.

Cufi. X, Munoz. X, Freixenet. J and Marti. J, 2000, "**A Concurrent Region Growing Algorithm Guided By Circumscribed Contours**", Pattern Recognition, 2000. Proceedings. 15th International Conference on, vol.1, pp. 432 – 435.

Daw-Tung Lin, Chung-Chih Lei and Siu-Wan Hung, "**Computer-Aided Kidney Segmentation On Abdominal CT Images**", Information Technology in Biomedicine, IEEE Transactions, Vol. 10, Issue 1, pp. 59-65, Jan. 2006.

Din Yuen Chan, Chih Hsueh Lin, and Wen Shyong Hsieh, 2005, "**Image Segmentation with Fast Color Segmentation and Directional Region Growing**", IEICE Transactions on Information and Systems. vol. 88-D, no.10, pp 2249-2259.

Fondón. I , Serrano. C, and Acha. B, 2004, "**Colour Image Segmentation based on Multitolerance Region Growing**", A scientific and Technical Publishing company, pp. 452-476.

G. Fan and X. G. Xia, 2003, "**Wavelet- based Texture Analysis and Synthesis using Hidden Markove Models**", IEEE Trans. Circuits Syst. Fundam. Theory Appl., vol.50, no. 1, pp. 106-120.

Gonzalez C. Rafael, Richard E. Woods, steven L. Eddins, 2002, "**Digital Image Processing using Matlab**", second edition, prentice hall.

Graps, A, 1995, "**An Introduction to Wavelets**", Computational Science and Engineering, IEEE, Vol. 2, Issue 2, pp. 50 – 61.

Gunawan. D, 2001, "**Microcalcification Detection Using Wavelet Transform**", Communications, Computers and signal Processing, 2001. PACRIM. 2001 IEEE Pacific Rim Conference, Vol. 2, pp. 694 – 697.

Haihua Liu, Zhouhui Chen, Xinhao Chen and Yaguang Chen, 2005, "**Multiresolution Medical Image Segmentation Based On Wavelet Transform**", Engineering in Medicine and Biology Society, 2005. IEEE-EMBS 2005. 27th Annual International Conference, pp. 3418 – 3421.

Han Zhang, Say Wei Foo, Krishnan. S.M and Choon Hua Thng, 2004, "**Automated Breast Masses Segmentation In Digitized Mammograms**", Biomedical Circuits and Systems, 2004 IEEE International Workshop, pp. S2/2 - S1-4.

Hu. C, Wang. X, Mandal. M.K, Meng. M and Li. D, 2003, "**Efficient Face and Gesturree Recognition Techniques For Robot Control**", Electrical and Computer Engineering, 2003. IEEE CCECE 2003. Canadian Conference, Vol. 3, pp. 1757 – 1762.

Ikonomatakis. N, Plataniotis. K.N, Zervakis. M and Venetsanopoulos. A.N, 1997, "**Region Growing And Region Merging Image Segmentation**", Digital Signal Processing Proceedings, 1997. DSP 97., 1997 13th International Conference on, vol.1, pp. 299 - 302.

Jianping. Fan, Yau. D.K.Y, Elmagarmid. A.K and Aref. W.G, 2001, "**Automatic Image Segmentation by Integrating Color Edge Extraction and Seeded Region Growing**", Image Processing, IEEE Transactions, Vol. 10, Issue 10, pp. 1454 – 1466.

Jiasheng Hao, Yi Shen and Yan Wang, 2006, "**Segmentation for MRA Image: An Improved Level Set Approach**", Instrumentation and Measurement Technology Conference, 2006. IMTC 2006. Proceedings of the 23rd IEEE, pp. 382 – 385.

Jong Bae Kim, Chae Hyun Moon and Hang Joon Kim, 2002, "**Wavelet-Based Morphological Approach For Detection Of Human Face Regions**", Pattern Recognition, 2002. Proceedings. 16th International Conference, Vol. 1, pp. 417 – 420.

Jung. C.R, 2003, "**Multiscale Image Segmentation Using Wavelets and Watersheds**", Computer Graphics and Image Processing, 2003. SIBGRAPI 2003. XVI Brazilian Symposium, pp. 278 – 284.

Karras. D.A and Mertzios. B.G, 2003, "**On Edge Detection In MRI Using The Wavelet Transform And Unsupervised Neural Networks**", Video/Image Processing and Multimedia Communications, 2003. 4th EURASIP Conference focused, Vol. 2, pp: 461 – 466.

Kurnaz. M.N, Dokur. Z and Olmez. T, 2003,"**Segmentation Of Ultrasound Images By Using Wavelet Transform**", Engineering in Medicine and Biology Society, 2003. Proceedings of the 25th Annual International Conference, Vol. 1,pp. 657 – 659.

Leandro. J.J.G, Cesar. Jr. RM and Jelinek. H.F, 2001, "**Blood Vessels Segmentation In Retina: Preliminary Assessment Of The Mathematical Morphology And Of The Wavelet Transform Techniques**", Computer Graphics and Image Processing, 2001 Proceedings of XIV Brazilian Symposium, pp. 84 – 90.

Leandro. J.J.G, Soares. J.V.B, Cesar R.M.Jr and Jelinek. H.F, 2003, "**Blood Vessels Segmentation In Non-Mydriatic Images Using Wavelets And Statistical Classifiers**", Computer Graphics and Image Processing, 2003. SIBGRAPI 2003. XVI Brazilian Symposium, pp. 262 – 269.

Lei Zhang and Bao. P, 2002, "**A Wavelet-Based Edge Detection Method By Scale Multiplication**", Pattern Recognition, 2002. Proceedings. 16th International Conference, Vol. 3, pp: 501 – 504.

Liming Zhang and Lenders. P, 2001, "**Locating The Head Boundary With 2d Continuous Wavelet Transform**", Intelligent Multimedia, Video and Speech Processing, 2001. Proceedings of 2001 International Symposium, pp. 336 – 339.

Maeda. J, Anh. V.V, Ishizaka, T and Suzuki, Y, 1996, "**Integration Of Local Fractal Dimension And Boundary Edge In Segmenting Natural Images**", Image Processing, 1996. Proceedings., International Conference, Vol. 1, pp: 845 – 848.

Mendonca. A.M and Campilho. A, 2006, "**Segmentation of Retinal Blood Vessels by Combining the Detection of Centerlines and Morphological Reconstruction**", Medical Imaging, IEEE Transactions, Vol. 25, Issue 9, pp. 1200 – 1213.

Mostafa. M.G, Tolba. M. F, Gharib. T.F and Megeed. M. A, 2001, "**Medical Image Segmentations Using A Wavelet Based On Multiresolutions Em Algorithm**", International Conference on Industrial Electronics Technology & Automation, ieta'2001.

Neyhart. J.T, ciocco. M.D, polikar. R, mandayam. S and Tseng. M, 2001, "**Dynamic Segmentation Of Breast Tissue In Digital Mammograms**", proceeding of the 23rd annual EMBS international conference, pp. 2669 – 2672.

Niya. J.M and Aghagolzadeh. A, 2004, "**Edge Detection Using Directional Wavelet Transform**", Electrotechnical Conference, 2004. MELECON 2004. Proceedings of the 12th IEEE Mediterranean, Vol. 1, pp: 281 – 284.

Pauwels. E.J, Fiddelaers. P and Van Gool. L.J, 1996, "**Autonomous Grouping Of Contour-Segments Using An Adaptive Region-Growing Algorithm**", Proceedings of the 13th International Conference, Vol. 2, pp. 586 – 590.

Potocnik. B and Zazula. D, 2000, "**Automated Ovarian Follicle Segmentation Using Region Growing**", Image and Signal Processing and Analysis, 2000. IWISPA 2000. Proceedings of the First International Workshop, pp. 157 – 162.

Qing-Hua Lu and Xian-Min Zhang, 2005, "**Multiresolution Edge Detection In Noisy Images Using Wavelet Transform**", Machine Learning and Cybernetics, 2005. Proceedings of 2005 International Conference, Vol. 8, pp: 5235 – 5240.

Rafael C. Gonzalez, Richard E. Woods, 2002, "**Digital Image Processing**", second edition, prentice hall.

Rajpoot. K.M and Rajpoot. N.M, 2003, "**Wavelet Based Segmentation Of Hyperspectral Colon Tissue Imagery**", Multi Topic Conference, 2003. INMIC 2003. 7th International, pp. 38 – 43.

Rao. A and Gillies. D, 2001, "**Vortex Segmentation from Cardiac MR 2D Velocity Images Using Region Growing about Vortex Centres**", Medical Imaging and Augmented Reality, 2001. Proceedings. International Workshop, pp. 222 – 225.

Shu-Yen Wan and Nung. E, 2001, "**Seed-Invariant Region Growing: Its Properties And Applications To 3-D Medical Ct Images**", Image Processing, 2001. Proceedings. 2001 International Conference, Vol. 1, pp.710 – 713.

Slobodan Ilic and Branislav Ulicny, 2000, "**Seeded Region Growing Method For Image Segmentation**", The Swiss Federal Institute of Technology.

Sophie Liu Xiao Fan, Zhihong Man and Rashi Samur, 2004, "**Edge Based Region Growing–A New Image Segmentation Method**", the Association for Computing Machinery, Inc. ACM, pp.302-305.

Strickland. R.N and Hee Il Hahn, 1996,"**Wavelet Transforms For Detecting**

Microcalcifications In Mammograms", Medical Imaging, IEEE Transactions, Vol. 15, Issue 2, pp. 218-229.

Theo Pavlidis and Yuh-Tay Liow, 1990, "**Integrating Region Growing And Edge Detection**", IEEE transactions on Pattern Analysis and Machine Intelligence, vol. 12 no. 3, pp. 225-233.

Tuduki. Y, Murase. K, Izumida. M And et al, 2000, "**Automated Seeded Region Growing Algorithm For Extraction Of Cerebral Blood Vessels From Magnetic Resonance Angiographic Data**", Engineering in Medicine and Biology Society, 2000. Proceedings of the 22nd Annual International Conference of the IEEE, Vol. 3, pp. 1756 – 1759.

Wan. S - Y and Higgins, W.E, 2003, "**Symmetric Region Growing**", Image Processing, IEEE Transactions on, vol. 12, no.9, pp. 1007-1015.

Wei. Xu, Cumming. I, 1999, "**A Region-Growing Algorithm For InSAR Phase Unwrapping**", Geoscience and Remote Sensing, IEEE Transactions, Vol. 37, Issue: 1, Part 1, pp. 124 – 134.

Wenlong Qian, Zujun Hou, Qingmao Hu, Aamer. A and Nowinski. W.L, 2004, "**Segmentation Of The Sylvian Fissure In Brain Mr Images**", Bioinformatics and Bioengineering, 2004. BIBE 2004. Proceedings. Fourth IEEE Symposium, pp. 115 – 121.

Wesolkowski. S and Fieguth. P, 2003, "**Color Image Segmentation Using Connected Regions**", Electrical and Computer Engineering, 2003. IEEE CCECE 2003. Canadian Conference, vol.2, pp. 1203 – 1206.

Xiaohui Hao, Bruce. C, Pislaru. C and Greenleaf. J.F, 2000,"**A Novel Region Growing Method For Segmenting Ultrasound Images**", Ultrasonics Symposium, 2000 IEEE, Vol. 2, pp. 1717 – 1720.

Xie, 2002,"**A Method Of Tumors Detection In Digital Mammography**", Communications, Circuits and Systems and West Sino Expositions, IEEE 2002 International Conference, Vol. 2, pp. 1007 – 1011.

Xu Jie and Shi Pengzfei, 2003, "**Natural Color Image Segmentation**", Image Processing, 2003. ICIP 2003. Proceedings. 2003 International Conference, Vol. 1, pp. 1 - 973-6.

Yanjiang Wang and Baozong Yuan, 2000, "**Human Eyes Location Using Wavelet And Neural Network**", Signal Processing Proceedings, 2000. WCCC-ICSP 2000. 5th International Conference, Vol. 2, pp. 1233 – 1236.

Yinpeng Jin, Elsa Angelini, and Andrew Laine, 2000, "**Wavelets in Medical Image Processing: De-noising, Segmentation, and Registration**".

Yishu Zhai and Xiaoming Liu, 2006, "**Adaptive Edge Detection Based On Multiscale Wavelet Features**", Intelligent Control and Automation, 2006. WCICA 2006. The Sixth World Congress, Vol. 2, pp: 10289 – 10293.

Yu-Bu Lee, Soo-Min Song, Jae-Sung Lee and et al, 2005, "**Tumor segmentation from small animal PET using region growing based on gradient magnitude**", Enterprise networking and Computing in Healthcare Industry, 2005. HEALTHCOM 2005. Proceedings of 7th International Workshop, pp. 243 – 247.

Zheng Lin, Jesse Jin and Hugues Talbot, 2001, "**Unseeded Region Growing For #D Image Segmentation**", Australian Computer Society, Inc.

Zhu Hongqing, Shu Huazhong and Luo Limin, 2004, "**Blood Vessels Segmentation In Retina Via Wavelet Transforms Using Steerable Filters**", Computer-Based Medical Systems, 2004. CBMS 2004. Proceedings. 17th IEEE Symposium, pp. 316 – 321.



تقسيم الصور الملونة بالاعتماد على خوارزمية التدرجات اللونية

إعداد

محمد إبراهيم الفراهيد

إشراف

د. ياس السلطاني

قدمت هذه الرسالة للمتطلبات الجزئية للحصول على درجة الماجستير في العلوم بتخصص علم

الحاسبات

قسم علم الحاسب

كلية الدراسات الحاسوبية العليا

جامعة عمان العربية للدراسات العليا

أيار، 2007

